MARMARA UNIVERSITY
INSTITUTE FOR GRADUATE STUDIES
IN PURE AND APPLIED SCIENCES

ELECTROCHEMICAL AND SPECTROELECTROCHEMICAL CHARACTERIZATION OF PHTHALOCYANINES AND DETERMINATION OF THEIR ELECTROCHEMICAL APPLICATION FIELDS

FARUK DEMİR

MASTER THESIS
Department of Chemical Engineering

ADVISOR
Assoc.Prof.Dr. Atıf KOCA

ISTANBUL, 2013

MARMARA UNIVERSITY
INSTITUTE FOR GRADUATE STUDIES
IN PURE AND APPLIED SCIENCES

ELECTROCHEMICAL AND SPECTROELECTROCHEMICAL CHARACTERIZATION OF PHTHALOCYANINES AND DETERMINATION OF THEIR ELECTROCHEMICAL APPLICATION FIELDS

FARUK DEMİR
524510009

MASTER THESIS
Department of Chemical Engineering

ADVISOR
Assoc.Prof.Dr. Atıf KOCA

ISTANBUL, 2013

ACKNOWLEDGEMENT

First of all, I would like to give thanks to God for without him this would not have been possible.

Several people have been instrumental during the research and writing of this thesis. Their contributions to this work were valuable and I am truly grateful.

I am deeply indebted to my thesis supervisor, Assoc. Prof. Dr. Atıf KOCA, for his kind guidance, valuable comments, suggestions, support, offering invaluable help in all possible ways and helpful criticism throughout this research.

I'd like to thank my friend Yeliz İPEK for her continuous support, her contributions towards the writing up and proof reading this thesis.

Many thanks to Prof. Dr. Halit KANTEKİN, Assoc. Prof. Dr. Zekeriya BIYIKLIOĞLU and Assoc. Prof. Dr. Ali ERDOMUS, for their remarkable help throughout the duration of this project and their newly synthesized phthalocyanines. Thanks also to Assoc. Prof. Dr. Fatma KARACA for his help.

I am also thankful to my colleagues at Pendik Municipality for their cooperativeness and friendly support.

Finally, during all stages involved in the beginning of this thesis I want to thank to my family members who supported and encouraged me.

May, 2013 **Faruk DEMİR**

TABLE OF CONTENTS

ABSTRACT

ELECTROCHEMICAL AND SPECTROELECTROCHEMICAL CHARACTERIZATION OF PHTHALOCYANINES AND DETERMINATION OF THEIR ELECTROCHEMICAL APPLICATION FIELDS

It is well known that that modern electrochemical technology can offer the preferred solution to a range of problems in chemical industry. Therefore in this thesis, we have aimed to use electrochemical methods for the analysis of some newly synthesized phthalocyanines and their practical applications. The unique properties of phthalocyanines have generated world-wide interest in their use in chemical sensors, fuel cells, molecular metals, molecular computers, pollution control, and information technology.

In this study, electrochemical and spectroelectrochemical characterizations of newly synthesized free, titanyl, cobalt and nickel phthalocyanines, which were peripheral and nonperipheral substituted, were performed and according to these results their possible applications in different electrochemical technologies were determined. Multiple and reversible, diffusion controlled and multi-electron redox reaction of titanyl phthalocyanines indicate possible usage of the complexes especially in electro sensing and electrocatalytic applications. The complexes sense some heavy metals, such as Ag^{+} and Pd^{2+} in solution and in solid states and catalyzed molecular oxygen in aqueous and nonaqueous solutions.

Diethylamino and dimethylamino groups on the substituents of the free, nickel and cobalt complexes cause electropolymerization of the complexes on the working electrode during the oxidation reactions. Changing the potential window of the voltammetric cycles alters the electropolymerization mechanisms. Types of the metal center of the complexes also affect the electropolymerization mechanism.

Reversible and multi-electron metal based electron transfer properties of the relevant phthalocyanines indicated their possible electrochemical application in the fields of electrocatalyst, photocatalyst and sensors. Different color of the oxidized and reduced species of these compounds indicated their possible application in especially electrochromic, solvatochromic and optically light emitting diodes.

Electron transfer reactions of diethyl amine substituted phthalocyanine complexes alter the optical responses of the complex in solution as well as in solid state due to the disappearance of the Q band of the complex and observation of new bands in the visible region of the light spectrum. Optical changing’s in the visible light spectrum are the desired properties for a material for the usage in the display technologies.

In situ spectrochronocoulometric measurements indicate that electro polymerized Pc films illustrate excellent electrochromic properties with fast response time, high efficiency, high columbic and optic stability, and high optical contrast.

May, 2013 **Faruk DEMİR**

ÖZET

FTALOSİYANİNLERİN ELEKTROKİMYASAL VE SPEKTROELEKTROKİMYASAL KARAKTERİZASYONU VE ELEKTROKİMYASAL UYGULAMA ALANLARININ BELİRLENMESİ

Modern elektrokimya teknolojisinin kimya sanayindeki birçok probleme öncelikli çözümler sunduğu iyi bilinmektedir. Bu tez çalışmasında, yeni sentezlenmiş ftalosiyaninlerin ve elverişli uygulama alanlarının analiz edilmesi amacıyla elektrokimyasal metotlar kullanılmıştır. Ftalosiyaninlerin benzersiz özellikleri; kimyasal sensörler, yakıt pilleri, moleküler metaller, moleküler bilgisayarlar, kirlilik kontrolü ve bilgi teknolojisinde kullanımında dünya çapında bir ilgi oluşmasını sağlamıştır.

Bu çalışmada, yeni sentezlenmiş hidrojen, titanyum, kobalt ve nikel ftalosiyaninlerin elektrokimyasal ve spektroelektrokimyasal karakterizasyonu gerçekleştirilmiş ve bu sonuçlar ışığında farklı elektrokimyasal teknolojilerde olası kullanım alanları belirlenmiştir. Titanil ftalosiyaninlerinin çoklu ve tersinir, difüzyon kontrollü ve çok elektronlu redoks reaksiyonları bu komplekslerin özellikle elektro algılama ve elektrokatalitik uygulamalarda kullanılabilirliğini göstermektedir. Bu kompleksler Ag^{+} ve Pd^{+2} gibi ağır metalleri çözelti içerisinde ve katı halde algılamaktadır ve oksijeni sulu ve sulu olmayan çözeltilerde katalizlemektedir.

Hidrojen, nikel ve kobalt komplekslerinin çevresindeki dietilamin ve dimetilamin grupları indirgenme reaksiyonları esnasında çalışma elektrodu üzerinde elektrokimyasal olarak polimerleşmesini sağlamaktadır. Voltametrik dönüşümlerin potansiyelinin değiştirilmesi elektrokimyasal polimerleşme mekanizmasını etkilemektedir. Ayrıca merkezde bulunan metallerde ayrıca polimerleşmenin değişmesine katkı sağlamaktadır.

Söz konusu ftalosiyaninlerin tersinir ve çok elektronlu metal merkezli elektron transfer özellikleri, elektrokatalizör, fotokatalizör, sensör ve benzeri uygulama alanlarında elektrokimyasal uygulamalarının mümkün olduğunu göstermektedir. Bu komplekslerin yükseltgenmiş ve indirgenmiş türlerinin farklı renkleri özellikle elektrokromik ve solvatokromik uygulamalarda, ışık saçan diyotlarda ve benzer işlemlerde uygulanabilirliğini göstermektedir.

Q bandının kaybolması ve görünür bölgede yeni bantların oluşmasından ötürü dietilamin bağlı ftalosiyanin komplekslerinin elektron transfer reaksiyonları hem çözeltide hem de katı haldeki optik değişimlerini etkilemektedir. Görünür bölge spektrumundaki optik değişimler görüntüleme teknolojilerindeki kullanımı açısından uygun özellikleri sahip olduğunu göstermektedir.

Spektrokronokolometrik ölçümler elektrokimyasal olarak polimerleşebilen ftalosiyanin filmlerinin hızlı değişim, yüksek verim, yüksek kolombik ve optik kararlılık yüksek optik kontrast gibi mükemmel elektrokromik özelliklere sahip olduğunu göstermektedir.

Mayıs, 2013 **Faruk DEMİR**

LIST OF SYMBOLS

C : electrocatalyst

A : Analyte

Ox : oxidized form of redox couple

Red : reduced form of redox couple

Ox : oxidized form of redox couple

R_{ed} : reduced form of redox couple

C_{ox} : concentrations of oxidized form

C_{red} : concentrations of reduced form

E_0 : standard electrode potential for redox reaction

i_d : limiting current (μA)

m : mass flow rate (mg/sec)

t : drop lifetime in seconds(s)

C : analyte concentration (mol/cm^3)

n : number of electrons involved in overall electrode reaction

D : diffusion coefficient (cm^2/s).

i_p : the peak current

A : area of the electrode

v : scan rate of the applied potential

F : faraday constant

LIST OF ABBREVIATIONS

Pc : phthalocyanine
MPc : metallophthalocyanine
HOMO : highest occupied molecular orbital
LUMO : lowest unoccupied molecular orbital
NHE : normal hydrogen electrode
SCE : saturated calomel electrode
TEAP : tetraethylammonium perchlorate
TBAP : tetrabutylammonium perchlorate
$TBABF_4$: tetrabutylammonium tetrafluoroborate
ITO : indium tin oxide
MLCT : metal to ligand charge transfer
LMCT : ligand to metal charge transfer
CME : chemically modified electrode
PDT : photodynamic therapy
WE : working electrode
RE : reference electrode
DMF : dimethylformamide
DMSO : dimethylsulfoxide
EDTA : ethylenediaminetetraacetic acid
CV : cyclic voltammetry
NPV : normal pulse voltammetry
DPV : differential pulse voltammetry
SWV : square wave voltammetry
OTE : optically transparent electrode
OTTLE : optically transparent thin layer electrode
LB : langmuir-blodgett
DCM : dichloromethane
AN : acetonitrile

LIST OF FIGURES

LIST OF TABLES

1. INTRODUCTION

Electrochemistry is the branch of chemistry concerned with the interrelation of electrical and chemical effects. A great part of this field deals with the study of chemical changes caused by the passage of an electric current and the production of electrical energy by chemical reactions. The synthesis of new compounds as well as the electronic and magnetic properties of solids are of principal interest in the field of solid state chemistry.[1] Electrochemical organic synthesis has seen enormous progresses in recent years. One of the most promising areas for development of electrochemical methodology is within the field of organic synthesis, where it can enable the simplification of synthetic routes.[2] Thus a precipitous growth in the discovery of new phthalocyanine-based compounds has already been observed. While the basic principles of electrochemistry discussed in this text apply to all of these, the main emphasis here is on the application of electrochemical methods to the study of chemical systems.

Phthalocyanines (Pcs) and metallophthalocyanines (MPcs) are macrocyclic π-electron conjugated molecules. Metallo-phthalocyanine compounds demonstrate a high potential for various applications. MPcs and Pcs, primarily due to their π-electron conjugation, may exhibit a series of electrochemical processes and can consequently be used as efficient electron mediators. Hence, this work uses MPcs attached to electrodes as electrochemical sensors. [3] The primary aim of these investigations was to probe the electrochemical and material science aspects of some selected metal phthalocyanines (MPcs).Metal phthalocyanines characterized by an exclusive planar molecular structure. As a single class of compounds they have been the subject of ever increasing number of physicochemical and technological investigations. During the last two decades the literature on these compounds was flooded by an out pour of original publications and patents. Almost every branch of materials science has benefited by their application- surface coating, printing, electrophotography, photoelectrochemistry, electronics and medicine to name a few. The present study was confined to electrochemical and spectroelectrochemical properties of free, titanium, cobalt, nickel and copper phthalocyanines.

1.1 Discovery and History of Phthalocyanines

The first recorded observation of a phthalocyanine occurred in 1907 (Braun and Tscherniac, 1907). During the synthesis of o-cyanobenzamide from phthalamide and acetic anhydride, Braun and Tcherniac observed the production of a colored impurity of unknown structure and origin [4]. The first metal-free phthalocyanine (H_2Pc) was also reported in 1927 de Diesbach and von der Weid made CuPc [5]. However, none of them characterized the products, so the discovery of Pcs is attributed to chemists at Scottish Dyes Ltd, who later made and characterized iron phthalocyanine (FePc), whose structure was elucidated by Linstead [6] at Imperial College and confirmed by Robertson [5-6] using X-ray diffraction (XRD). A patent describing the manufacturing process was filed in 1928 [7]. Linstead (1933) to describe both its origin from phthalic anhydride (*phthalo*) and its strikingly beautiful blue color which was similar to *cyanine* dyes. Phthalocyanines (Pcs) are man's synthetic analogues of the porphyrins, such as chlorophyll, cyanocobalamine (vitamin B12) and hemoglobin[8]. Subsequently, work carried out by Robertson was the first example of a single crystal X-ray study being used to confirm a structure postulated from conventional chemical analysis [9-10]. In 1929, another Pc derivative, iron (II) phthalocyanine, was found as a green/blue impurity coming from a defect in the iron vats of which phthalimide was being produced from phthalic anhydride and ammonia [11] Dandridge and Dunsworthreported that the compound was very stable, insoluble and resistant to heat (500°C) and concentrated acid. One year later, a patent for iron (II) phthalocyanine was granted to Dandridge, Drescher and Thomas of Scottish Dyes, Ltd., being the first for Pc compounds.

Up to 1929, none of the observers of the blue coloring matters attempted to determine its structure. Professor Linstead and his students, at the University of London, supported by grants from Imperial Chemical Industries, starting in 1929, determined and announced the structure of Pc and several metallophthalocyanines (MPcs) in 1933 and 1934 [12]. Not only are the Pcs a new class of organic compounds but also they constitute a new class of coloring matter or chromogen.

Moderate cost of manufacture, good stability and tinctorial properties, in a region of the visible spectrum which had been lacking in chromogens of as good color properties, stability, and manufacturing cost, have led the Pcs to become. The potential of phthalocyanines as pigments was immediately obvious to workers at ICI, which began trading copper (II) phthalocyanine under the name Monastral Blue in 1935 [13].

I.G. Farbenindustrie and Du Pont also commenced production. Industrial manufacture of phthalocyanine was based on the methodology developed by Wyler at the ICI research center at Blackley, Manchester. The Wyler method involves heating inexpensive phthalic anhydride in a melt of urea, metal salt, and suitable catalyst (e.g., ammonium molybdate) and this is still the method of choice for industrial-scale manufacture of phthalocyanine colorants. Water-soluble dyes based on sulfonated phthalocyanines and, subsequently, reactive dyes for permanent textile coloration were developed in the 1950s and 1960s.

Since 1934 and continuing to the present day, the object of intensive world-wide investigations, particularly with respect to applications in the field of color. Also, numerous production facilities for the manufacture of the principal Pc coloring matter, copper phthalocyanine have been constructed throughout the world. Today, many thousands of tons of phthalocyanines are produced worldwide, per annum, to help satisfy the demand for colorants and optoelectronic materials.

1.2 General Properties Of Phthalocyanines

Phthalocyanines consists of 16 carbon and 8 nitrogen atoms and have a two-dimensional 18π electron conjugated system, in which more than 70 different metals and non-metals such as those shown in red, Fig.1.1. Incorporation of different ring substituents in the peripheral and non peripheral positions is also possible.

For instance, the structure of a Pc ring is versatile and thus allows the incorporation of different substituents on the peripheral {(2, 3), (9, 10), (16, 17) or (23, 14)} or non-peripheral {(1, 4), (8, 11), (15, 18) or (22, 25)} positions of the ring. Fig.1.2.

The above alterations change the properties of phthalocynanines such as solubility. Solubility can be varied by changing the central metal ions, axial ligands and ring substituents. [14]

In MPc, the macrocycle is dianionic, i.e. Pc^{-2}, and thus acts as a ligand which complexes with most metal ions thanks to its rich coordination chemistry. Two Pc nitrogens covalently bond with the central atom through loss of the central hydrogens, and two other nitrogens (N_{30} and N_{32}) have a co-ordinate linkage with the metal.

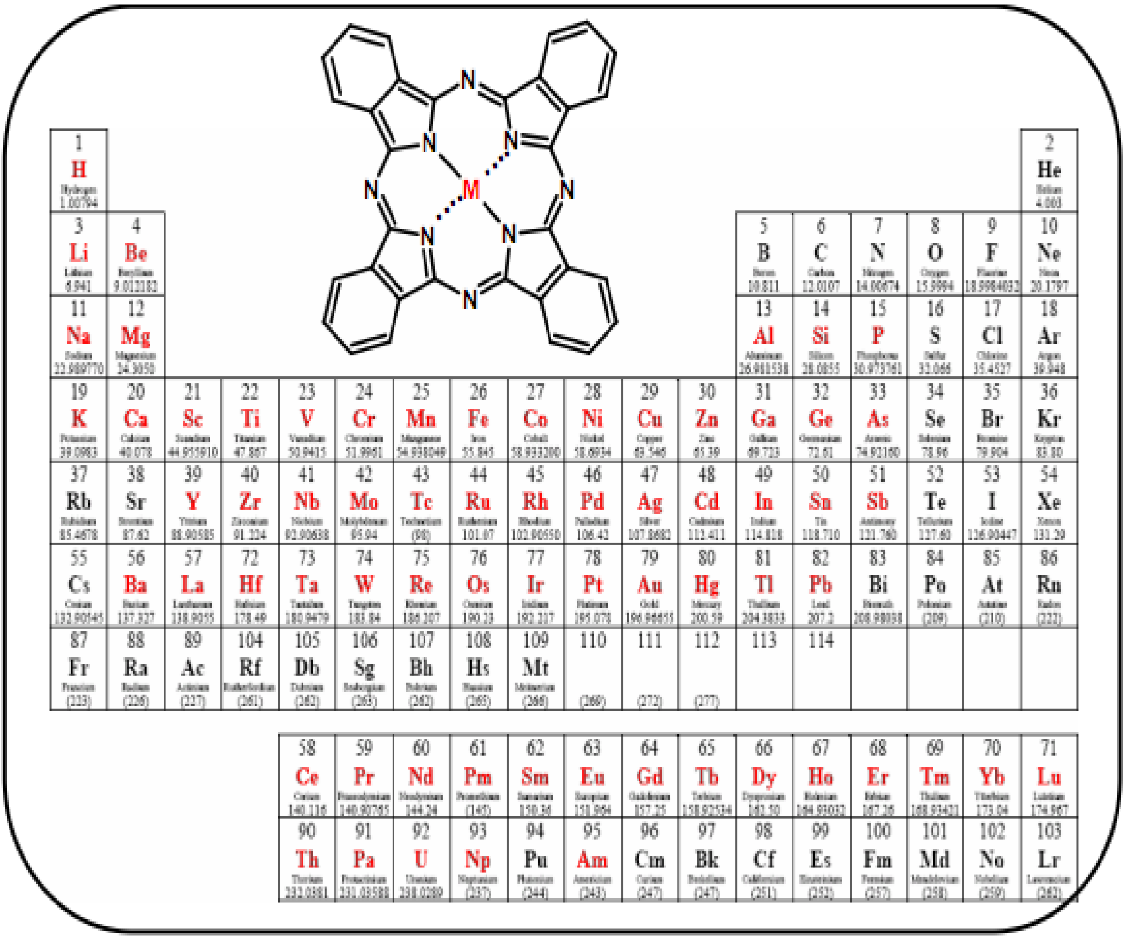

Figure 1.1. Metals and Non-Metals which are conjugated phthalocynanines shown in red.

A metal-free phthalocyanine (H_2Pc) is generally considered to be of square planar geometry, with a π-electron system of D_2h symmetry.

Most metal ions in an oxidation state +2, which closely fit inside the cavity of the ring, complex with the Pc ring to form a stable 1:1 planar metal-ligand complex, thus increasing the symmetry from D_2h to D_4h.

These types of phthalocyanine complexes, e.g. NiPc and CuPc, are generally strong such that removal of a metal ion results in the destruction of the Pc ring.

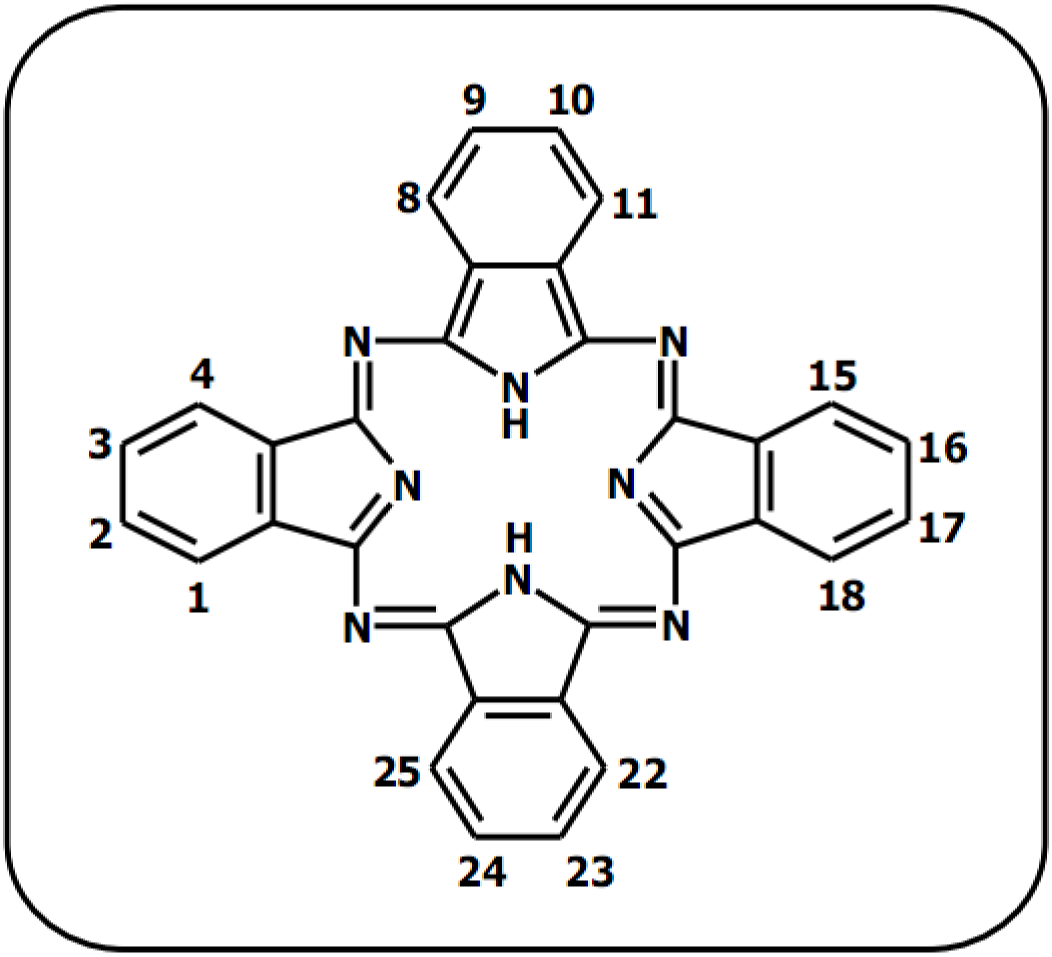

Figure 1.2. Phthalocyanine Molecular Complex

They are also not affected by strong acids such as concentrated H_2SO_4 or strong bases; however, they can be broken down to phthalimide or phthalic acid by strong oxidizing agents such as dichromate or ceric salts [15, 16, and 17]. Larger metal ions tend to distort the geometry of the macrocycle to some extent as they do not fit into the cavity of the ring. The molecular symmetry is decreased to C_4v (i.e. square pyramidal) and thus the metal ions tend to lie above the ring to adopt a 'shuttlecockshaped' configuration [18, 19]. Fig. 1.3(i). MPcs such as Pb2+ [20], Sn2+, [21,22] and Ge2+ [23], form these non-planar structures of C_{4v} symmetry as a result of the rotation of the rigid isoindole units that reduce the internal stress induced by the large metals.

It is worth mentioning that the introduction of two chloride ions to SnPc and GePc leads to both change of valence as well as molecular symmetry from C_{4v} to D_{4h} of C_{l2}SnPc and C_{l2}GePc as shown in Fig. I.3 (ii).

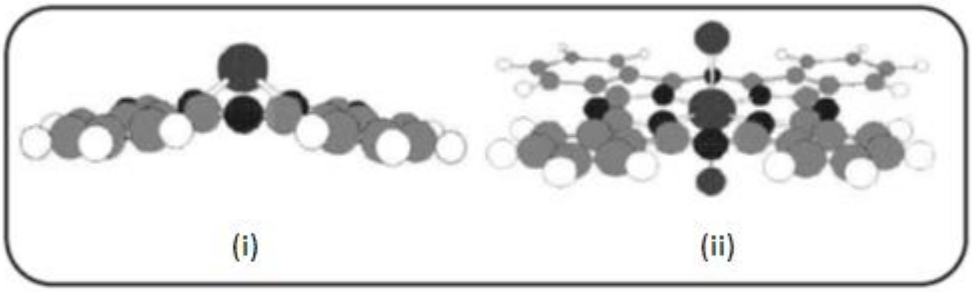

Figure 1.3. MPc structures showing (i) 'shuttlecock-shaped' C_{4v} symmetry and (ii) D_{4h} symmetry.

On the contrary, 2:1 metal-ligand derivatives of smaller monovalent ions such as Li^+, Na^+, K^+ are formed where both metal ions lie on each face of the Pc plane [24,25], Fig.1.4(i). The protrusion enhances their solubility in polar organic solvents by disrupting the intermolecular forces between the Pc rings [25, 26]. The Li^+, Na^+, K^+ ions are also labile such that they are either easily replaced by robust metal ions that have stronger interactions with the ring or are easily removed by dilute acids to produce metal-free phthalocyanines. Therefore they are used as precursors for the synthesis of novel MPcs such as tetra-, octa-substituted and sandwich-type MPcs [27-30]. The use of the "dilithium-method" in MPc formation is advantageous over many other routes in that MPc that require low boiling point solvents and stoichiometric amounts of Pc and metal salts can be prepared in large amounts. Titanium phthalocyanines (TiPcs) may additionally adopt different coordination geometries, depending on whether the axial ligand is 'O' or 'Cl'. OTiPc is square pyramidal with C4v symmetry [31] while C_{l2}TiPc has trigonal prism geometry of *D*3h symmetry [32]. MPcs with coordination number 7 such as in the case with C_{l3}TaPc [33], have a C_{2v} symmetry and exhibit a capped trigonal prism geometry. In the case of rare-earth metals such as lutetium, a 1:2 metal: ligand complex (known as sandwich complex or bisphthalocyanine) is formed when the large metal ion complexes with two Pc units [34, 35].

The formation of bisphthalocyanines is possible through metal coordination to all isoindole nitrogens in each Pc macrocycle.

The Pc macrocycles are rotated by a staggering angle, with the sandwich complexes either adopting a cubic geometry, or square antiprism geometry as in the case with *bis* (phthalocyaninato) M (III) complexes (M = neodymium and lutetium).

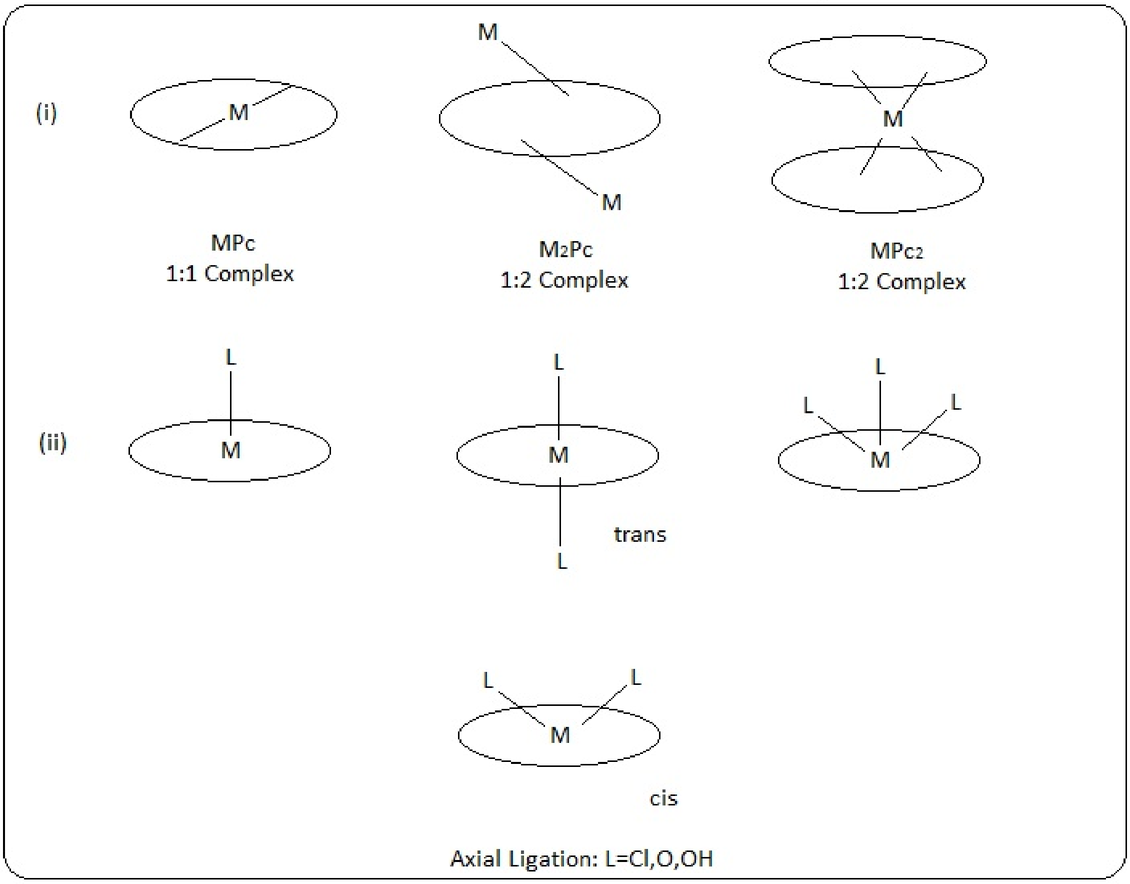

Figure 1.4. (i) Various forms of MPc complexes (ii) MPc in which metals in oxidation states greater than +2 are bonded to axial ligands.

1.2.1. Physical Properties

The density of β-phthalocyanine, H_2Pc, is 1.43 g/cm^3; β-copper phthalocyanine, CuPc, 1.61 g/cm^3; and polychloro-copper phthalocyanine, 2.14 g/cm^3. The color of most phthalocyanines ranges from blue-blackto a metallic bronze, depending on the manufacturing process and the chemical and crystalline form of the material. The colors of the newly divided pigment forms vary from dark blue to green, as phthalocyanines absorb in the visible region at 600–700μm.

Most compounds do not melt but sublime above 200°C. CuPc can be sublimed without decomposition at 500–580°C under an inert gas and normal pressure and at 900° C under vacuum. It decomposes vigorously, however, at 405–420°C in air and in nitrogen between 460–630° C.

1.2.2. Chemical Properties

The chemical properties of phthalocyanines depend mostly on the nature of the central atom. Phthalocyanines are stable to atmospheric oxygen up to approximately 100°C. Mild oxidation may lead to the formation of oxidation intermediates that can be reduced to the original products. In aqueous solutions of strong oxidants, the phthalocyanine ring is completely destroyed and oxidized to phthalimide. Oxidation in the presence of ceric sulfate can be used to determine the amount of copper phthalocyanine quantitatively. Oxidation can also occur at the central metal atom of the phthalocyanine system. Mn phthalocyanine, for instance, can be produced in these different oxidation states, depending on the solvent. The carbon atom of the ring system and the central metal atom can be reduced, some reversibly, e.g., in vatting. Phthalocyanine compounds exhibit favorable catalytic properties which makes them interesting for applications in dehydrogenation, oxidation, electrocatalysis, gas-phase reactions, and fuel cells (qv).

1.2.3. Electrochemistry of Phthalocyanines

The electrochemical characterizations of the MPcs as well as their ability to electrocatalyst analytes are studied, hence a review of electrochemical techniques follows. Over the past 40 years the electrochemistry of MPcs has been an area of intense research [36]. From rather primitive beginnings, the electrochemistry of the macrocycles was not investigated sooner (unlike porphyrins) due to their poor solubility and hence relative purity. Phthalocyanines have the capacity to gain or lose electrons and it is these interesting electronic properties that make them useful in many areas including solar cells and electricity production. The Pc skeleton exists as a dianion, Pc (-2), successive removal of up to two electrons from the HOMO (a1u) results in the formation of Pc (-1) and Pc (0) -cation radicals, respectively [37].

The Pc ring redox activity is directly related to the frontier orbitals in the molecule where oxidation is the removal of electron(s) from the HOMO (a1u) while reduction is the addition of electron(s) to the LUMO (e.g.).

The electrochemical activity of unmetallated Pcs is related to processes occurring on the ring; on the other hand, the MPcs containing electro active central metals exhibit electro activity associated with the central metals, in addition to ring processes. Examples of electro active metals include cobalt, iron and manganese while electrochemically inactive metals include zinc, nickel and magnesium. Furthermore, electro active ligands substituted on the Pc also demonstrate their own characteristic redox peaks or couples [38]. Metallophthalocyanines (MPcs) containing electro active central metals show electro activity associated with the central metals, in addition to ring processes [39]. Peaks or couples linked to oxidation or reduction of the central metal usually lay between those for ring oxidation or reduction processes [40]. The MPc electrochemistry is characterized by multiple and often reversible redox processes that are localized on the metal center or the Pc ring [41-47], both in solution or when adsorbed on electrode surfaces. MPcs can be reduced or oxidized, but still retain their molecular structure and stability [46]. The Pc^{2-} ring can be oxidized ($Pc^{2-} \rightarrow Pc^{1-} \rightarrow Pc^{0}$) or can be successively reduced ($Pc^{2-} \rightarrow Pc^{3-} \rightarrow Pc^{4-} \rightarrow Pc^{5-} \rightarrow Pc^{6-}$). The electro active transition-metal Pcs (Cr, Mn, Co and Fe) whose orbitals lie between HOMO and LUMO of the Pc ligand [48-50] have their metal oxidations or reductions occurring in between those corresponding to ligand reduction or oxidation [51-52], in the presence of coordinating species that would stabilize the metal center [52-54]. For MPcs containing non-redox metals such as Ni, Cu, Zn, Pd, the redox processes take place on the Pc ring. Their redox chemistry will be similar to those of MPcs containing a non-electro active metal [55]. Changes in the nature of the peripheral substituents affects the electron density and consequently the redox chemistry of the Pc macrocycles [56, 57, and 58]. Electron-donating substituents (e.g. amine, ether, thioether, methoxy) shift redox processes towards negative potentials while the presence of an electron withdrawing group (e.g. fluoro, sulphonate, nitro, ester, carboxylic acid) shift redox processes towards positive potentials [59]. Since the electron transfer abilities of Pcs depend on the kind and the number of the substituents and also on the interaction between the Pc ring and the metal center [53, 60-63], Pc redox chemistry can be easily tuned.

Thus up to four electrons can be successively added to the doubly degenerate e.g. orbitals of the LUMO to form Pc^{-3}, Pc^{-4}, Pc^{-5} and Pc^{-6}, and two electrons can be removed from the HOMO to form Pc^{-1} and Pc^{0} [64].

MPc electrochemistry in the solution phase is typified by multiple and often reversible redox processes localized on the metal centre and the Pc ring.

Fig. 1.5 shows the energy level diagrams of neutral, one-electron ring reduced, and one-electron ring oxidized MPc complexes. A small black arrow represents electrons in Fig. 1.5

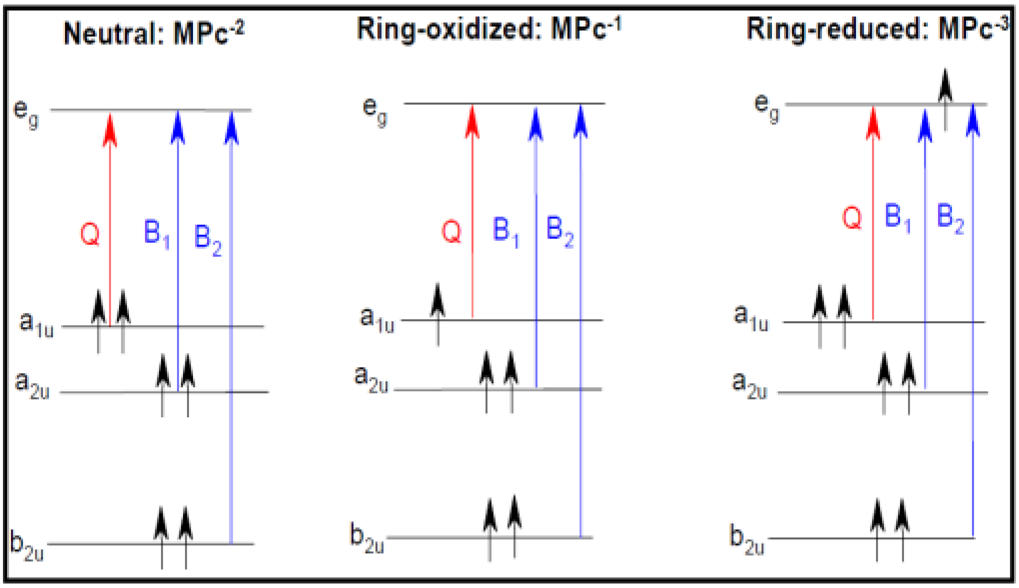

Figure 1.5. Energy level diagrams of neutral, one-electron ring reduced, and one-electron ring oxidized MPc complexes.

This redox activity is typical of H_2Pcs and phthalocyanines with redox inactive metals, i.e. complexes with closed-shell central ions such as Mg^{2+} and Zn^{2+}. In light of this, the metal orbitals (b2g, e.g., a1g and b1g) of redox inactive metals are buried inside filled Pc orbitals while those of redox active metals lie between the HOMO and LUMO of the Pc ligand. [65,66] Thus the nature and oxidation state of the central metal, the nature of axial ligands and solvents as well as the nature of substituents on the ring periphery determine the redox properties of a given complex [67]. Significant alteration of phthalocyanine electrochemical properties occurs with substituents at the non-peripheral positions.

Electron-donating substituents, e.g. alkoxy or alkylthio groups, increase the electron density of the central metal atom, thereby making it easier to oxidize and harder to reduce MPc complexes [68]. In contrast, electron withdrawing substituents, e.g. CN groups, decrease the electron density thereby lowering the LUMO energy levels of the conjugated system.

As a result, the electron affinity of the macrocycle is increased and hence MPcs are easier to reduce. In general, central metal ion redox energies are a function of their polarizing power, expressed as charge/radius (*ze*/*r*).

Thus in most redox reactions, there is an apparent well-defined pattern, i.e. oxidation of MPcs with more positive central metal ions is difficult [69]. MPc electrochemical reactions are often performed at platinum or a carbon [70] working electrode, the latter being popular as it is cheaper and is a suitable alternative to platinum. Examples of carbon electrode materials – depending on percentages of crystalline graphite - include glassy carbon, pyrolytic graphite, carbon paste, carbon fiber and many more. The most common reference electrode whose potential does not change with time is silver-silver chloride (Ag|AgCl). Other reference electrodes employed include normal hydrogen electrode (NHE) and saturated calomel electrode (SCE). Platinum wire is usually used as the counter electrode as it is inert and therefore is resistant to corrosion. As in all electrochemical reactions, inert electrolytes which carry the task of ion transportation between electrodes are required. Tetraalkylammonium salts are employed in organic media, e.g. tetraethylammonium perchlorate (TEAP), tetrabutylammonium perchlorate (TBAP) and tetrabutylammonium tetrafluoroborate (TBABF4). Sodium hydroxide and potassium chloride or nitrate are utilized in aqueous media whereas buffer salts are employed for pH controlled experiments. In addition, solvents influence Pc electrochemical properties due to protic or aprotic and electrophilic or nucleophilic properties. For example oxidation is easier in DMF than in pyridine for a divalent FePc [66] due to stabilization in the latter solvent.

1.2.4. Spectroelectrochemistry of Phthalocyanines

Electro active ligands substituted on the Pc also exhibit their own characteristic redox peaks or couples. Potentials at which redox couples are observed depend on the nature of the molecule and solvent.

Redox processes of MPc complexes are assigned successfully using spectroelectrochemistry. This technique involves recording UV/Vis spectra as potential is applied. It therefore requires unique electrodes such as indium tin oxide (ITO), which are optically transparent, conductive, mechanically strong, and resistant to corrosion and exhibit low background currents. Central metal or phthalocyanine ring oxidation and reduction can be afforded by other non-electrochemical methods. Oxidation is afforded by use of oxidizing agents such as bromine, and photo chemically by irradiation with light of suitable wavelength in the presence of an appropriate electron acceptor.

On the other hand, reduction is achieved by use of reducing agents such as sodium borohydride and by photochemical irradiation in the presence of an appropriate electron donor. Ring oxidation to cation radical is accompanied by loss of intensity of the Q band , formation of new bands near 500 nm (charge transfer), 830 nm (Pc-1 monomer), 720 nm and 1040 nm due to (Pc^{-1}) dimer and solution color change to purple . Ring reduction involves addition of electrons to the e.g. LUMO energy level resulting in the collapse of the Q-band and formation of two bands in the 500 - 600 nm regions. Additional bands are observed near 780 and 860 nm. Ring reduction is accompanied by color change to bluish purple, purple, blue and blue-green for Pc^{-3} anion, Pc^{-4} dianion, Pc^{-5} trianion and Pc^{-6} tetra anions respectively.

Furthermore, oxidation or reduction processes occurring at the central metal of MPcs are characterized by a shift of the Q band without a drastic decrease of peak intensity. Intensities of B and Q bands are not affected since they are due to π-π* transitions. However, charge transfer bands near 500 nm due to metal to ligand (MLCT) or ligand to metal (LMCT) transitions may be lost or formed.

Classical (e.g. infra-red (IR) spectroscopy) and recent (e.g. matrix-assisted laser desorption ionization (MALDI)) methods have been used for characterization of Pcs. The Q and B bands are those occurring most frequently in all Pcs. Fig. I.6 shows a typical MPc UV-visible spectrum with the described absorption bands. The most common method is by UV-visible spectroscopy. A UV/Visible absorption spectrum of MPcs, Fig. 1.6, is characterized by a Q band in the red area of the visible region, which has been explained, using the Gouterman's model [71, 72].

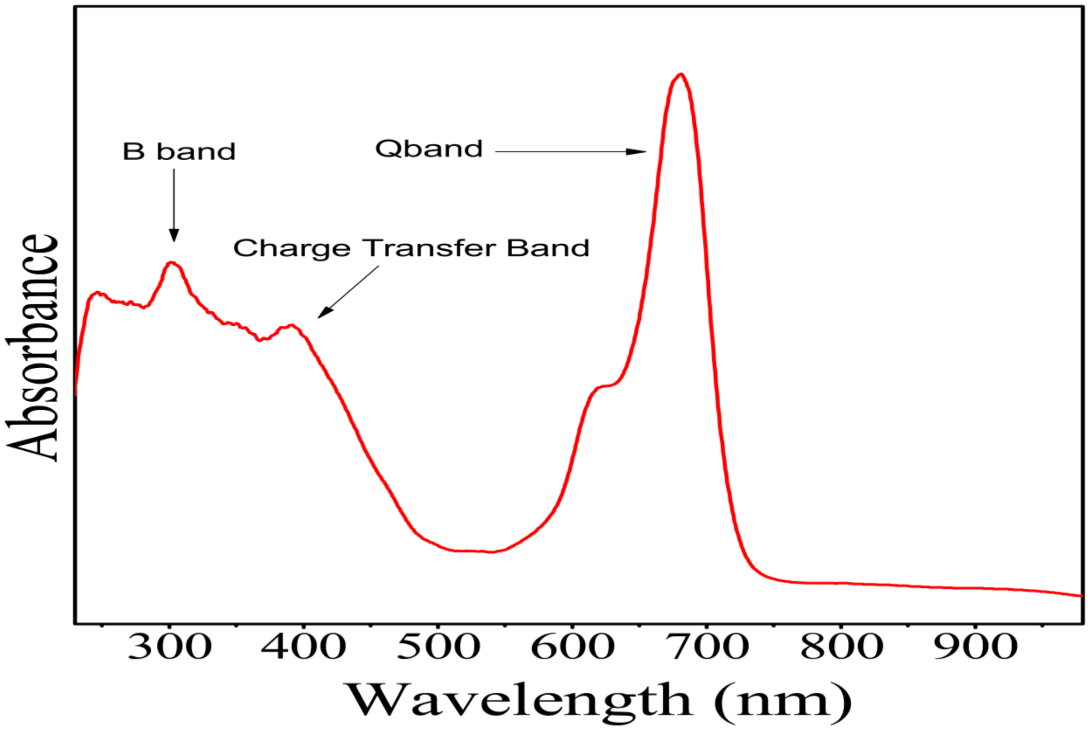

Figure 1.6. MPc classic electronic absorption spectra showing the common absorption bands.

The Q band is a transition from the highest occupied molecular orbital (HOMO), a1u, to the lowest unoccupied molecular orbital, e.g. There is also the B band which is observed at the blue end of the spectrum, and consists of an overlap of B1 and B2 bands, Fig. 1.7. B1 is due to a transition from the a2u to the e.g. and B2 is due to a transition from the lower lying b2u to the e.g. orbital. The B1 and B2 bands are usually observed as a single broad band around the 340 nm region [73]. There are also the N, L and C band that are associated with MPcs. These are observed at wavelengths that are shorter than 300 nm and are due to transitions from the deeper HOMO orbitals. They are observed when UV transparent solvents are used.

The position of the Q band is influenced by the point of substitution, which is whether the substituents are on the a or b positions. It has been observed that substitution at the position results in greater shifts of the Q band to the infrared region [74, 75]. This can be attributed to a greater destabilization of the HOMO when the substituent is at the position in comparism with the b position.

The position of the Q band is also influenced by the nature of the substituent with electron donating groups such as alkylthio and alkoxy groups leading to a more red shifted Q band [76,77].

This is due to the destabilization of the HOMO in a way that the distance between the HOMO and LUMO is shortened and hence lower energies are experienced [78]. Even though the sulphur and the oxygen atoms are both electron donating, it has been found that the alkylthio substituted phthalocyanines lead to a redder shifted spectrum when it is compared [79]. This has been attributed to the fact that the 3p orbital of the sulphur group interacts more with the π bond cloud compared to the alkoxy group [80]. Electron withdrawing groups, tend to shift the Q band to the blue region [81]. The nature of the substituent together with the number of substituents affects the position of the Q band with an increase in the number from tetra to octa alkylthio substituents resulting in a shift to the near infrared region, this shift is clearly observed for MPcs that are substituted at the a position.

The nature of the central metal has been observed to influence the position of the Q band, with a bath chromic shift being observed with an increase in the size of the central metal [82]. The oxidation state of the central metal also influences the Q band position, with a bath chromic shift being observed with increase in the oxidation state of the metal [83]. Normally an unmetallated MPc has a Q band that is split; this is due to the fact that the e.g. orbital of the LUMO is non-degenerate. It has been found that as the position of the Q band of the unmetallated MPc moves more to the infrared region; it becomes observed as single band. This is due to the fact that there is generation of degeneracy as the Q band shifts to the red region [84].

There can be metal to ligand charge transfer (MLCT) or a ligand to metal charge transfer (LMCT) bands [85], Fig. 1.7. These weak bands are normally observed in the visible region between the Q band and B band or after the Q band in the near infra red or infra red region. Charge transfer bands are observed for phthalocyanines with electro active metal centers.

This has been accounted by the fact that the d-orbitals of the electro active metal [86] are found within the HOMO and LUMO of the phthalocyanine. The observed CT bands are due to the movement of electrons between the d-orbitals of the metal centre and the HOMO/LUMO state of the phthalocyanine.

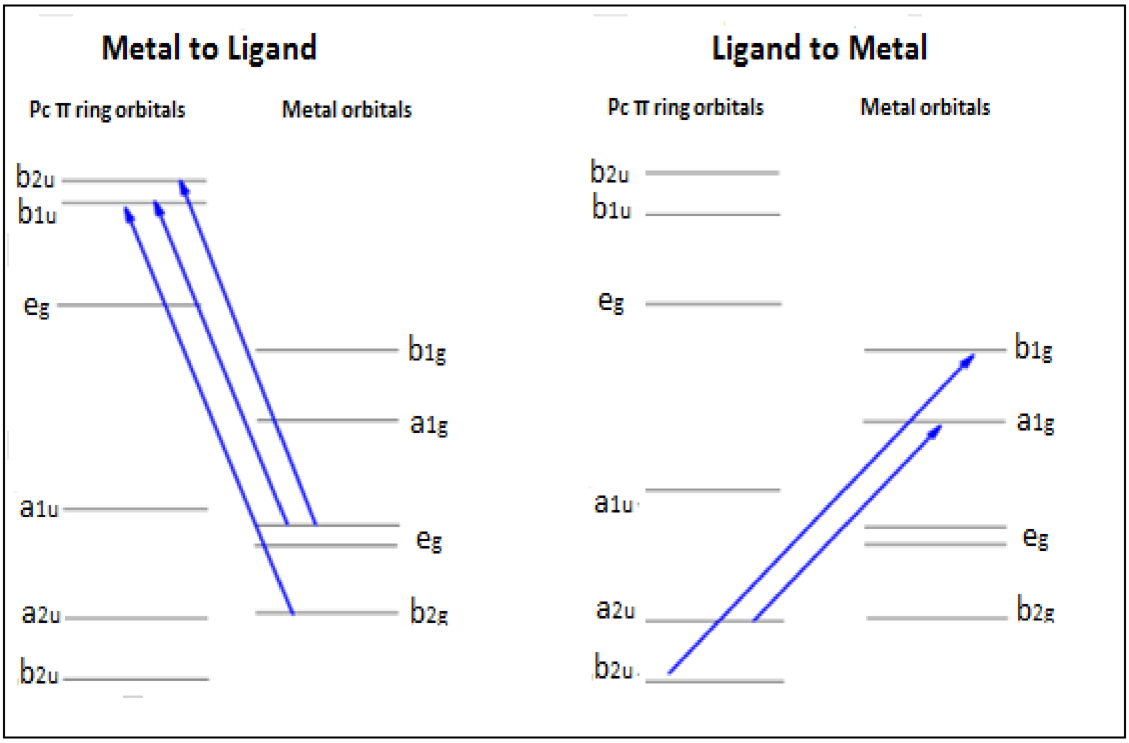

Figure 1.7 Probable directions for charge transfer transitions between central metal and ligand.

The Q band originates from the π-π* electronic transitions from the highest occupied molecular orbital (HOMO) to the lowest unoccupied molecular orbital (LUMO) of the Pc^{2-} ring whilst the B bands occur as a result of deeper π levels to LUMO transitions, Fig. 1.8.

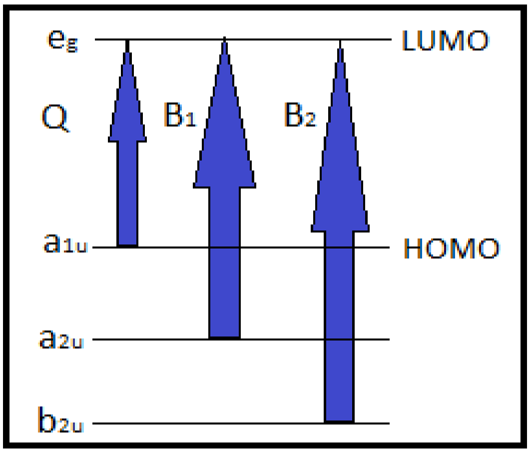

Figure 1.8. Pc electronic transitions showing origin of the Q and B absorption bands.

From Fig. 1.8, the Q, B1, and B2 bands are shown as due to: a1u to e.g.; a2u to e.g.; b2u to e.g. electronic transitions respectively.

The spectral position and intensity of the Q band are important in tailoring new Pc types for particular applications. The positions of the Pc spectral absorption bands, especially the Q band, are affected by factors such as central metal, symmetry, substituents, aggregation, and solvents [87, 88].

Pcs are mostly blue/green in color [89, 90] because the intense Q band usually lies at the red end of the visible spectrum. In MnPcs the Q band is shifted out of the visible region into the near infrared region so that the color of the complex is now determined by the absorption at the blue end of the spectrum and MnPcs consequently appear red or brown. Absorption can be moved into the near-infrared region by appropriate substitution of the Pc ring and by varying the central metal atom. The effect of the central Pc metal atom on the absorption maximum is especially significant for the Q band spectral position (λmax), spanning from the most hypsochromic metal, iron, to the most bath chromic metal, manganese [91,92]. The effects of non-peripheral substitution of a Pc on its Q band position are larger than observed for peripheral substitution [88]. Peripherally substituted derivatives also have a stronger tendency to aggregate [93, 94] and show a broader Q band than non-peripherally substituted complexes [95]. Furthermore, the consequence of incorporating sulfur donors, as was done in this work, is to shift the Q-band to the longer (near-infrared) wavelengths [96] essential for high-technology applications, such as PDT and near-infrared detection. This work studies the electronic transition properties of the synthesized substituted phthalocyanines for characterization and spectroelectrochemistry purposes.

1.3. General Synthetic Methods of Phthalocyanines

Synthesis of phthalocyanines can be achieved using different paths depending on the type of phthalocyanines to be synthesized; metal free, symmetrical and asymmetrical metallophthalocyanines. Historically, the eldest method for phthalocyanine synthesis is the reaction of 2- cyanobenzamide in the presence of metal or metal salt in a bulk reaction or in a solution.

However, this method is limited to very few cases and has not received much attention in daily lab practice. The complexation of metal-free phthalocyanine is usually a clean and efficient reaction. Various precursors such as phthalonitrile, phthalic acid, phthalic acid anhydride, phthalimide, diiminoisoindoline and o-cyanobenzamide have been developed for these syntheses. This synthesis of phthalocyanine involved the reaction of o-cyanobenzamide in refluxing ethanol from which was recovered in low yield. Linstead and co workers reported that the yield could be improved if magnesium, antimony or magnesium salts such as its oxide and carbonate are mixed with o-cyanobenzamide and heated over 230 ^{o}C followed by demetallating the resultant metallophthalocyanine with cold concentrated H_2SO_4 . Use of substituted analogues of o-cyanobenzamide in order to synthesize substituted Pcs has been rare.

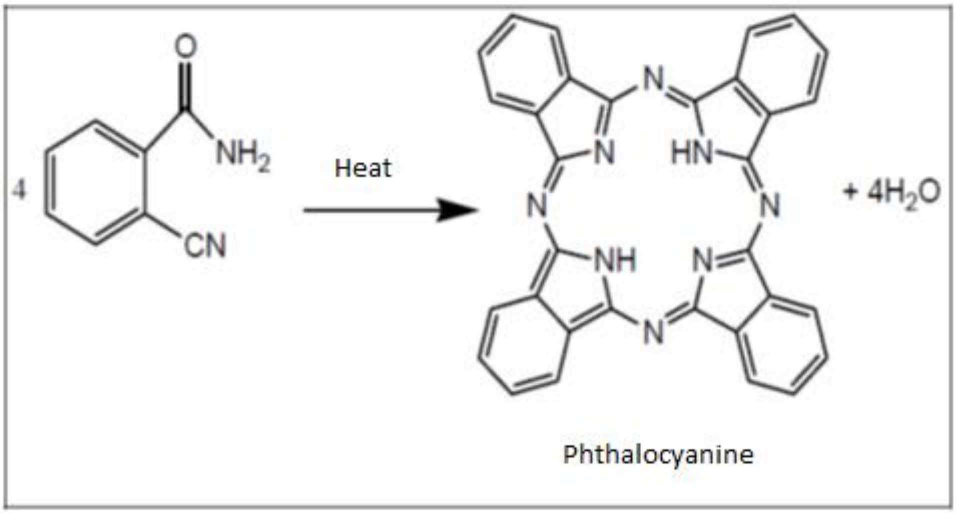

Figure 1.9. The accidental discovery of phthalocyanine from o-cyanobenzamide.

A Pc is formed from the cyclotetramersation of its precursor units so the synthetic strategy starts from the molecules which make up these units. MPcs can form from precursors through a metal templated cyclotetramerization reaction. Typical precursors are phthalic acid (1), phthalonitrile (2), phthalic anhydride (3), phthalimide (4), diiminoisoindoline (5), and o-cyanobenzamide (6), Figure 1.10.

The variety of starting materials for Pc synthesis and the diversified methods for their preparation, Figure1.10, allow Pcs to fulfill their promise. The most useful of the un-substituted MPc precursors is phthalonitrile (2). This compound readily gives MPc complexes in good yields with most metals except silver and mercury.

Reactions often involve simply heating the phthalonitrile in the presence of a metal-ion source and base as either a melt of reagents or in a suitable high boiling point solvent. Phthalonitrile (2) as a precursor leads to products of high purity but, because phthalonitriles are generally more expensive, their use tends to be restricted to high-technological applications (e.g. electrophotography) and small scale syntheses (e.g. laboratory synthesis) where quality, and not cost, is the main consideration.

Un-substituted MPcs commonly exhibit poor solubility in most organic solvents and water due to the molecular interactions between their π-systems. These interactions lead to the Pcs stacking upon themselves to form a strong and hydrophobic crystal lattice. This insolubility significantly limits the usefulness of un-substituted Pcs.

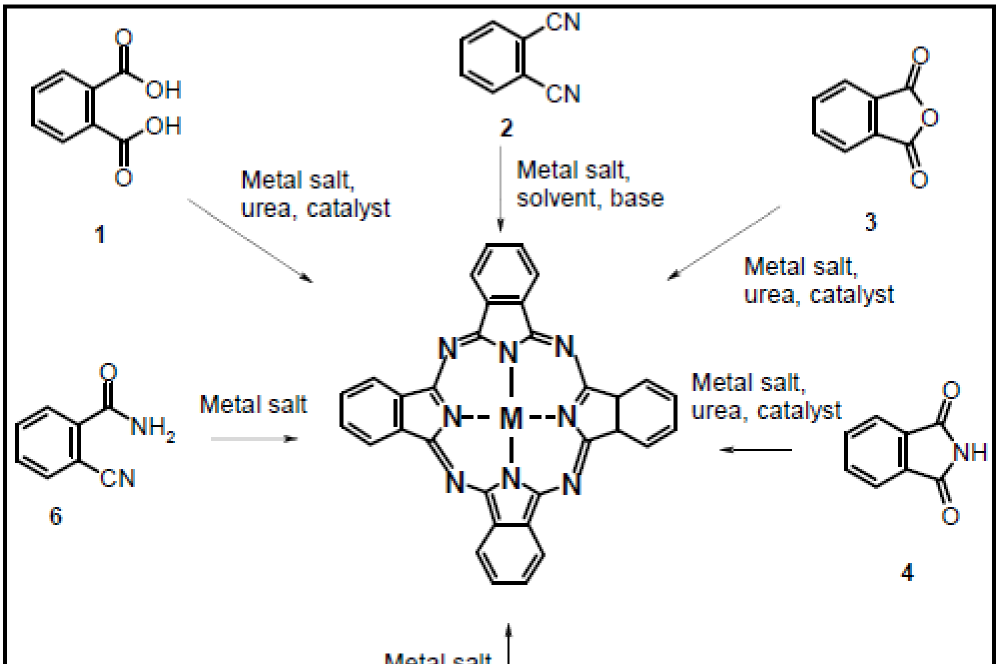

Figure 1.10 Synthesis of metallophthalocyanines (MPcs) from typical starting materials.

Taking into consideration all these facts, today it is possible to prepare bespoken phthalocyanine derivatives with highly tailored properties (*e.g.* Q-band position, solubility, light absorption, self-assembling, *etc.*).

There are two excellent reviews on phthalocyanines preparation; one by Leznoff et al. [97] and the other, actually the most up-to-date, by Neil B. McKeown [98]. Pc and related compounds synthesis has been rapidly developing field with yearly appearing new achievements and publications.

1.3 Application Fields of Phthalocyanines

Pcs have found commercial applications in photocopying, laser printing, information storage, odor removal, oil sweetening, computer disk writing and infrared security devices, display devices (electrochromism and electroluminescence), organic catalysis, electrocatalysis, photo catalysis, photovoltaic devices, lithium batteries, gas sensors and fuel cells [99,100].

For example, MPcs are valued for their color and therefore are important in visible applications such as electrophotography [101,102], ink-jet printing [103,104] and xerography [105]. In electrophotography, light and electricity are used to produce an image, a process familiar in photocopying and laser printing. A type IV polymorph of ox titanium (OTiPc) has been found [106] to be the best material to generate the latent image in laser printers through its excellent compatibility with the semiconductor infrared lasers. In color photocopiers, the cyan toner used to produce images is based on CuPc pigment, namely CI Pigment Blue 15. Ink-jet printing produces images by using electromagnetic fields that guide electrically charged ink streams onto a page. Copper phthalocyanines [107] are cyan dyes of choice as they possess all-round properties, namely, high chroma, high strength and high light-fastness. Xerography involves a photocopying process which forms a negative image by a resinous powder on an electrically charged plate, such that the image is transferred to and thermally fixed as positive on paper. Use of Pcs, e.g. OTiPc, NiPc, CuPc [108], as active components is favored because they are less toxic and many absorb in the infrared (IR) region such that use of infrared lasers is possible.

Pcs have also attracted much attention in oncology as photosensitisers for malignant tumor treatment by photodynamic therapy (PDT). In PDT, O_2, light and a photosensitizing drug, e.g. phthalocyanines, are used in combination.

Briefly, PDT involves the selective uptake and retention of a photo sensitizer in a tumor, followed by irradiation with light of a particular wavelength. Tumor necrosis is then initiated, through the formation of singlet oxygen, the cytotoxic species. Biochemical molecules [109] can suffer significant damage that may lead to death through singlet oxygen ingestion.

In vitro/vivo studies utilizing diode laser and using axially substituted silicon NiPchthalocyanine (formed through annulations of further benzene units on MPc) have been found to be effective in cell destruction [110]. Phthalocyanine research activity in the PDT field has expanded tremendously during the past 20 years [111-114]. For instance, commercially available Photo senses, composed of differently sulphonated aluminum phthalocyanines has been successfully used for both diagnosis and clinical PDT of various cancers including small lung tumors.

Since Pcs strongly absorb light in the red region, introduction of electron donating substituents can shift their main absorption band to the near-IR region. Infrared-absorbing Pcs such as sulphur-substituted Pcs find use in energy conversion and optical applications for laser thermal transfer, solar screens, optical data storage (ODS) as in CD-RW and security, e.g. brand protection. Pcs absorbing at around 780 nm to match the 780 and 830 nm semiconductor lasers are used for ODS whilst for security applications; Pcs are used in lasers to cover the 700-1000 nm range. Near-IR Pcs have also been investigated for their non-linear optical (NLO) applications needed for eye protection against pulsed lasers, photonics and photo electronics. Lead [115] and indium [116] Pcs have shown to be very good materials for optical limiting as their heavy atom effect reveal enhanced optical limiting behaviours. MPcs are well known as catalysts for both homogeneous and heterogeneous reactions, which in most cases involve the transfer of electrons. Both the catalyst and analyte are in solution for homogeneous catalysis whereas for homogeneous catalysis, the catalyst is in solid form. For both homogeneous and heterogeneous systems, reactions are possible through usage of oxidants such as hydrogen peroxide (H_2O_2) or may be light-driven and thus promote reactions photo catalytically.

In homogeneous reactions, MPcs exhibit enzyme-like catalytic activities since they are similar in structure to protohemes found in home-enzymes that are important for many biological reactions [117].

The degree of importance is extended to heterogeneous systems in which MPcs catalyze a number of environmentically toxic pollutants such as chlorophenols by being immobilized or supported onto resins [118] or polymer matrixes [119]. Oxidative decompositions of pollutants such as chlorophenols have been observed with iron, manganese and cobalt Pcs [120]. Furthermore, MPcs may be insoluble in water-based reactions and thus can be deposited onto electrodes in order to electrochemically catalyze reactions [121]. Here, the surface of the electrode is modified in some way such that reactions are accelerated at the electrode and over potentials significantly reduced. Modification includes adsorption on the electrode surface thus forming an electro active film of a chemically modified electrode (CME). Also mixing MPcs with micro particles such that they become part of the electrode constituents, results in the formation of a composite paste electrode, e.g. carbon paste electrode.

Oxygen electro reduction to hydrogen peroxide or water [122-124], electro oxidation of mercaptans, [125-127] hydrazine [128-130] and nitrite [131-132], are some of the reactions catalyzed by MPcs at the electrode surface.

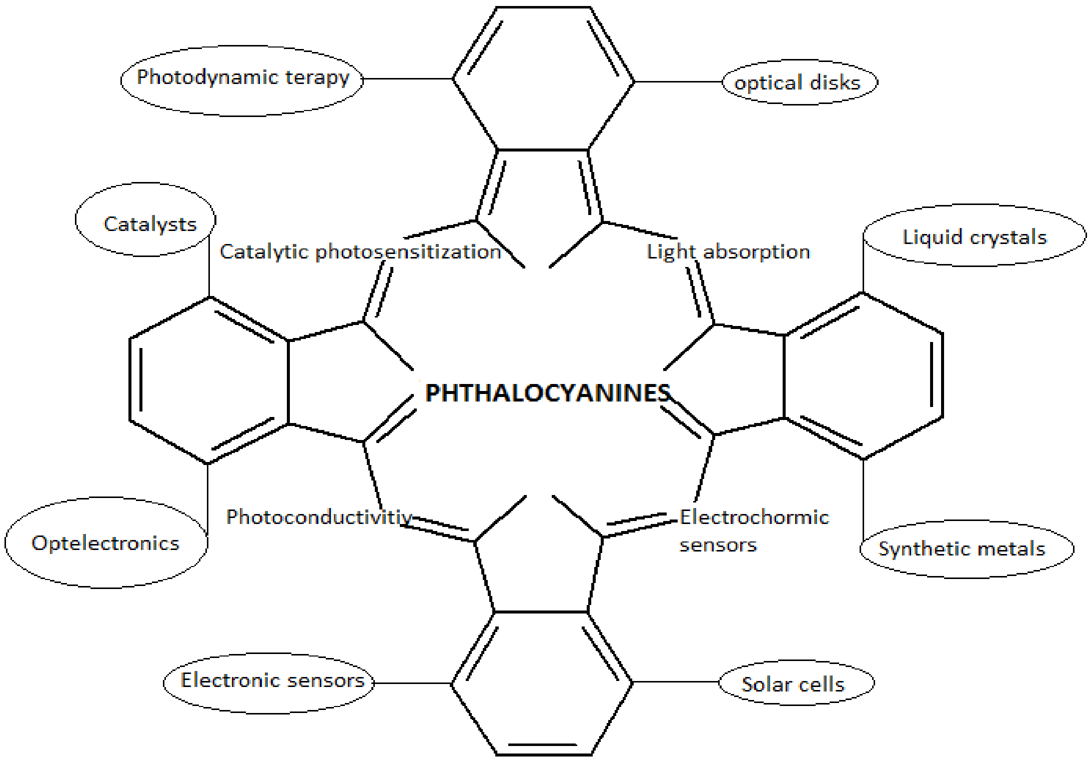

Figure 1.11. Typical function of phthalocyanine derivatives.

As stated above, metallophthalocyanines (MPcs) are unique in terms of physical and chemical properties, which have resulted to a wide range of applications. Over the years phthalocyanine complexes have attracted many applications in areas such as catalysis sensors and photodynamic therapy (PDT).New applications of MPcs are emerging, these include ink jet printing, electrophotography, photocopying and laser printing, electrochromic display devices, optical computer re-writable discs and information storage systems, liquid crystal display devices, photovoltaic cells, fuel cells, molecular electronics, semi-conductor devices and electrochemical sensors [133].

1.4.1. Pigments and Dyes

The phthalocyanines are widely used in textile, paint, printing ink and plastic industries. The no colorant applications include catalysts, lubricating greases, analytical reagents, clinical diagnostic agents and electrical devices.

Although the shade range of the phthalocyanines is rather limited and covers only the blue green regions of the spectrum, their excellent fastness to light, and high absorptivity render them apt for many applications. The insolubility of phthalocyanines necessitates preparation of soluble derivatives for application as dyes for textile fibers. Phthalocyanine pigments in the fon of aqueous dispersions is used in pad-dyeing with resin emulsions. Because of their excellent stability to acids, alkalis and solvents phthalocyanines are particularly useful in spin dying. They have also been used in coloring polyvinylchloride fibers, viscose, cuprommonium cellulose, nylon, 'perIon L', etc. Both phthalocyanine blue (copper phthalocyanine) and phthalocyanine green (copper polychloro phthalocyanine) have found wide use as paint pigments. Metal surfaces can be coated by forming the metal phthalocyanine directly on them. 804 Large metal surfaces can be coated with metal phthalocyanine by dipping in a solution of phthalonitrile in acetone, drying, and subjecting the metal to temperatures of around 3500°C in a sealed oven.

The coating is very adherent and the shade of color depends on the metal used. Phthalocyanines have been used to color rubber, poly styrene, poly urethane foams, cellulose acetate sheeting, polyesters, polyamides, vinyl chloride polymers and other plastic and polymeric materials.

IS-BB Copper phthalocyanine-sodium sulfonate have been used in photographic processes to produce colored prints. Copper phthalocyanine is also used as a certified food color**.** [134]

1.4.2. Catalyst

The first mention of phthalocyanines as catalyst is on the activation of molecular hydrogen [135] and found that crystals of phthalocyanine and copper phthalocyanine catalyze atomic interchange between molecular hydrogen and water vapour, and oxygen.[136] Phthalocyanines catalyze the oxidation of many organic compounds.[137] Cobalt, nickel and iron phthalocyanines catalyze the oxidation of a-pinene to verbenone. Nickel phthalocyanine catalyses the auto oxidation of saturated ketones such as 2-octanone, 4-heptanone and cyclo hexanone at 120-130°C to adiketones and aldehyte. The aerobic oxidation of unsaturated fatty acids catalyzed by iron and cobalt phthalocyanine has been reported. [138]

Iron, cobalt, tin and copper phthalocyanines and their derivatives have been used as rubber emulsification catalysts. When cobalt tetrasulphophthalocyanine is attached to poly (vinyl amine) it can catalyze the auto oxidation of thiols. [139]

1.4.3. Electrocatalyst

Keto acids, e.g., pyruvic, phenylpyruvic, a-ketobutyric, a-ketoglutaric and a-keto isocaproic undergo electrocatalyzed reduction at carbon past electrode modified with cobalt phthalocyanine.[140] CoPc modified electrodes can catalyze numerous electron transfer processes in addition to those of hydrazine and thiol compounds.[141] Metal phthalocyanines have received much attention in the electrocatalytic reduction of dioxygen.[142] The phthalocyanines assume importance in electrocatalysis for two reasons:

1) Metal phthalocyanines are structural and electronic analogues of porphyrins whose electrochemistry is important in understanding electron transfer processes in biological systems.

2) Electrocatalytic reduction of dioxygen is important in fuel cells. Of the metal complexes of phthalocyanine, iron and cobalt have been examined in detail.

Because of the lower solubility of phthalocyanines, water soluble phthalocyanines such as tetrasulphophthalocyanine [143] and tetracarboxy phthalocyanine [144] have been used as facile catalysts in aqueous medium. The electrocatalytic activity of dioxygen reduction was improved at a glassy carbon electrode when modified with polypyrrole/tetrasulfonatophthalocyaniato cobalt electrode. [145] The glassy carbon/polypyrrole/cobalt tetrasulfophthalocyanine (GC/PPY /CoTSP) electrode was formed by electro polymerization of pyrrole on a glassy carbon electrode in methanol solution containing CoTSP. Oxygen reduction reaction at the GC/PPY/CoTSP electrode in O.5M ~SO 4 showed about O.5V more anodic onset 'potential than the value obtained with a GC electrode in the same medium.

The reduction of dioxygen at iron tetrasulfonatophthalocyanine (FeTSP) incorporated into polypyrrole was also studied.[146] It was found that thicker films are stable and mediate four-electron reduction of dioxygen. It was indicated that dimeric FeTSP species are responsible for the marked shift in the reduction onset potential.

Polymeric iron phthalocyanine precipitated on activated carbon, when heated to 200-5000 °C showed a higher rate of deactivation for the electrochemical reduction of dioxygen. [147]

The iron, cobalt, copper phthalocyanine function as a catalyst layer and oxygen sensor in fuel cells and air batteries.[148] A porous electrocatalyst material was prepared by soaking activated carbon in iron phthalocyanine pyridine solution and in perfluorodecalin - CCI solution and then mixing with P_1Fe. The material in the form of sheet was bonded on a nickel mesh. The electrode was used in a zinc-air battery having a discharge current density of 63 mAlcm^2.

1.4.4. Electrochromic Displays

Electrochromic (Electrochemichromic EC) effect is the production, by faradaic reaction, of a color change in materials localized at an electrode surface. A thin film of lanthanide diphthalocyanine deposited on optically transparent electrode shows change in absorption spectrum of polarization in contact with an aqueous electrolyte. [149,150]

Rare earth phthalocyanine can be sublimed onto conducting glass and can therefore be used as materials for EC displays. These electrochemichromic materials are also useful for full-color imaging and graphic and alphanumeric displays.[151] The rapid decay of EC characteristics of rare earth diphthalocyanine film electrodes on potential cycling in neutral aqueous solution has been considerably retarded by using ethylene glycol as solvent.[152]

1.4.5. Gas Sensors

Devices based on metal phthalocyanine such as PbPc show useful response towards NO_2. A thin film PbPc sensor has successfully been used to monitor NO" produced by shone firing in coal mines. [153] Pc based devices offer much promise as resistance modulating sensors for toxic gases. They are thus complementary to metal oxide devices which are most useful in the detection of flammable gases. The lanthanide diphthalocyanine complexes have been used as gas detectors for acidic and basic gases.

2. MATERIAL AND METHOD

This section sets out to represent the electrochemical methods used to study phthalocyanines presented in this work.

2.1. Mass Transport

Electrochemistry may be broadly defined as the study of the chemical response of a system to an electrical stimulation. Electrochemistry may more specifically be defined as the study of chemical reactions to produce electric power or, on the other hand, the use of electricity to affect chemical processes or systems. [154]

The three mechanisms of mass transport are migration, convection and diffusion. In most electrochemical techniques, conditions are chosen so that transport of the electro active species is affected by a single mechanism, typically diffusion. A description of each mechanism is given below:

• ***Migration*** is the movement of ions under the influence of an electric field. Migrational effects are removed by adding a large excess of an easily ionisable salt (the supporting electrolyte) e.g. KCl which dissociates to produce inert ions. These ions become the migration current carriers and also increase the conductivity of the solution;

• ***Convection*** is mass transport resulting from movements of the solution as a whole. In short experiments (as in this work), convection is not a factor in mass transport provided the solution is quiescent and the electrodes are stationary;

• ***Diffusion*** is mass transport driven by a gradient of chemical potential. Anytime that the concentration of a molecule or ions (charge is not considered here) is uneven throughout a solution, mass transport will occur to restore the homogeneity of the solution.

2.2. The Electrochemical Cell

The normal material for cell construction is Pyrex glass for reasons of both visibility and general chemical inertness. The size of the cell is variable and depends upon the volume of the sample being studied.

Some electrochemical measurements can be run in cells under an atmosphere of air. Oxygen however is electrochemically active and its solubility in water is sufficiently high that oxygen reduction interference can be a problem. As a consequence, most measurements are carried out under an inert atmosphere of either nitrogen or argon. A three-electrode electrochemical cell (Figure 2.1) is often used in electrochemical experiments. The electrochemical reaction takes place at the working (or indicator) electrode (labeled W.E. in Figure 2.1). This is the electrode at which the electrochemical phenomena being investigated takes place. [155] The working electrode should provide high signal-to-noise characteristics, including a reproducible response. [155] Hence working electrode selection depends on essentially two factors: the redox behavior of the target analyte and the background current over the potential region required for the measurement. The reference electrode is labeled R. E. in Figure 2.1. This is the electrode whose potential is constant enough that it can be taken as the reference standard against which the potentials of the other electrodes present in the cell can be measured. [155] Reference electrodes with large surface areas are often employed in order to maintain low current densities and hence minimize polarization. The complete elimination of reference electrode polarization is only possible with modern potentiostatic instrumentation based on operational amplifiers. The potentiostat maintains a potential difference, ΔE, between the R. E. and W. E., and supplies the current (i) needed for affecting the changes occurring at the W. E.[156-158] An ideal R. E. is one whose potential does not shift from equilibrium (non-polarisable).

The other electrode, which is called the counter electrode, serves to complete the electric circuit and provides a reference potential against which the working electrode's potential is measured. Ideally the counter electrode's potential remains constant so that any change in the overall cell potential is attributed to the working electrode.

In a dynamic method, where the passage of current changes the concentration of species in the electrochemical cell, the potential of the counter electrode may change over time. This problem is eliminated by replacing the counter electrode with two electrodes: a reference electrode, through which no current flows and whose potential remains constant; and an auxiliary electrode that completes the electric circuit and through which current is allowed to flow [159].

The choice of an electrode material depends greatly on the useful potential range of the electrode in the particular solvent used and the qualities and purity of the material. One or more of the following limits the usable potential range: [160]

• Solvent decomposition;

• Decomposition of the supporting electrolyte;

• Electrode dissolution or formation of a layer of an insulating/semiconducting substance on its surface;

• Poisoning through contact with solutions containing contaminants.

There are several reference electrodes used in electro analytical experiments, silver-silver chloride (Ag-AgCl) being the most common. This consists of a piece of silver wire anodized with silver chloride in a glass tube. The wire is in contact with concentrated KCl or NaCl solution.[161] A semi-permeable salt bridge protects the electrode from the bulk solution. Many materials have been used as working electrodes. Mercury, carbon and “inert” (or noble) metals such as gold and platinum have been found to be essential working electrode materials. The geometry of these electrodes must also be considered. An inert conducting material, such as platinum wire or graphite rod, is usually used as the current carrying auxiliary electrode.

Supporting electrolytes are usually used in conjunction with solvents for electrochemical experiments. The choice of the solvent is based upon the solubility of the analyte including its redox activity and the solvent properties (e.g. electrical conductivity, electrochemical activity and chemical reactivity). The solvent should not react with the analyte (or products) and should not undergo electrochemical reactions over a large potential range. [162]

Solvent types include water, acetonitrile, dichloromethane, dimethylformamide (DMF), dimethylsulfoxide (DMSO) or methanol. Certain applications may require mixed solvents. Supporting electrolytes are necessary in order to: decrease the resistance of the solution; eliminate electro migration effects; maintain constant ionic strength (by eliminating the effects of erratic amounts of naturally occurring electrolyte). The inert supporting electrolyte may be an inorganic salt, a mineral acid or a buffer. While potassium chloride or nitrate and sodium hydroxide are usually used when employing water as a solvent, tetraalkylammonium salts are often utilized in organic media. Buffer systems (e.g. acetate) are used when pH control is essential.

The supporting electrolyte should be prepared from highly purified reagents and must not be easily oxidized or reduced. A large excess of the electrolyte concentration is used (e.g. 0.1 – 1.0 M).[160]. Supporting electrolytes are required in controlled-potential experiments to decrease the resistance of the solution, to eliminate electro migration effects, and to maintain a constant ionic strength. The inert supporting electrolyte may be an inorganic salt, a mineral acid, or a buffer. While potassium chloride or nitrate, ammonium chloride, sodium hydroxide, or hydrochloric acid are widely used when using water as a solvent, tetraalkylammonium salts are often employed in organic media. Buffer systems (such as acetate, phosphate, or citrate) are used when a pH control is essential. The composition of the electrolyte may affect the selectivity of voltammetric measurements. For example, the tendency of most electrolytes to complex metal ions can benefit the analysis of mixtures of metals. In addition, masking agents [such as ethylenediaminetetraacetic acid (EDTA)] may be added to “remove” undesired interferences. The supporting electrolyte should be prepared from highly purified reagents, and should not be easily oxidized or reduced. The usual electrolyte concentration range is 0.1-1.0 M, in other words, in large excess of the concentration of all electro active species. Significantly lower levels can be employed in connection with ultra micro working electrodes.

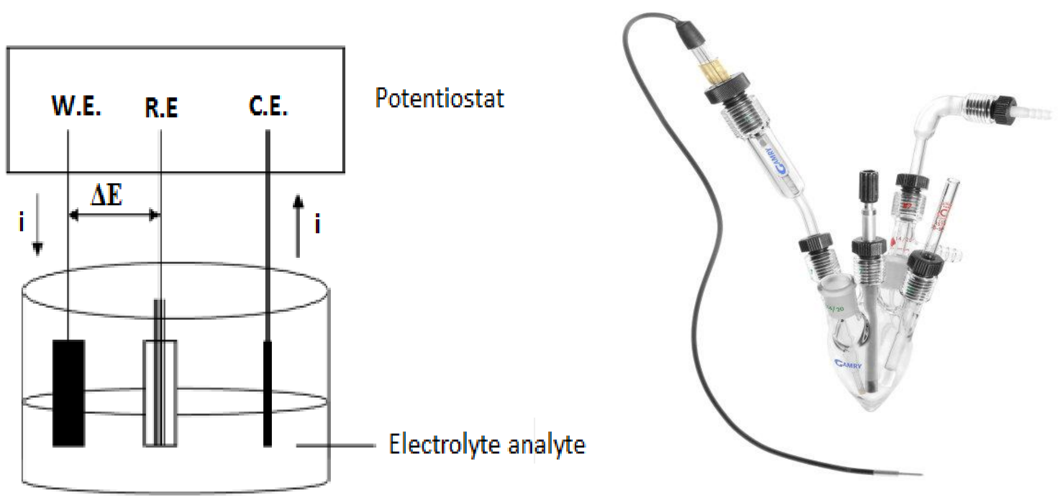

Figure 2.1. A typical three-electrode electrochemical cell.

2.3 Electroanalytical Methods

Galvanostatic method is also named as Chronopotentiometry and carried out by applying a constant current between the working and auxiliary electrodes using a galvanostat. Only a simple, two-electrode configuration is required for galvanostatic electrolysis. The galvanostat ensures a constant current density and thus a controlled rate of the electrochemical reaction. Common applications of the galvanostat include constant current stripping potentiometry and constant current electrolysis. One advantage of all constant current techniques is that the ohmic drop due to solution resistance is also constant, as it is equal to the product of the current and the solution resistance. However, as the reaction proceeds, the potential on the working electrode may change, new electrochemical processes may occur at different potentials and a change in the composition or character of the product may result and for that reason, complications may arise in initiation and propagation steps.

Potentiostatic method is conducted with a three-electrode system. The potential between the working and reference electrodes is maintained by a potentiostat. An electronic feedback circuit continually compares and controls the working electrode potential with respect to the reference electrode. Several factors should be considered in choosing the appropriate electrolysis potential, including the threshold reaction potential determined by voltammetry, the potential at which interfering reactions may occur and the desired rate of the electrochemical reaction. The voltage between the working and the reference electrode may be called the polymerization potential. By keeping the potential constant, creation of undesired species is prevented; hence the initiation becomes selective, that is, through the monomer itself. Chronoamperometry, i.e. measuring the current as a function of time, is the method of choice to study the kinetic of polymerization and especially the first steps.

2.3.1 Voltammetry

Voltammetry may be defined as an electrolysis process limited by the mass transport rate at which molecules move from the bulk of the solution to the electrode. The current is followed as a function of the potential applied using a three-electrode cell of 1-50 ml working volume.

Voltammetric methods are limited to easily reducible or oxidizable compounds and are more practical for low-level quantification, possessing an extensive linear dynamic range (10-3 to 10-8 M).

Voltammetry represents a wide range of electrochemical techniques. These techniques can be used to study the solution composition through current-potential relationships in an electrochemical cell and with the current-time response of a microelectrode at a controlled potential.

The advantages of voltammetry quickly demonstrate that it is apotent analytical tool. The foremost advantage is sensitivity. Voltammetry ranks among the most sensitive analytical techniques available; it is routinely used for the determination of electro active substances in the sub-parts per million ranges. Analysis times of seconds are possible. The simultaneous determination of several analytes by a single scan is often possible with a voltammetric procedure. Voltammetric techniques have a unique capability to distinguish between oxidation states that may affect a substance's reactivity and toxicology. The theory of voltammetry is well developed, and reasonable estimates of unknown parameters can be made.

The target of voltammetric studies is to provide a current response for analytes. The current is related to the concentration of the basis analyte. This is achieved by monitoring the transfer of electrons throughout redox process of the analyte.

$$Ox + ne^{-} \rightarrow Red \qquad (2.1)$$

Here Ox: oxidized form and red: reduced form of the redox couple. At the electrode surface at 250 ^{0}C according to the Nernst equation:

$$E = E^{0} + \frac{0.059}{n} \log \left(\frac{C_{Ox}}{C_{red}}\right) \qquad (2.2)$$

Here Cox and Cred are concentrations of oxidized and reduced form at the electrode surface. E_0 is the standard electrode potential for redox reaction.

In direct-current voltammetry using a dropping mercury electrode , it is a formidable problem to develop an expression for the current at expanding spherical electrode when the surface concentration is held at zero. The original equation was solved by Ilkovič, who assumed semi-infinite linear diffusion to an expanding plane rather than to an expanding sphere. The limiting current or diffusion current is related to analyte concentration by the Ilkovic equation (Eq. 2.3) and this equation is used in quantitative analysis.

$$i_d = 708.n.D^{1/2}.m^{2/3}t^{1/6}C \qquad (2.3)$$

where i_d is the limiting current (μA), m is the mass flow rate of Hg through the capillary (mg/sec), t is the drop lifetime in seconds and C is analyte concentration in mol/cm^3 , n is number of electrons involved in overall electrode reaction and D is diffusion coefficient (cm^2/s).

2.3.1.1 Cyclic Voltammetry

A more commonly used variation of the technique is cyclic voltammetry, in which the direction of the potential is reversed at the end of the first scan. This has the advantage that the product of the electron transfer reaction that occurred in the forward scan can be probed again in the reverse scan. In addition, it is a powerful tool for the determination formal redox potentials, detection of chemical reactions that precede or follow the electrochemical reaction and evaluation of electron transfer kinetics. The basic shape of the current response for a cyclic voltammetry experiment is shown in Figure 2.2. At the start of the experiment, the bulk solution contains only the reduced form of the redox couple (R), so that at potentials lower than the redox potential, i.e. the initial potential, there is no net conversion of R into O, the oxidized form As the redox potential is approached, there is a net anodic current that increases exponentially with potential. As R is converted into O, concentration gradients are set up for both R and O, and diffusion occurs down these concentration gradients. At the anodic peak , the redox potential is sufficiently positive that any R that reaches the electrode surface is instantaneously oxidized to O.

Upon reversal of the a net reduction of O to R occurs which causes a cathodic current that eventually produces a peak shaped response If there is no reversal of potential then a Linear Sweep voltammogram is obtained.

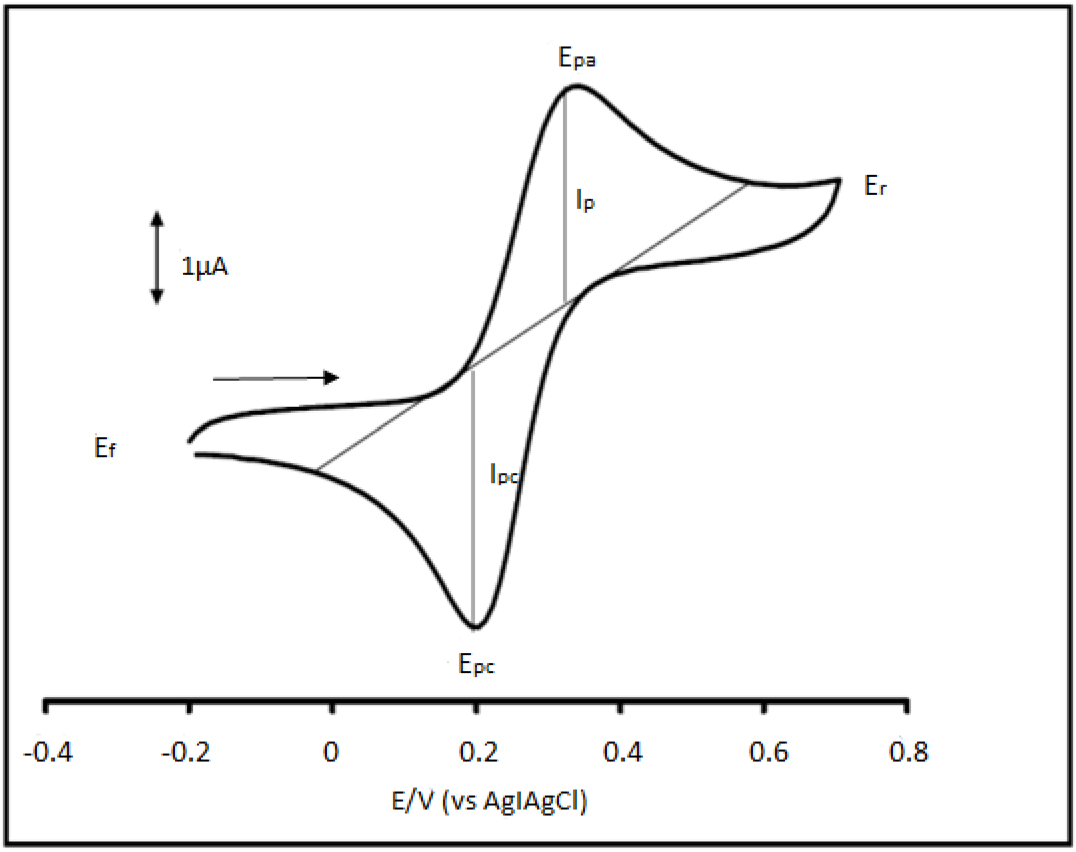

Figure 2.2. A typical cyclic voltammogram for a reversible system.

If a redox system remains in equilibrium throughout the potential scan, the electrochemical reaction is said to be reversible. This is to say equilibrium requires that the surface concentrations of O and R be maintained at the values required by the Nernst equation. Under these conditions, the following parameters characterize the cyclic voltammogram of the redox process:

• The peak potential separation (Epa - Epc) is equal to 59/n mV for all scan rates where n is the number of electron equivalents transferred during the redox process;

• The peak width is equal to 28.5/n mV for all scan rates;

• The peak current ratio (ipa/ipc) is equal to 1 for all scan rates.

Cyclic voltammetry (CV) is the most widely used technique for acquiring qualitative information about electrochemical reactions. The power of CV results from its ability to rapidly provide considerable information on the thermodynamics of redox processes and the kinetics of heterogeneous electron transfer reactions and on coupled chemical reactions or adsorption processes.

CV is often the first experiment performed in an electro analytical study. In particular, it offers a rapid location of redox potentials of the electro active species, and convenient evaluation of the effect of media on the redox process.

Cyclic voltammetry involves the reduction and oxidation of the species. Oxidation occurs on application of a positive going potential, an increase in the peak current with an increase in the potential is observed until the potential where the analyte is oxidized is reached. Thereafter a decrease in current occurs. The reduction of the species occurs with application of a negative going potential. The movement of the species to the electrode can be facilitated by migration, convection and diffusion. Diffusion is the movement of analyte due to concentration gradient. The latter is the one that is of interest when dealing with electro analytical reactions. When working with voltammetry, specifically cyclic voltammetry, a system can be characterized as a reversible, quasi-reversible and irreversible. This is dependent on the ease of the redox reaction of the species and whether both the oxidized and reduced species are redox active. A reversible system shows the redox reaction of the species in the forward scan followed by the redox reaction upon application of a reverse scan. An irreversible system is observed by the occurrence of a forward peak with a peak in the reverse direction being very weak or not observed at all due to failure to regenerate the starting electro active species. A shift in the potential with change in scan rates is observed for an irreversible system because of the slow electron transfer.

The problem with cyclic voltammetry is that it has high background currents due to the charging current, this limits sensitivity. Hence another voltammetric method such as square wave voltammetry has to be used concurrently with cyclic voltammetry to increase the sensitivity.

Conclusions can also be drawn from the cyclic voltammograms regarding the rate of charge transfer, charge transport processes, and the interactions that occur within the polymer segments, at specific sites and between the polymer and the ions and solvent molecules. For very thin films and/or at low scan rates, when the charge transfer at the interfaces and charge transport processes within the film are fast, i.e., electrochemically reversible (equilibrium) behavior prevails, and if no specific interactions (attractive or repulsive) occur between the redox species in the polymer film.

2.3.1.2 Pulse Voltammetry

The potential step is the basis of pulse voltammetry. Pulse techniques were initially developed for the dropping mercury electrode, the objective being to synchronize the pulses with drop growth and reduce the capacitive current contribution by current sampling at the end of drop life. After applying a pulse of potential, the capacitive current dies away faster than the faradaic current; thus the current is measured at the end of the pulse [163].

Normal Pulse Voltammetry (NPV)

This technique uses a series of potential pulses of increasing amplitude. The current measurement is made near the end of each pulse, which allows time for the charging current to decay. It is usually car- ride out in an unstirred solution at either DME (called normal pulse polarography) or solid electrodes. The potential is pulsed from an initial potential Ei . The duration of the pulse, t, is usually 1 to 100 msec and the interval between pulses typically 0.1 to 5 sec. The resulting voltammogram displays the sampled current on the vertical axis and the potential to which the pulse is stepped on the horizontal axis. [164]

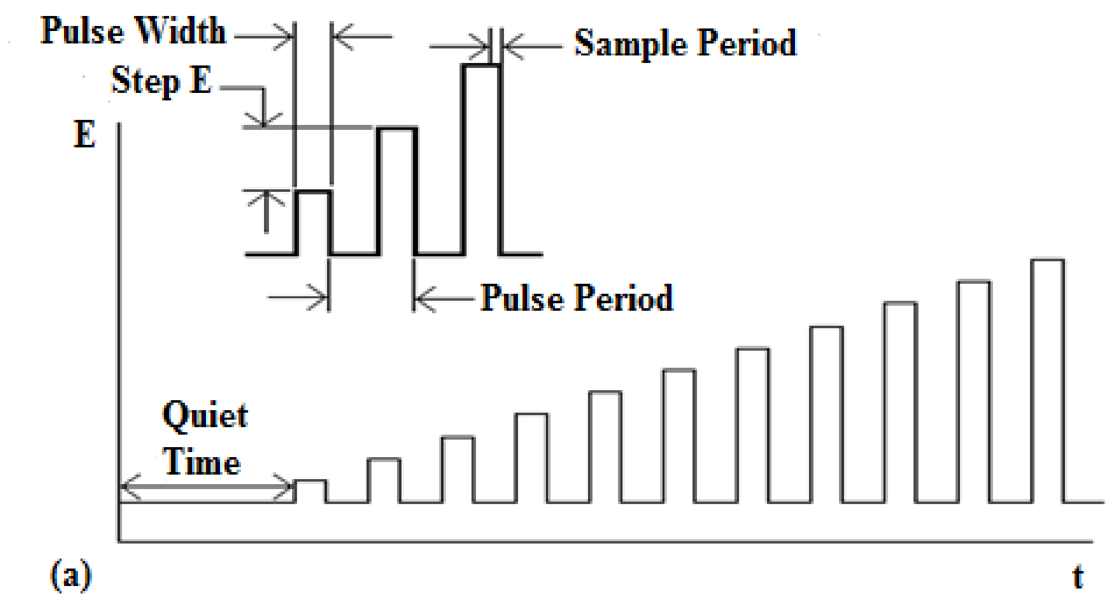

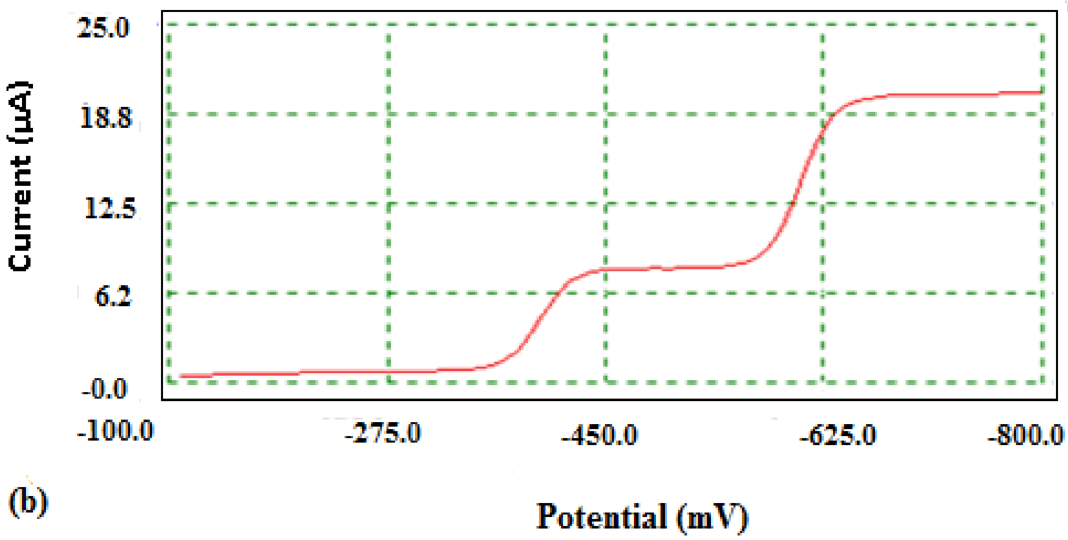

Figure 2.3. Normal pulse voltammetry. (a) operation and (b) response.

Differential Pulse Voltammetry (DPV)

DPV is an extremely useful technique for measuring trace levels of organic and inorganic species. In DPV, fixed magnitude pulses superimposed on a linear potential ramp are applied to the working electrode at a time.

The current is sampled twice, just before the pulse application and again late in the pulse life, when the charging current has decayed). The first current is instrumentally subtracted from the second, and this current difference is plotted against the applied potential.

This technique is comparable to normal pulse voltammetry in that the applied potentials are an overlapping of a fixed amplitude pulse and a linear potential ramp. However, it differs from normal pulse voltammetry because each potential pulse is fixed, of small amplitude (10 to 100 mV), and is superimposed on a slowly changing base potential. Current is measured at two points for each pulse, the first point just before the application of the pulse and the second at the end of the pulse. These sampling points are selected to allow for the decay of the nonfaradaic (charging) current.

The difference between current measurements at these points for each pulse is determined and plotted against the base potential.

2.3.1.3 Square Wave Voltammetry

Square Wave Voltammetry (SWV) is a useful method for studying redox reactions with overlapping waves. This type of polarography is often named Osteryoung Square Wave Voltammetry. In SWV a square wave potential superimposed to a staircase potential is applied to the working electrode.

For reversible processes the peaks are Gaussian shaped and the peak potentials (Ep) are equal to the half potentials ($E_{1/2}$) of the redox processes. An estimate of the number of electrons (n) involved in the redox process under each peak can be obtained from the peak height (i.e. the peak current), which is approximately proportional to n. A more exact evaluation of the number of electrons involved can be calculated from the half peak widths ($W_{1/2}$) which depend on factors such as temperature and the number of electrons involved.

The ability to analyze both the forward and reverse currents as well as the net current in Square Wave Voltammetry proves useful as information about reaction reversibility can be obtained easily. Square wave voltammetry (SWV) is a sensitive electro analytical technique used to investigate redox reactions that may otherwise be impossible with CV. The more popular technique is known as Osteryoung square wave voltammetry (OSWV) after its inventors in the 1950s [165]. Current signals are sampled at two points, the difference of which is plotted as a function of applied potential, such that peaks rather than voltammetric waves are observed.

SWV eliminates the charging current caused by the electrode double layer, thus an increased signal-to-noise ratio results. Therefore shortcomings observed with CV, e.g. overlapping or closely spaced peaks with poor resolution are overcome by SWV. Optimal peak separation, greater analysis speed, lower electro active species consumption and lower detection limits of up to 10-8 M, are advantages that can be obtained with this technique.

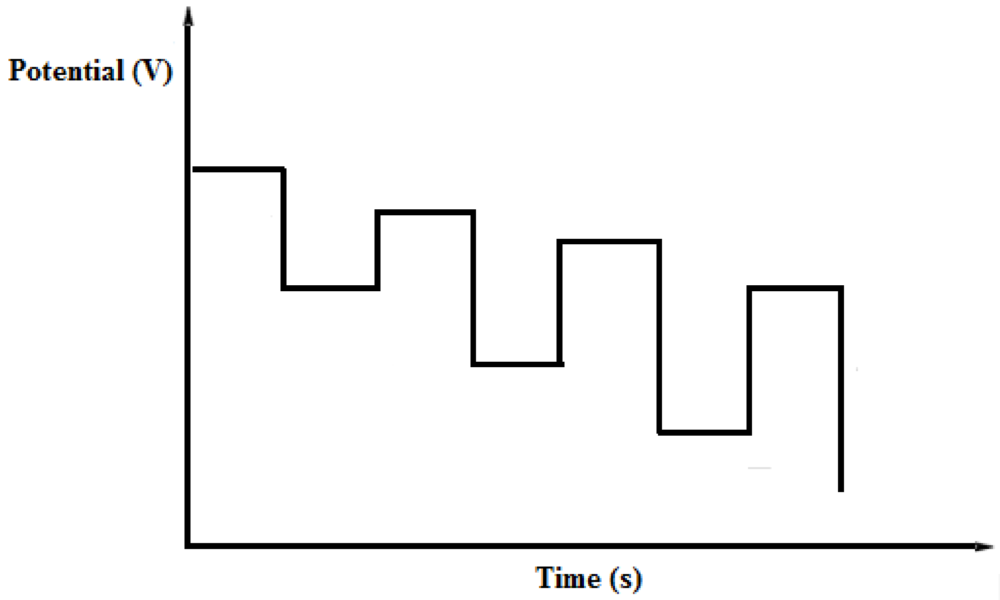

Figure 2.4. Diagrammatic representation of a Square Wave curve**.**

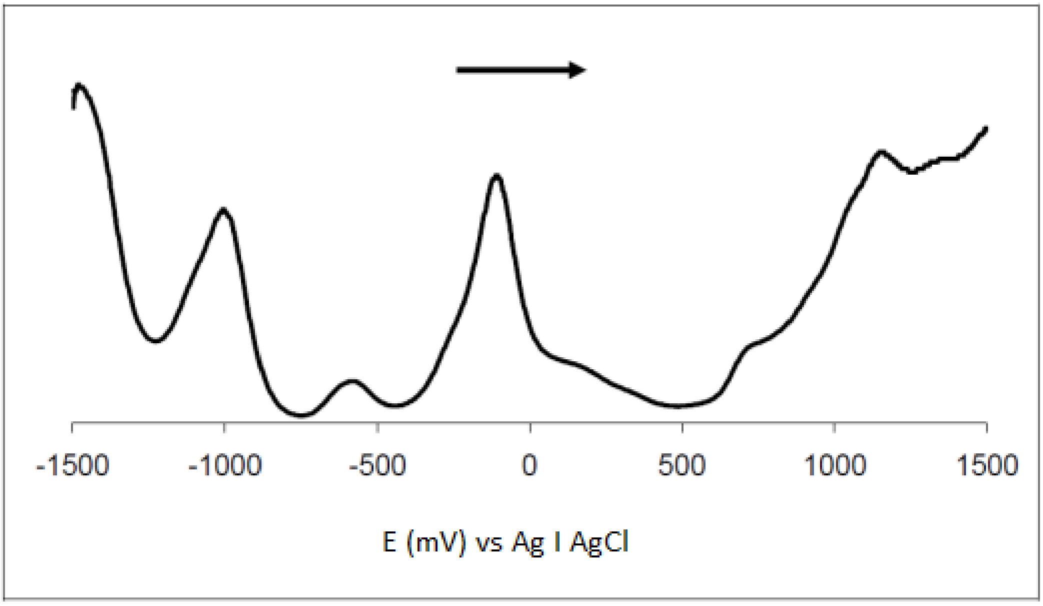

Figure 2.5. Typical Square Wave voltammogram.

2.3.2. Spectroelectrochemistry

Spectroscopic measurements can be carried out concurrently with electrochemical control, with each technique providing complementary information about the chemical systems of interest. These studies mainly involve two modes, transmission and reflection, and the measurements can be *in situ* or *ex situ*.

In transmission experiments, the typical setup involves a light beam passing through the working electrode. Spectroelectrochemistry allows the simultaneous acquisition of electrochemical and spectroscopic data . In spectroelectrochemistry, the current and spectral absorbance bands are concurrently monitored.

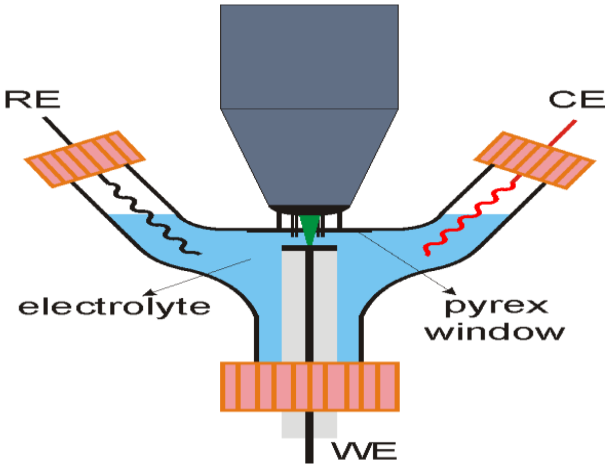

Figure 2.6. Typical Spectroelectrochemical Cell.

Spectroelectrochemistry may also be used to characterize the products of oxidation or reduction of redox complexes. The use of spectroelectrochemistry in MPc studies is based on the well known fact that the spectra of ring-based processes drastically affects the Q band while the metal-based redox processes result only in the shift in the Q band without much change in intensity. Spectroelectrochemistry may consequently be used to: monitor electron transfer reactions; investigate the stability of the oxidation or reduction products; determine the reversibility of an electrochemical reaction. Information gathered from spectroelectrochemistry can be applied to Faraday's Law, equation 2.4:

$$Q = nFvco \qquad [2.4]$$

where Q is the charge read from the spectroelectrochemical instrument; F is Faraday's constant, v is the volume (usually 0.5 ml), and the initial concentration, co, is attained from Beer's Law (A = εcol). Hence one may find n, the number of electrons occurring in the electrochemical process.

The main problem encountered in *in situ* spectroelectrochemical experiments is that light must be able to pass through the electro analysis cell, so everything (cell walls, solution, and electrode) must be highly transparent.

To construct a cell from quartz or silica is simple, and to work with transparent solutions is generally problem-free, but transparent electrodes are a greater challenge. Nevertheless, the use of a wire mini-grid optically transparent electrode (OTE) overcomes this challenge. Modern methods commonly use a relatively cheap, thin (~0.3 μm) film of a semiconductor: either tin oxide doped with fluoride (SnO_2:F) or indium doped with tin oxide otherwise known as indium-tin oxide (ITO). This is a method that makes use of spectroscopy with electrochemistry. The simplest spectroelectrochemical method is the one that makes use of UV/Visible spectroscopy. There is passage of charge while a change in the species is monitored by the change in absorption. There are two modes that can be utilized when using UV/visible spectroscopy. There is use of optically transparent electrodes (OTEs); these can be made of thin film semiconductors such as tin oxide and indium oxide or a fine wire mesh that is made of metals such as platinum, gold.

There is also the use of an optically transparent thin layer electrode (OTTLE), which is an enclosed chamber with the electrodes within the chamber together with the solution. Spectroscopic changes can be observed within a shorter time-frame, in seconds when making use of the OTTLE cell because of the low volumes used, 30-50 μl.

Spectroelectrochemical experiments can be used to probe various adsorption-desorption processes. In particular, changes in the absorbance accrue from such processes can be probed utilizing the large ratio of surface area to solution volume of OTEs with long optical path length. In addition to transmission experiments, it is possible to use more sensitive reflectance protocols. In particular, in internal reflectance, spectroscopy (IRS) the light beam is introduced to the electrode at an angle, and the spectrum is recorded from the reflected beam at the solid/solution interface. Prisms are used to allow the radiation enter and leave. In addition to its higher sensitivity, IRS is less prone to solution resistance effects.

2.4 Electrode Modification (Chemically Modified Electrode)

Compared with other electrode concepts in electrochemistry, the distinguishing feature of a CME(is that a generally quite thin film (from a molecular monolayer to perhaps a few micrometers-thick multilayer) of a selected chemical is bonded to or coated on the electrode surface to endow the electrode with the chemical, electrochemical, optical, electrical, transport, and other desirable properties of the film in a rational, chemically designed manner. The range of electrode surface properties includes, but is more diverse than, that of ion-selective electrodes (ISEs) which also involve, in their highest forms, rational design of the phase-boundary, partition and transport properties of membranes on or between electrodes.

While CMEs can operate both amperometrically (or voltammetrically) and potentiometrically, they are generally used amperometrically, a faradaic (charge transfer) reaction being the basis of experimental measurement or study, whereas ISEs are generally used in potentiometric formats where a phase-boundary potential (interfacial potential difference) is the measured quantity [166]. Gas-sensing electrodes (e.g., for $C0_2$, NH_3, NO_x) are also potentiometrically based [167] although the oxygen electrode, which functions amperometrically, is an exception [168].

Chemically sensitive field effect transistors (CHEMFETs) are basically non-faradaic electrode systems in which electric field variations in the semiconductor gate region control the magnitude of the source-drain current [169]. Enzyme-based electrodes detect the product(s) of a reaction between an immobilized enzyme layer and a reaction substrate in many ways, including both amperometric and potentiometric means.

2.4.1.Dip-Coating

Dip-coating is an ideal method to prepare thin layers from chemical solutions since it is a low-cost and waste-free process that is easy to scale up and offers a good control on thickness.

For such reasons, it is becoming more and more popular not only in research and development laboratories, but also in industrial production, as testified by the increasing number of annual publications.

This procedure consists of immersing the electrode material in a solution of the polymer for a period sufficient for spontaneous film formation to occur by adsorption. The film quantity in this procedure may be augmented by withdrawing the electrode from the solution and allowing the film of polymer solution to dry on the electrode.

2.4.2.Spin coating

In the spin coating process, solution is first deposited on the substrate, and the substrate is then accelerated rapidly to the desired rotation rate. Liquid flows radially, owing to the action of centrifugal force, and the excess is ejected off the edge of the substrate. The film continues to thin slowly until disjoining pressure effects cause the film to reach an equilibrium thickness or until it turns solid-like due to a dramatic rise in viscosity from solvent evaporation. The final thinning of the film is then due solely to solvent evaporation. An excellent description of the basic principles involved in the spin coating process is given in a review by Bornside, Macosko, and Scriven. A droplet of a dilute solution of the polymer is applied to the surface of a rotating electrode. Excess solution is spun off the surface and the remaining thin polymer film is allowed to dry. Multiple layers are applied in the same way until the desired thickness is obtained. This procedure typically produces pinhole-free thin films.

2.4.3.Electrochemical Polymerization

A solution of monomer is oxidized or reduced to an activated form that polymerizes to form a polymer film directly on the electrode surface. This procedure results in few pinholes since polymerization would be accentuated at exposed (pinhole) sites at the electrode surface. Unless the polymer film itself is redox active, electrode passivation occurs and further film growth is prevented.

2.4.4. Langmuir-Bloddget Films

The Langmuir-Blodgett (LB) technique is one of the most promising methods for the preparation of thin films as it enables ;

- Precise control of the monolayer thickness,
- Homogeneous deposition of the monolayer over large areas and
- The possibility to make multilayer structures with varying layer composition.

An additional advantage of the LB technique is that monolayers can be deposited on almost any kind of solid substrate.

There exists a wide range of surfactants with an amphiphilic nature which drastically lower the surface tension of water. Many of these amphiphilic substances insoluble in water can, with the help of a volatile and water insoluble solvent, be easily spread on a water surface to form an insoluble monolayer at the air/water interface. These monolayers, also called Langmuir (L) films, represent the extreme case when considering adsorption to interfaces because all molecules are concentrated in a one molecule thick layer at the interface. The amphiphilic nature of the surfactants dictates the orientation of the molecules at the interface (air/water or oil/water) in such a way that the polar head group is immersed in the water and that the long hydrocarbon chain is pointing towards air, gas or oil.

The hydrocarbon chain of the substance used for monolayer studies has to be long enough in order to be able to form an insoluble monolayer. A rule of thumb is that there should be more than 12 hydrocarbons or groups in the chain ($(CH_2)n$, $n > 12$). If the chain is shorter, though still insoluble in water, the amphiphile on the water surface tend to form micelles.

These micelles are water soluble, which prevents the build-up of a monolayer at the interface. On the other hand if the length of the chain is too long the amphiphile tends to crystallize on the water surface and consequently does not form a monolayer. It is difficult to determine the optimal length for the hydrocarbon chain because its film forming ability also depends on the polar part of the amphiphile.

Furthermore, the amphiphile has to be soluble in some organic solvent which is highly volatile and water insoluble (to transport the surfactant to the surface, chloroform or hexane is commonly used). Langmuir-Blodgett films are built up by a process of successive deposition of individual Langmuir monolayers onto a solid substrate.

The monolayer is formed by spreading the organic molecules on the water subphase. The molecules usually have hydrophilic (head) and hydrophobic (tail) parts, so when the film is formed the molecules stand on their heads. When the molecules first are spread on the water they are very loosely packed and form a so called gas phase. This means that the area on the water available for each molecule is rather large and the surface pressure is low. The surface pressure is usually measured using a Wilhelmy plate and a precision scale. The surface pressure can be increased by means of one or two sliding barriers. At a certain point the surface pressure starts to rise more rapidly indicating a transition to the liquid phase. As the barrier is moved even further the onset of the solid phase can be noted by an even steeper rise in the surface pressure.

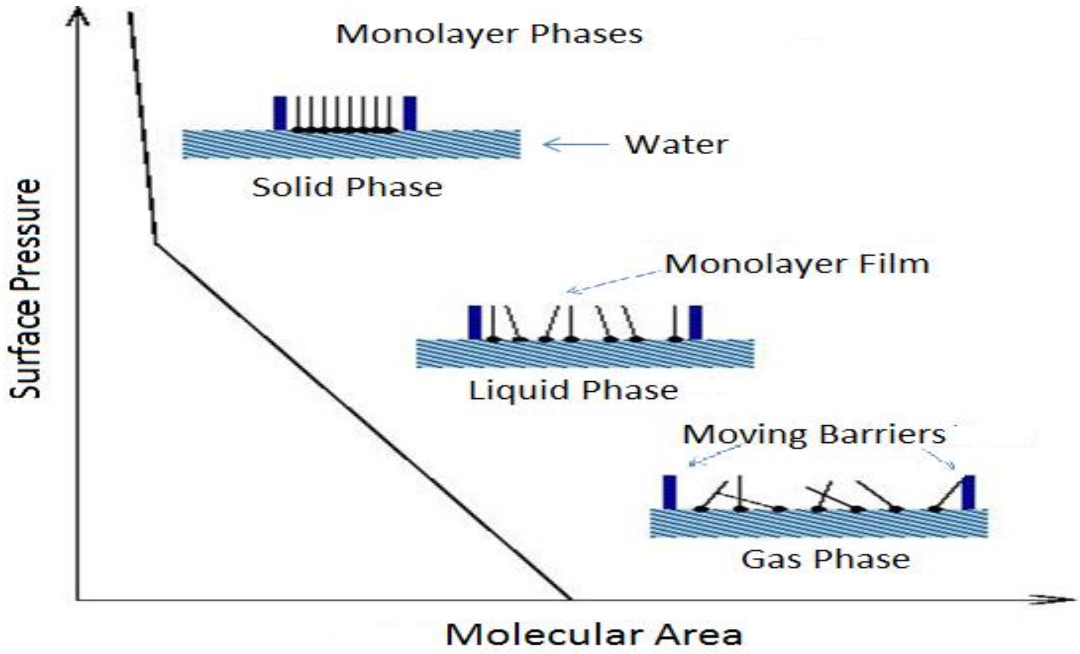

Figure 2.7. Surface pressure - area isotherm.

One or more monolayers can be transfered to a substrate by dipping the substrate through the monolayer. The monolayer is kept uniform by controlling the surface pressure with the barriers throughout the process.

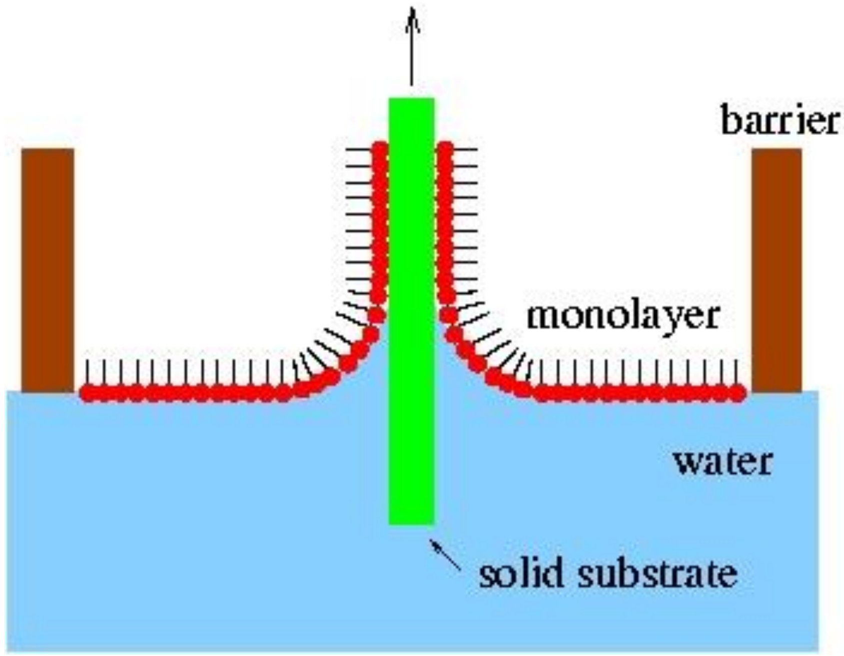

Figure 2.8. Deposition of a monolayer on a solid substrate.

3. RESULTS AND DISCUSSION

3.1.Experiments

Electrochemical analyses of the complexes were investigated in solution to propose possible applications of the complexes in electrochemical technologies.This chapter consists of the materials (chemical reagents used for electrochemical and spektroelectrochemical measures,) equipment and experimental procedures used in this study.

3.1.1 Materials

Ultra pure dimethylsulfoxide (DMSO),dichloromethane (DCM), Acetonitrile (AN) electrochemical grade tetrabutylammonium perchlorate (TBAP), other reagents were purchased from Aldrich and used without further purification. MPcs used in this thesis were obtained from the authors of the published papers.Triple distilled water was used as solvent for electrocatalytic measurements. A platinum disk electrode, glassy carbon electrode (GCE), and an indium tin oxide (ITO) plate were purchased from BAS and SPI Supplies respectively. All sensor applications were performed in phosphate-buffer solution (0.1 mol.dm^{-3} KH_2PO_4 + 0.1 mol.dm^{-3} H_3PO_4) containing 0.1 mol.dm^{-3} $LiClO_4$ as supporting electrolyte.

3.1.2 Apparatus and Experimental Procedures

The electrochemical measurements were carried out with Gamry Reference 600 potentiostat/galvanostat controlled by an external PC and utilizing a three-electrode configuration at 25 ˚C. The working electrode was a Pt disc with a surface area of 0.071 cm^2. A Pt wire served as the counter electrode.

Saturated calomel electrode (SCE) was employed as the reference electrode and separated from the bulk of the solution by a double bridge. Electrochemical TBAP in ultra pure DCM and/or DMSO were employed as the supporting electrolyte at a concentration of 0.10 mol dm-3.

High purity N_2 was used to remove dissolved O_2 at least 15 minute prior to each run and to maintain a nitrogen blanket during the measurements.

UV-Vis absorption spectra and chromaticity diagrams were recorded by an Ocean Optics QE65000 diode array spectrophotometer. In situ spectroelectrochemical measurements were carried out by utilizing a three-electrode configuration of thin-layer quartz thin-layer spectroelectrochemical cell at 25˚C. The working electrode was a semipermeable Pt sheet. Pt wire counter electrode separated by a glass bridge and a SCE reference electrode separated from the bulk of the solution by a double bridge were used. In situ electrocolorimetric measurements, under potentiostatic control, were obtained using an Ocean Optics QE65000 diode array spectrophotometer at color measurement mode by utilizing a three-electrode configuration of thin-layer quartz spectroelectrochemical cell.

Langmuir experiments were carried out using a KSV/Nima 5000. 0.1 M $CdCl_2$ dissolved ultrapure water (resistivity greater than 18M/cm) from a Milli-Q Millipore system was used as the subphase (pH 5.9). LB films were prepared by spreading chloroform solution of the compounds on subphase. A 100 μl aliquot of the spreading solution was uniformly spread over the aqueous subphase by adding small drops at different locations on the water surface. A time period of 15 min was allowed for the solvent to evaporate before the area enclosed by the barriers was reduced. The π–A isotherm was recorded using a compression speed of barriers of 10 mm min^{-1}. A surface pressure (π) vs. molecular area isotherm was measured to characterize the quality of the monolayer on the subphase. The surface pressure was measured by the Wilhelmy method. After 30min waiting for the stabilization of the monolayer, a vertical dipping procedure was performed at the selected surface pressure with a speed of 5 mm min^{-1} for both the down and up strokes to transfer the monolayer on the ITO substrates. LB film samples were left to dry after each up stroke. 20 monolayers were transferred to the ITO glass by Y-type deposition.

To characterize the coating ability of the LB film, a transfer ratio was calculated by dividing the area of deposited film by the area of substrate. Sensor measurements of the modified electrodes were carried out in aqueous solution with the CV and SWV techniques.

During the measurements in solid state, first of all, an adequate number of SWV cycles were applied to reach the steady state and then, metal ion solutions were added to the aqueous solution gradually. After an efficient stirring, SWVs and CVs were recorded.

3.2 Results and Commentary

3.2.1. Titanyl derivatised phthalocyanines

The solution redox properties of the complexes (shown in Figure 3.1.) were studied using CV, DPV,SWV and CPC in DCM and/or DMSO on platinum electrode.

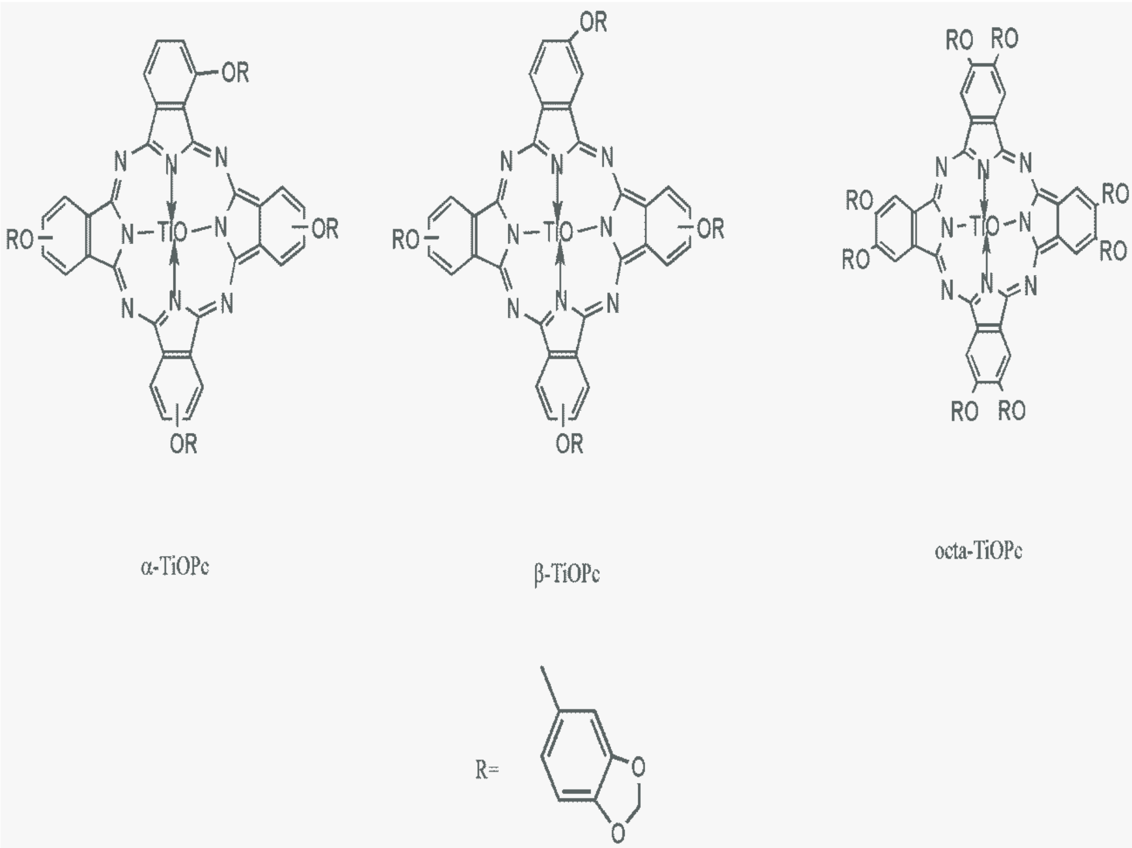

Figure 3.1. Structure of TiOPc complexes. β-TiOPc: Titanyl phthalocyanine nonperipherally tetra substituted with 3,4-(methylendioxy)-phenoxy moieties; α -TiOPc: Titanyl phthalocyanine peripherally tetra substituted with 3,4-(methylendioxy)-phenoxy moieties; octa-TiOPc: Titanyl phthalocyanine peripherally octa substituted with 3,4-(methylendioxy)-phenoxy moieties.

Table 3.1 lists the assignments of the redox couples and estimated electrochemical parameters including the half-wave peak potentials (E1/2), ratio of anodic to cathodic peak currents ($I_{p,a}/I_{p,c}$), peak to peak potential separations (ΔEp), and difference between the first oxidation and reduction processes (ΔE1/2).

3.2.1.1. Titanyl phthalocyanine nonperipherally tetra substituted with 3,4-(methylendioxy)-phenoxy moieties (β –TiOPc)

CV and SWV responses of peripherally tetra substituted TiOPc (β – TiOPc) is shown in DCM/TBAP electrolyte system.(Fig. 3.2.) β-TiOPc displays five well-resolved electrochemically reversible and diffusion controlled reduction (R1 at -0.22 V, R2 at -1.00 V, R3 at -1.40 V, R4 at -1.40 V and R5 at -1.40 V) and two irreversible oxidation processes (O1 at 0.95 V and O2 at 0.95 V). SWVs clearly show the chemical and electrochemical reversibility of the redox processes (Fig. 3.2b). When compared with the responses of internal reference ferrocene, ΔE_p values of all reduction processes of β-TiOPc are in electrochemical reversibility range. The effect of coupled chemical reactions to the electron transfer reactions is illustrated with $I_{p,a}/I_{p,c}$ ratio change as a function of the scan rate.

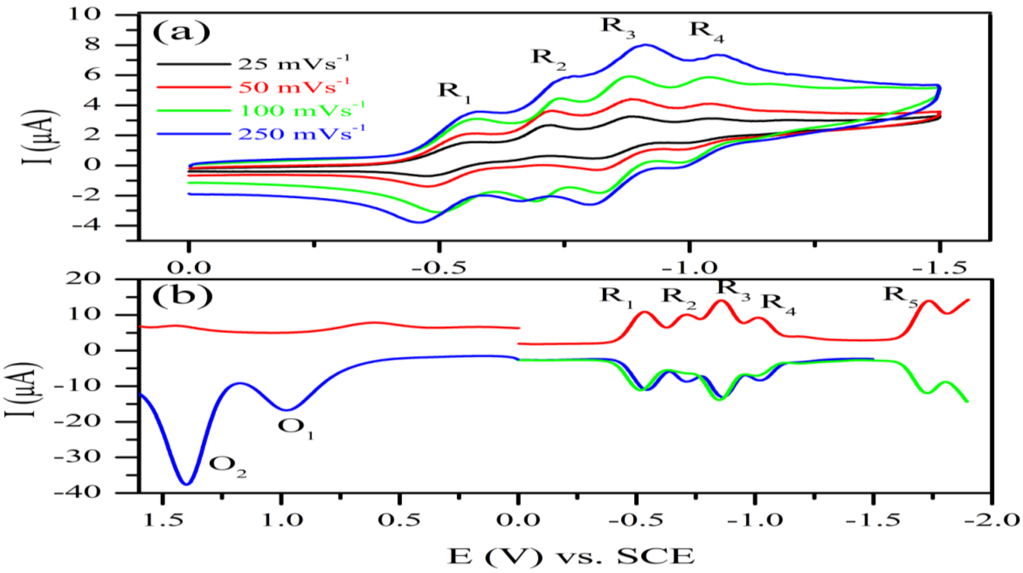

Figure 3.2. (a) Cathodic CVs of β-TiOPc at various scan rates on a Pt working electrode in DCM/TBAP and (b) SWV of β -TiOPc recorded with SWV parameters: step size = 5 mV; pulse size = 100 mV; Frequency = 25 Hz.

Table 3.1 Voltammetric data of the complexes with the related MPcs. All voltammetric data were given versus SCE.

Complex		Pc^{1-}/Pc^{0}	Pc^{2-}/Pc^{1-}	$Ti^{IV}O/ Ti^{III}O$	$Ti^{III}O/ Ti^{II}O$	Pc^{2-}/Pc^{3-}	Pc^{3-}/Pc^{4-}	Pc^{4-}/Pc^{5-}	$^{d}\Delta E_{1/2}$	Ref
TiOPc (β)	$^{a}E_{1/2}$	1.54[e]	1.02	-0.53	-0.86	-0.71	-1.02	-1.74[e]	1.55	
(in DCM)	$^{b}\Delta E_{p}$ (mV)	-	-	63	58	55	62	-		tw
	$^{c}I_{p,a}/I_{p,c}$	-	-	0.92	0.67	0.85	0.80	-		
TiOPc (β)	$^{a}E_{1/2}$	0.85	0.55	-0.44	-0.79	-0.59	-0.94	-1.64	1.00	
(in DMSO)	$^{b}\Delta E_{p}$ (mV)	84	75	80	66	61	-	-		tw
	$^{c}I_{p,a}/I_{p,c}$	0.27	0.33	0.95	0.98	0.92	-	-		
TiOPc (α)	$^{a}E_{1/2}$	-	0.82	-0.55	-0.91	-0.74	-1.09[e]	-1.45[e]	0.98	
(in DCM)	$^{b}\Delta E_{p}$ (mV)	-	86	80	107	90	-	-		tw
	$^{c}I_{p,a}/I_{p,c}$	-	0.77	0.58	0.47	0.66	-	-		
TiOPc (octa)	$^{a}E_{1/2}$	-	0.52	-0.38	-0.67	-0.86	-1.23	-1.56	1.00	
(in DCM)	$^{b}\Delta E_{p}$ (mV)	-	-	120	91	100	85	-		tw
	$^{c}I_{p,a}/I_{p,c}$	-	-	0.88	0.86	0.92	0.92	-		
	$^{b}\Delta E_{p}$ (mV)	-	-	170	110	100	150	-		tw
	$^{c}I_{p,a}/I_{p,c}$	-	-	1.10	0.95	0.56	0.45	-		
TiOPc (in DCM)	$^{a}E_{1/2}$		0.73	-0.54	-0.92	-1.81				32
TiOPc (in DCM)	$^{a}E_{1/2}$		1.03	-0.43	-0.72	-1.50				21
TiOPc (in DMSO)	$^{a}E_{1/2}$		0.54	-0.73		-1.19				22
TiOPc (in DCM)	$^{a}E_{1/2}$		0.75	-0.45	-0.85	-1.13				38

a: $E_{1/2}$ values ((E_{pa}+E_{pc})/2) were given versus SCE) at 0.100 Vs^{-1} scan rate. **b:** ΔE_{p}= E_{pa}-E_{pc}. **c**:$I_{p,a}/I_{p,c}$ for reduction ,$I_{p,c}/I_{p,a}$ for oxidation processes.**d**:$\Delta E_{1/2}$ = $E_{1/2}$ (first oxidation)-$E_{1/2}$ (first reduction). **e**: Recorded by SWV. **tw**: This work

The first reduction process is purely diffusion controlled with respect to unit $I_{p,a}/I_{p,c}$ ratio at all scan rates. However, while the $I_{p,a}/I_{p,c}$ ratio of R_1 is unity at fast scan rates, it decreases at slow scan rates and reverse couple of the process disappears completely at scan rates slower than 50 mVs^{-1}. These behaviors indicate presence of a chemical reaction after the R_1 process. SWV measurements recorded with different initial potentials also support the presence of this chemical reaction.

When the reverse SWV scan starts from -1.50 V (blue SWV), the reverse couple of all reduction process are present. However, when the reverse SWV shifts to -1.90 V, reverse couple of R_1 disappears and that of R_3 decreases in current intensity. These voltammetric behaviors indicate the presence of a chemical reaction succeeding the electron transfer processes.

The effects of vertex potential to the electrochemical behaviors of β - TiOPc in DCM/TBAP electrolyte system are illustrated in Fig. 3.3. During the cathodic potential scans at 0.10 Vs^{-1} scan rate, shifting of the vertex potential to the more negative potentials slightly decrease the reverse couple of the reduction processes due to the presence of a slow chemical reaction.

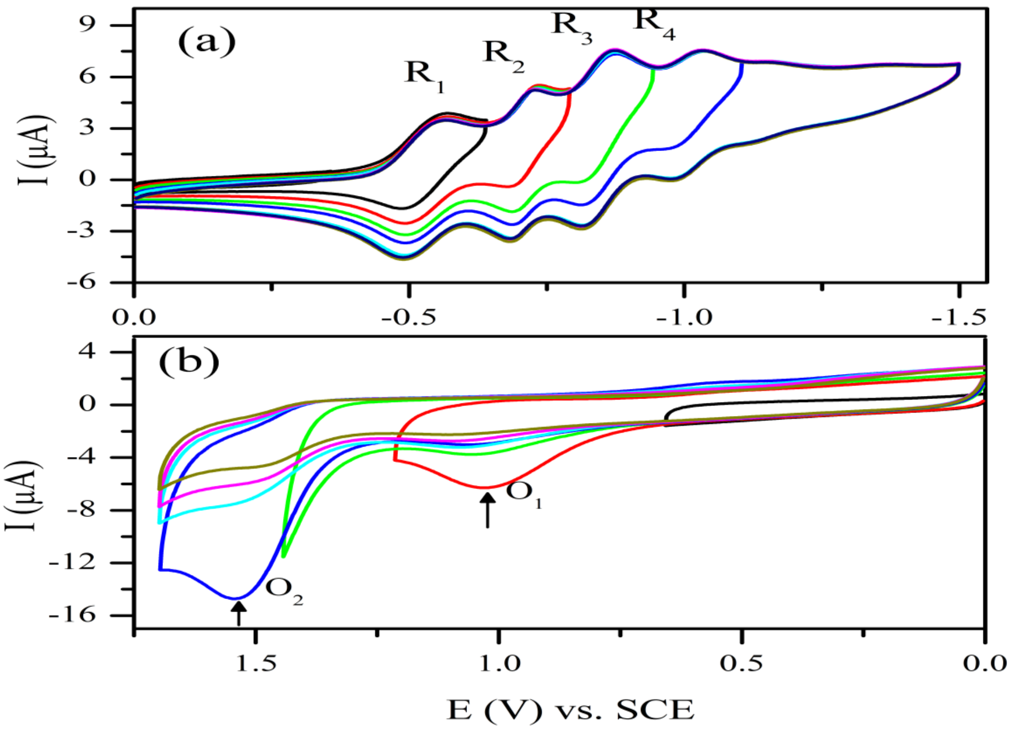

Figure 3.3. CVs of β -TiOPc recorded with different switching potentials (a) for reduction; (b) for oxidation processes at 0.100 Vs-1 scan rate on a Pt working electrode in DCM/TBAP.

Repetitive CV scans after the vertex application applications do not affect the reduction processes considerably. However irreversible oxidation couples decreases continuously in current intensity during the vertex and repetitive CV applications. This behavior indicates presence of a fast chemical reaction which is the reason of the chemical irreversibility of the oxidation processes.

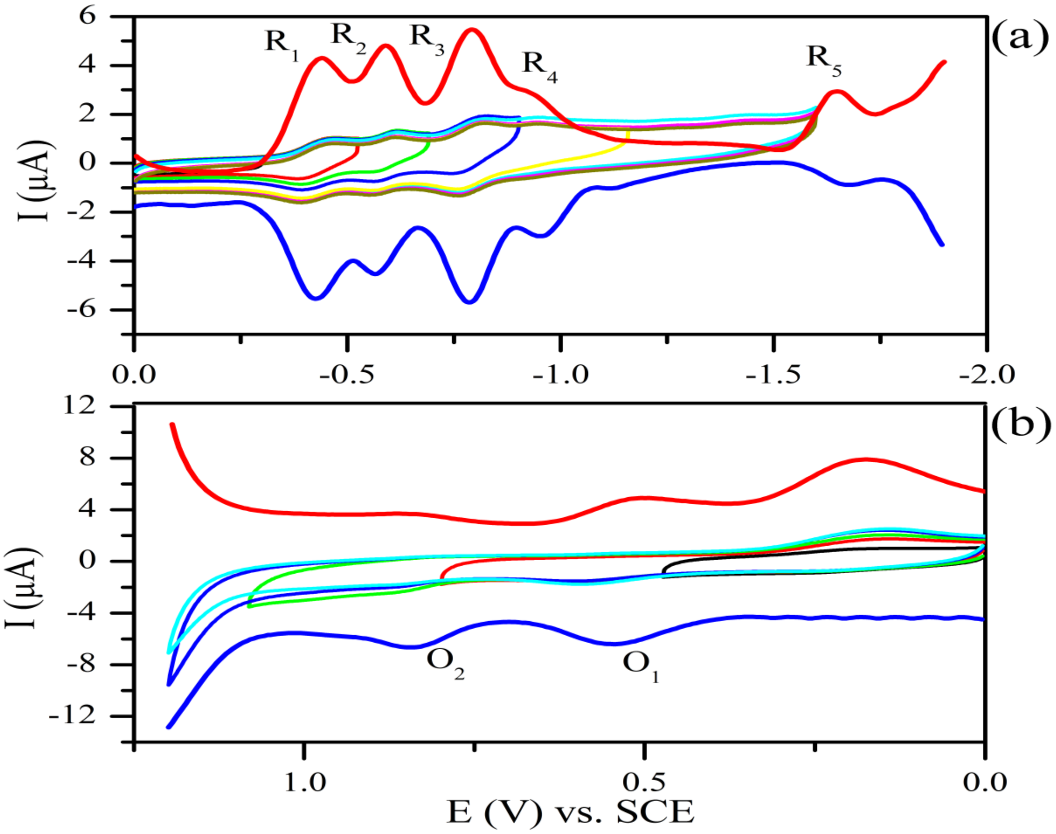

Figure 3.4. CVs (recorded with various vertex potential) and SWVs of β -TiOPc recorded during cathodic potential scan (a), and during anodic potential scan (b) at 0.100 Vs-1 scan rate on a Pt working electrode in DMSO/TBAP.

CV and SWVs were also recorded in DMSO, a coordinating polar solvent to investigate the solvent effect to the electrochemical behavior of the complex, β - TiOPc, (Fig. 3.4). β - TiOPc illustrates very similar voltammetric behaviors in both solvents, DCM and DMSO. Only the difference is the positions of the electron transfer reactions.

The reduction reactions shift approximately 10 mV towards the positive potentials, oxidation processes shift to negative potentials approximately 470 mV. Thus β - TiOPc is easily oxidized and reduced in DMSO.

All reduction processes are chemically and electrochemically reversible in DMSO, while a chemical reaction is coupled to the oxidation processes in DMSO.

In situ spectroelectrochemical studies were employed to perform the assignments for the redox processes recorded with the CVs and SWVs of the complexes and to investigate effect of the solvent to the peak assignments. The reduction of $Ti^{IV}OPc^{-2}$ species has been a subject of some controversy, with some reports proposing ring reduction and others suggesting metal reductions followed with the ring reduction processes.

To analyze the effect of the position of the substituents to the assignments of the redox couples of **TiOPcs**, spectroelectrochemical measurements of **β-TiOPc** in DCM/TBAP electrolyte system were performed in Fig. 3.5. The Q-band corresponding to the neutral $[Ti^{IV}OPc^{-2}]$ species shifts from 703 to 693 nm with increasing in the intensity during the controlled potential reduction of β -TiOPc at −0.60 V (Fig. 3.5a). Moreover while the B band at 295 nm ant the band at 435 nm decrease, a new band increases at 341 nm. As shown in Fig. 3.5a, the process occurred with clear isosbestic points at 330, 367, 577, and 710 nm in the spectra which demonstrate that there is no chemical reaction complicating the electron transfer reaction. These spectral changes are typical for a metal-based reduction process of titanyl phthalocyanine complexes, and assigned easily to $[Ti^{IV}OPc^{-2}]$ / $[Ti^{III}OPc^{-2}]^{-1}$ process Under the applied potential at −0.75 V, the Q band at 693 nm decreases without shifting, while a new band is recorded at 590 nm. Moreover, small new bands are also recorded at 626 and 763 nm. These spectral changes are easily assigned to a ring reduction process, $[Ti^{III}OPc^{-2}]^{-1}/[Ti^{III}OPc^{-3}]^{-2}$ redox process.

Because during the ring reduction reaction of MPc complexes, while the Q band decreases in intensity without a shift, new bands are recorded at MLCT regions. Fig. 3.4b inset indicates the spectral changes recorded during the third reduction reaction of β -TiOPc at -0.90 V. During this process, the Q band at 693 nm decreases without shift and finally disappears completely. At the same time the band at 590 nm shifts to 570 nm with increasing, while a new band is recorded at 535 nm. These spectral changes characterizes a ring-based reduction process and assigned to $[Ti^{III}OPc^{-3}]^{-2}/[Ti^{III}OPc^{-4}]^{-3}$. The spectral changes during the fourth reduction process indicate a metal-based reduction process (Fig.3.5c).

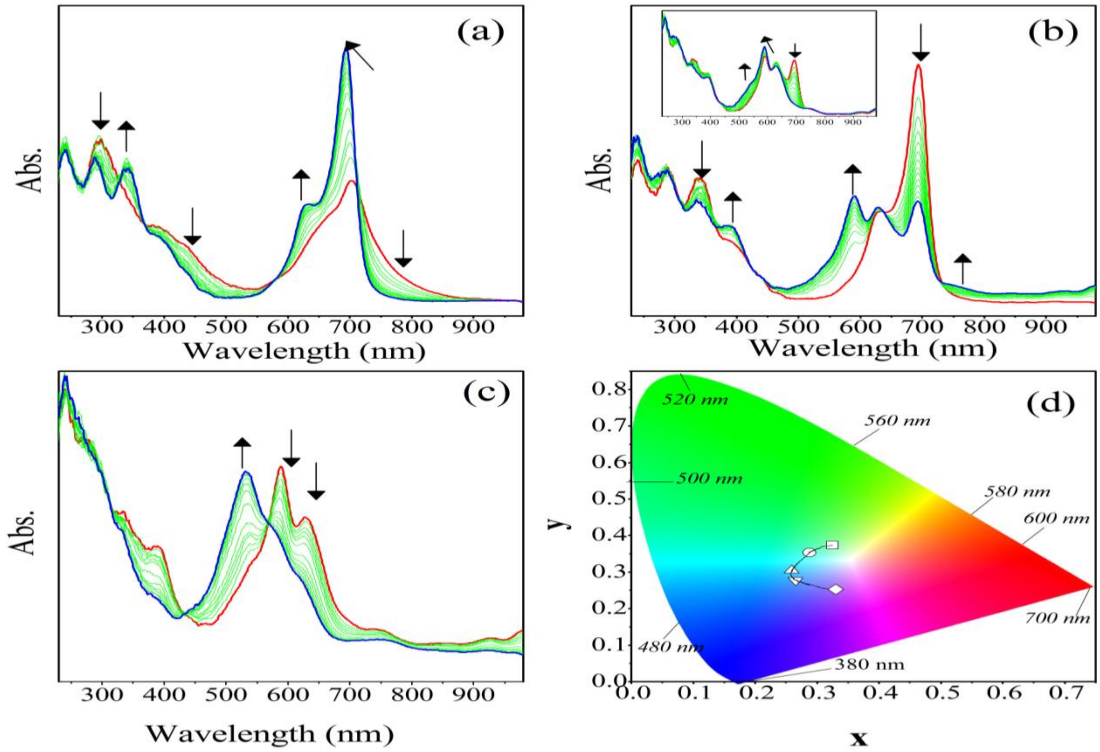

Figure 3.5. In situ UV-Vis spectral changes of β-TiOPc in DCM/TBAP. a) Eapp= -0.60 V. b) Eapp= -0.75 V (Inset: Eapp= -0.95 V). c) Eapp= -1.20 V. d) Chromaticity diagram (each symbol represents the color of electro-generated species; □ : $Ti^{IV}OPc^{-2}$, ○ : $Ti^{III}OPc^{-2}$, △ : $TiI^{II}OPc^{-3}$, ▽ : $Ti^{II}OPc^{-3}$, ◇ : $Ti^{II}OPc^{-4}$.

Because, the band at 590 nm shifts to 530 nm, while the band at 630 nm disappears completely. These spectral changes are easily assigned to $[Ti^{III}OPc^{-4}]^{-3}/[Ti^{II}OPc^{-4}]^{-4}$. β -TiOPc decomposed during the oxidation reaction, since all bands decrease in intensity. Color changes of the β -TiOPc in solution during the redox processes were recorded with in situ electrocolorimetric measurements and given in Fig. 3.5d.

Without any potential application, the solution of β -TiOPc is green (x = 0.3252 and y = 0.3746) (point in Fig. 3.5d). As the potential is stepped from 0 to -0.55 V, the color of the neutral β -TiOPc starts to changes and a bluish green color (x = 0.2879 and y = 0.3541) of monoanionic $[Ti^{III}OPc^{-2}]^{-1}$ was obtained at the end of the first reduction. Similarly the color of the complex changed during the further reduction processes, blue (point in Fig. 3.5d), dark blue (point in Fig. 3.5d) and a purple color (point in Fig. 3.5d) are obtained sequentially for the reduced species.

When we collect the responses of CV, SWV and spectroelectrochemical measurements and the data from the literature, we can propose the following mechanism for the electrochemical responses of β-TiOPc and α–TiOPc in DCM.

3.2.1.2. Titanyl phthalocyanine peripherally tetra substituted with 3,4-(methylendioxy)-phenoxy moieties (α –TiOPc)

CV and SWV of α- TiOPc in DCM/TBAP are represented in Fig. 3.6. Within the electrochemical window of DCM/TBAP in CV measurements, α - TiOPc complex undergoes an irreversible one-electron oxidation, and four reversible one-electron reduction processes.

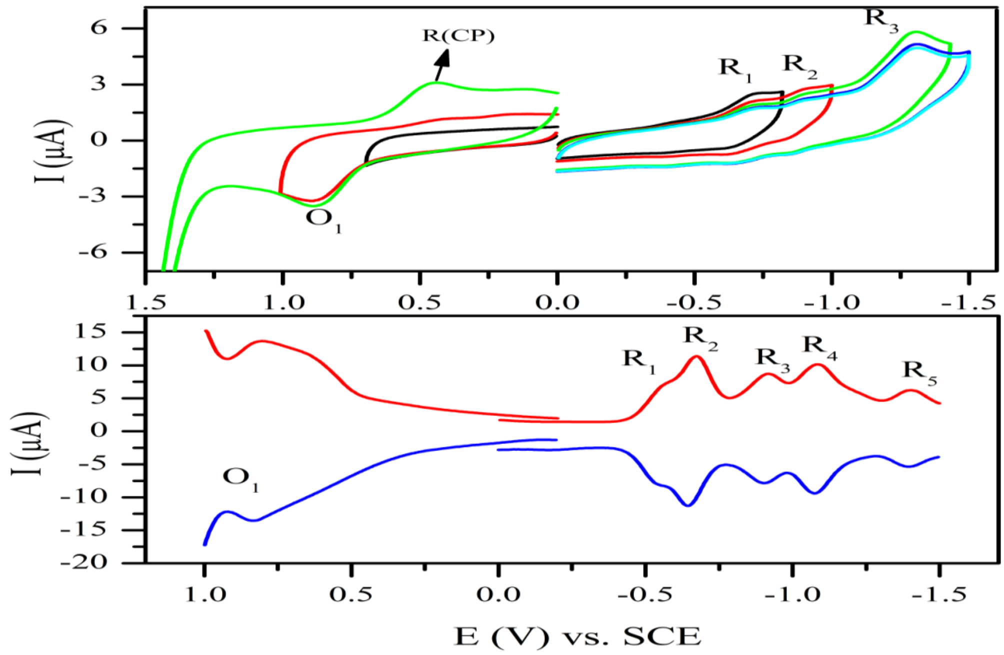

Figure 3.6. CVs (recorded with various vertex potential) (a) and SWVs (b) of α-TiOPc at 0.100 Vs-1 scan rate on a Pt working electrode in DCM/TBAP.

When compared with the voltammetric responses of β - TiOPc, redox processes of α - TiOPc shift to the negative potentials. It is well documented that electron releasing ability of a substituent at α position is more dominant that those at β position. Thus the results are in harmony with the literature. Moreover presence of the substituents at α position decreases the reversibility of the TiOPc complex. As shown in Fig. 3.6 and Table 1 the redox processes of α -TiOPc are all chemically irreversible at all scan rates.

Chemical and electrochemical reversibility is illustrated by the similarity of the peak currents and symmetry of the peaks in the forward and reverse SWVs (Fig. 3.6a). Changing the vertex potential affects the peak character of the oxidation process as shown in Fig. 3.6b. When the potential is shifted from the just positive sides of the O_1 process, O_1 has a electrochemically irreversible character and the process is diffusion controlled. However when the potential goes to the more positive potentials, a chemical reaction occurs and the product of this chemical reaction gives a cathodic wave R(CP) at 0.45 V during the reverse scan.

Fig. 3.7. illustrates the spectral changes recorded during the reduction reactions of α - TiOPc in DCM. When the spectral changes of α –TiOPc are compared with those of β - TiOPc, it is clear that both complexes have similar spectral changes during the electron transfer reactions.

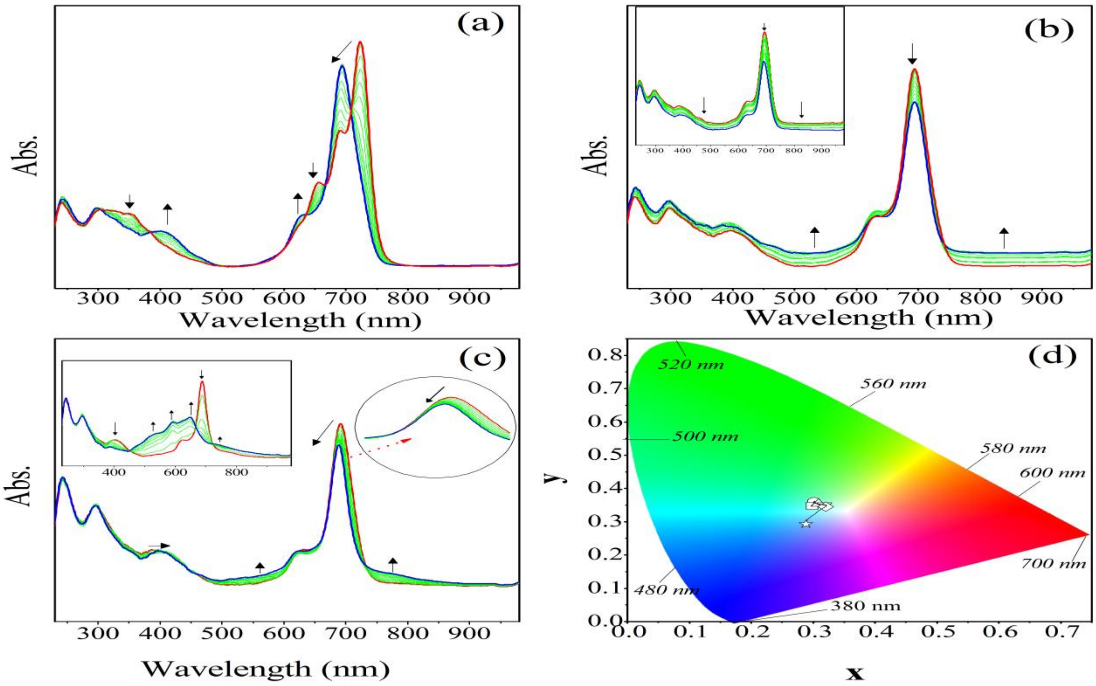

Figure 3.7. *In situ* UV-Vis spectral changes of **α-TiOPc** in DCM/TBAP. **a**) E_{app}= -0.60 V (R_1). **b**) E_{app}= -0.80 V (R_2) (Inset: E_{app}= -0.95 V (R_3)). **c**) E_{app}= -1.20 V (R_4) (Inset: E_{app}= -1.70 V (R_5)). **d**) Chromaticity diagram (each symbol represents the color of electro-generated species; □: $Ti^{IV}OPc^{-2}$, ○: $Ti^{III}OPc^{-2}$, △: $Ti^{III}OPc^{-3}$, ▽: $Ti^{II}OPc^{-3}$, ◇: $Ti^{II}OPc^{-4}$, ☆ : $Ti^{II}OPc^{-5}$.

As shown in Fig. 3.7a, the Q band of at 723 nm shifts to 694 nm during the first reduction process, which can be easily assigned to $[Ti^{IV}OPc^{-2}]$ / $[Ti^{III}OPc^{-2}]^{-1}$ process. Spectral changes shown in Fig. 3.7b and Fig. 3.7b inset recorded during the second and third reduction processes are characteristic changes for ring reduction processes.

However the spectral changes given in Fig 3.7c are characteristic changes for a metal based reduction reaction. Similarly α –TiOPc decomposed during the oxidation reaction like β -TiOPc. Distinct color changes recorded during the electro transfer reactions are represented in Fig 3.7d. The responses of CV, SWV and spectroelectrochemical measurements of α –TiOPc indicate the presence of same mechanism illustrated in eq. [3.1] proposed for β -TiOPc in DCM.

$$Decompose \xleftrightarrow{E_{1/2}=0.80\,V} \underset{original\ complex}{[Ti^{IV}OPc^{-2}]} \xleftrightarrow{E_{1/2}=-0.48\,V} [Ti^{III}OPc^{-2}]^{1-} \xleftrightarrow{E_{1/2}=-0.63\,V} [Ti^{III}OPc^{-3}]^{2-}$$

$$\xleftrightarrow{E_{1/2}=-0.83\,V} [Ti^{III}OPc^{-4}]^{3-} \xleftrightarrow{E_{1/2}=-0.99\,V} [Ti^{II}OPc^{-4}]^{4-} \xleftrightarrow{E_{1/2}=-1.70\,V} [Ti^{II}OPc^{-5}]^{5-} \qquad [3.1]$$

Octa-TiOPc has different electron transfer mechanism than those of β -TiOPc and α –TiOPc complexes. With respect to spectroelectrochemical measurements, while the first two reduction reactions are metal based, the following ones are ring based processes for octa-TiOPc. This order is different for β -TiOPc and α –TiOPc complexes as illustrated in eq.[3.1].

3.2.1.3. Titanyl phthalocyanine peripherally octa substituted with 3,4-(methylendioxy)-phenoxy moieties (octa-TiOPc)

The CV of octa-TiOPc in DMSO/TBAP is represented in Fig. 3.8. Within the electrochemical window of DCM/TBAP in CV measurements, octa-TiOPc complex gives an irreversible one-electron oxidation, and five one-electron reduction processes. When compared with the voltammetric responses of β-TiOPc, tetra substituted complex, the redox processes of octa-TiOPc shift to the positive potentials. General behaviors of all redox reactions have similar trend for both octa and tetra substituted complexes.

But,the redox processes of **octa-TiOPc** shift to the positive potentials with respect to the voltammetric responses of **β-TiOPc**, and **α -TiOPc** complexes.

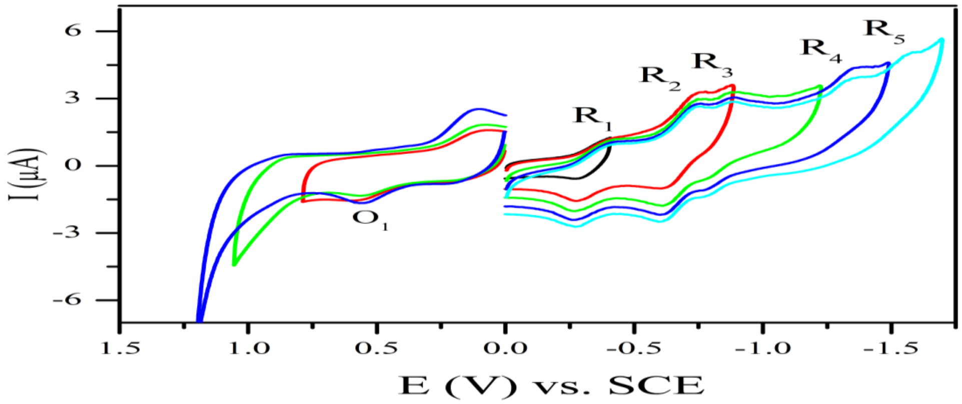

Figure 3.8. CVs of octa-TiOPc recorded with various vertex potential at 0.100 Vs-1 scan rate on a Pt working electrode in DMSO/TBAP.

As illustrated in Fig. 3.9a, the Q band of octa-TiOPc shifts from 701 nm to 689 nm with slight decreasing under the applied potential of -0.50 V. This spectral change is characteristic changes for a metal based reduction, thus can be easily assigned to $[Ti^{IV}OPc^{-2}]$ / $[Ti^{III}OPc^{-2}]^{-1}$ process.

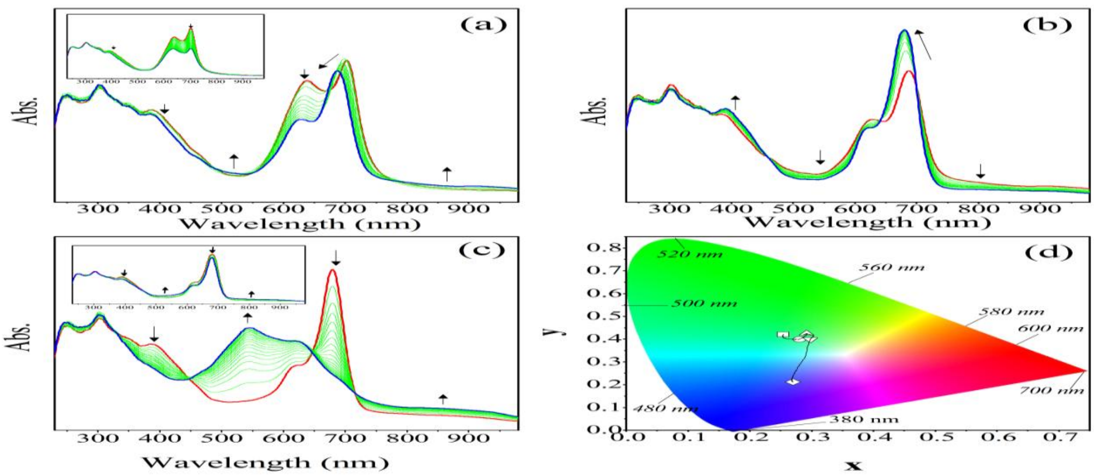

Figure 3.9. *In situ* UV-Vis spectral changes of **octa-TiOPc** in DCM/TBAP. **a**) E_{app}= -0.50 V. **b**) E_{app}= -0.75 V(Inset: E_{app}= -1.00 V). **c**) E_{app}= -1.30 V. **d**) Chromaticity diagram (each symbol represents the color of electro-generated species; □: $Ti^{IV}OPc^{-2}$, ○: $Ti^{III}OPc^{-2}$, △: $Ti^{II}OPc^{-2}$, ▽: $Ti^{II}OPc^{-3}$, ◇: $Ti^{II}OPc^{-4}$.

During the second reduction reaction, the band at 689 nm shift to 680 nm with increasing in intensity (Fig. 3.9b), which is assigned to the further metal based reduction, $[Ti^{III}OPc^{-2}]$ / $[Ti^{II}OPc^{-2}]^{-2}$ process. As shown in Fig. 3.5b and Fig.3.7b, this process is a ring based process for β -TiOPc and α –TiOPc complexes. As shown in Fig 3.9c inset under the applied potential of the third reduction reaction, the Q band decreases slightly without shifting and a small hand start to increases at around 600 nm, which are characteristic spectral changes for the ring reduction reactions of octa-TiOPc. During the fouth reduction process, the Q band disappears completely and a new huge band is recorded at 547 with a shoulder at 623 nm, which are also characteristic spectral changes of a Pc ring-based reduction reaction (Fig 3.9c). When the CV, SWV and the spectral changes are evaluated, the mechanism given in Eq.[3.2] can be proposed for the electron transfer reaction of octa-TiOPc. Similarly octa-TiOPc decomposed during the oxidation reaction like β -TiOPc and α –TiOPc, since all bands decrease in intensity during the oxidation of the complex (Fig. 3.9a inset).

While only the saturation of the green color of the complex changes during the first three reduction reaction a deep blue color(x = 0.2699 and y = 0.2122) (point in Fig. 3.9d) is obtained after the fourth reduction reaction.

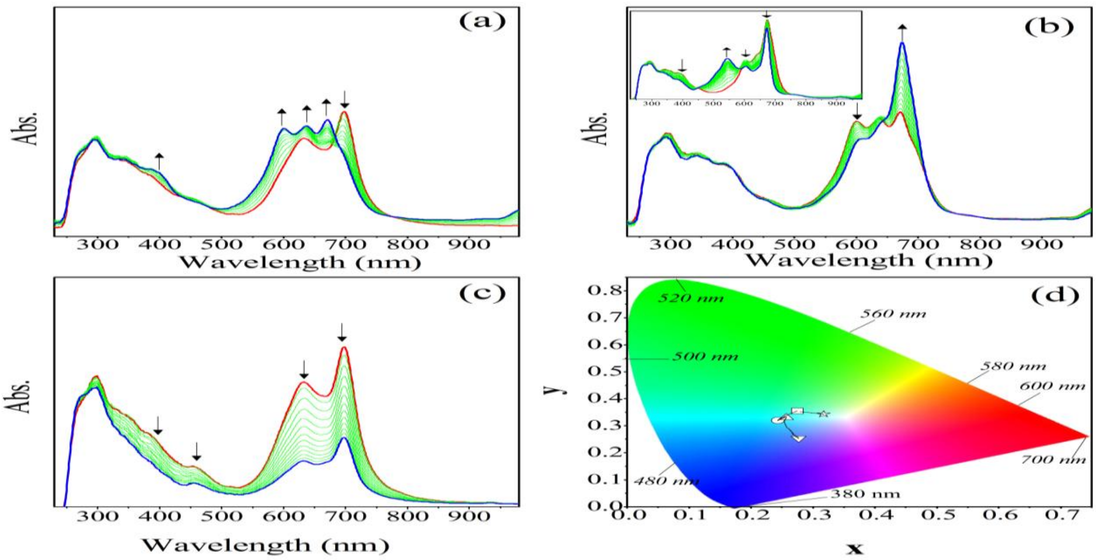

Figure 3.10. *In situ* UV-Vis spectral changes of octa-TiOPc in DMSO/TBAP. a) E_{app}= -0.40 V. b) E_{app}= -0.75 V(Inset: E_{app}= -0.90 V). c) E_{app}= -1.35 V. d) Chromaticity diagram (each symbol represents the color of electro-generated species; □: $Ti^{IV}OPc^{-2}$, ○: $Ti^{III}OPc^{-2}$, △: $Ti^{II}OPc^{-2}$, ▽: $Ti^{II}OPc^{-3}$, ◇: $Ti^{II}OPc^{-4}$.

Two investigate effects of the solvent to the spectral changes of the complexes, spectroelectrochemical measurements of octa-TiOPc were also recorded in DMSO instead of DCM. Fig. 3.10 illustrates the spectral changes of the complex in DMSO.

When compared with the spectral changes recorded in DCM (Fig. 3.9), general trends of the spectral changes in both solvent are similar and the redox processes have the same mechanism given in Eq.3.2.

$$Decompose \xLeftrightarrow{E_{1/2}=0.56\,V} \underset{original\ complex}{[Ti^{IV}OPc^{-2}]} \xLeftrightarrow{E_{1/2}=-0.34\,V} [Ti^{III}OPc^{-2}]^{1-} \xLeftrightarrow{E_{1/2}=-0.68\,V} [Ti^{II}OPc^{-2}]^{2-}$$

$$\xLeftrightarrow{E_{1/2}=-0.84\,V} [Ti^{II}OPc^{-3}]^{3-} \xLeftrightarrow{E_{1/2}=-1.28\,V} [Ti^{II}OPc^{-4}]^{4-} \xLeftrightarrow{E_{1/2}=-1.50\,V} [Ti^{II}OPc^{-5}]^{5-} \quad [3.2]$$

As shown in, the Q band at 700 nm shifts to 672 nm during the first reduction process. Differently a new band at 600 nm is recorded and the π to π* transition band at 637 nm increases in intensity. These bands are not observed in DCM (Fig.3.9a). During the second reduction processes, the band at 672 nm increases in intensity without shift and the band at 600 nm decreases in intensity (Fig.3.10b). Spectral changes during the further reduction processes (Fig.3.10b inset) characterize ring based processes. The complex decomposes also in DMSO during the oxidation reaction as shown in Fig.3.10c, because all bands decrease in intensity. Color changes of the complex during the redox reactions are illustrated in Fig.3.10d.

3.2.1.4. Peripherally tetra imidazole substituted oxo-titanium(IV) phthalocyanine.

Electrochemical analyses of the complex(shown in Figure 3.11) were investigated in solution to propose possible applications of the complexes in different fields of electrochemical technologies. Thus, CV and SWV analysis of the complexes were performed in deaerated DCM and/or DMSO/TBAP electrolyte system on a Pt working electrode.

Figure 3.11 Structure of oxotitanium(IV) phthalocyanine.

Fig. 3.12 and Fig. 3.13 show CV and SWVs of TiOPc in DMSO/TBAP and DCM/TBAP respectively. TiOPc illustrates very similar redox responses in both electrolyte systems. Five reduction and a completely irreversible oxidation processes are recorded. While the first four reduction processes are electrochemically and chemically reversible with respect to ΔE_p and the I_{pa}/I_{pc} ratio of the couples, the fifth one (**R_5**) is an irreversible reduction process.

R_5 process is followed with a chemical reaction, which decreases the chemical reversibility of the previous electron transfer reactions. The product of the chemical reaction gives a wave at around -0.20 V during the reverse potential scan. This chemical reaction is dominant in DMSO with respect to DCM solvent. The oxidation couple (O_1) at 1.05 V is completely irreversible.

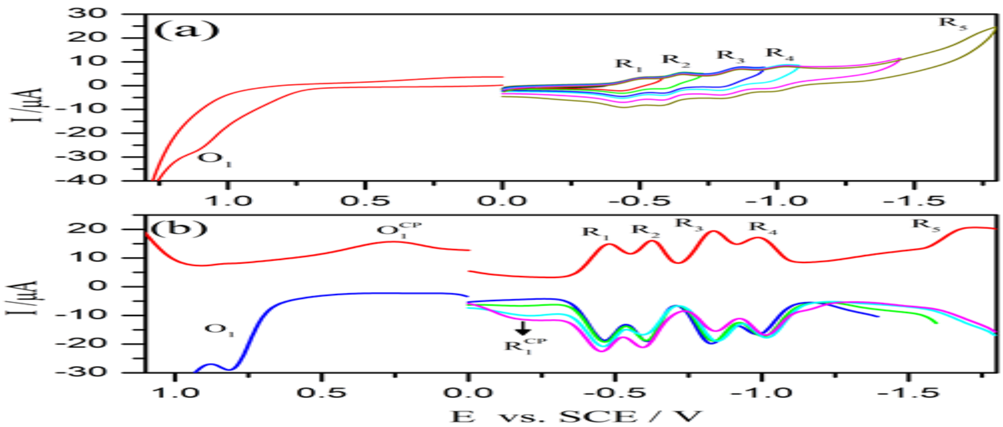

Figure 3.12. (a) CVs of TiOPc recorded with different switching potentials at 0.100 Vs-1 scan rate on a Pt working electrode in DMSO/TBAP. (b) SWV of TiOPc recorded with SWV parameters: step size = 5 mV; pulse size = 100 mV; Frequency = 25 Hz.

To investigate effect of the solvent to the electrochemical behavior of the complex, CV and SWVs responses of TiOPc were also recorded in DCM, a non-coordinating and nonpolar solvent.(Fig. 3.13.) TiOPc gives three well-resolved reversible and 2 irreversible reduction processes. (R_1 at -0.47 V, R_2 at -0.62 V, R_3 at -0.96 V, R_4 at -1.15 and R_5 at -1.35). These redox couples shift to the positive potentials in DCM due to the less electron donor ability of DCM, when compared with those in DMSO. The reduction processes are more reversible and diffusion controlled in DCM, while they are complicated with chemical reactions.

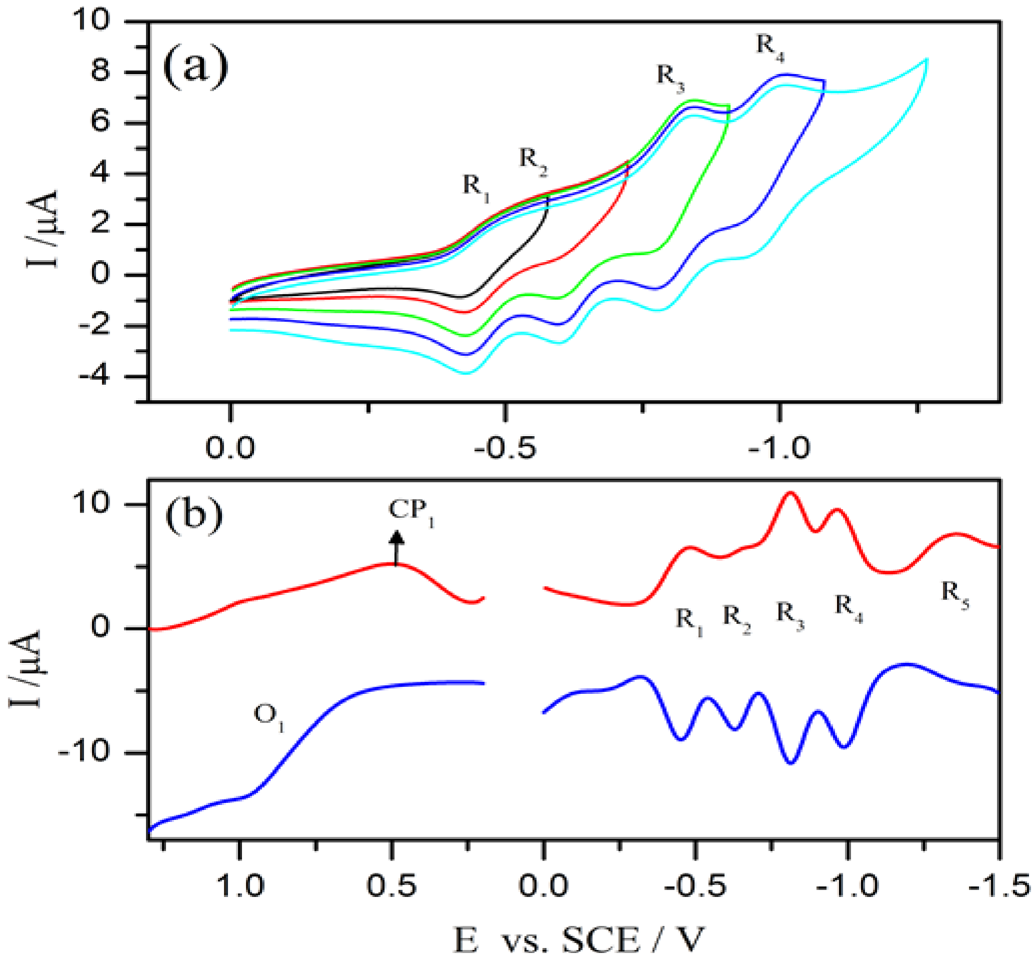

Figure 3.13. (a) CVs of TiOPc recorded with different switching potentials at 0.100 Vs-1 scan rate on a Pt working electrode in DCM/TBAP. (b) SWV of TiOPc recorded with SWV parameters: step size = 5 mV; pulse size = 100 mV; Frequency = 25 Hz.

The reduction of $Ti^{IV}OPc^{-2}$ species has been a subject of some controversy, with some reports proposing ring reduction and others suggesting metal reductions followed with the ring reduction processes.

To perform the assigments of the redox couples of TiOPc in this study, performed spectroelectrochemical measurements were given in Fig. 3.14. During the controlled potential reduction of TiOPc at −0.55 V (Fig. 3.14a), while the absorption of the Q-band corresponding to the neutral $[Ti^{IV}OPc^{-2}]$ species shifts from 704 to 635 nm, a new band is recorded at 590 nm.

As shown in Fig. 3.14a, the process occurred with clear isosbestic points at 640 and 756 nm in the spectra which demonstrate that there is no chemical reaction complicating the electron transfer reaction. These spectral changes are typical for a metal-based reduction process of titanyl phthalocyanine complexes, $[Ti^{IV}OPc^{-2}]$ /$[Ti^{III}OPc^{-2}]^{-1}$. During the second reduction of TiOPc at −0.70 V, the absorption for the Q band at 635 nm and the band at 590 nm decrease slightly, while a new band is recorded at 530 nm. These spectral changes are easily assigned to a ring reduction process, $[Ti^{III}OPc^{-2}]^{-1}$/$[Ti^{III}OPc^{-3}]^{-2}$ redox process. The spectral changes given in Fig. 3.14c indicate the spectral changes recorded during the third reduction at -0.90 V.

During this process, while the bands at 590 and 635 nm decrease in intensity, a new sharp band is recorded at 676 nm. At the same time, the band at 544 nm increases in intensity. These spectral changes characterizes a metal-based reduction process and assigned to the$[Ti^{III}OPc^{-3}]^{-2}$/$[Ti^{II}OPc^{-3}]^{-3}$. The spectral changes during the fourth reduction process indicate a ring-based reduction process (Fig.3.14d)

TiOPc decomposes under the applied potential at 1.00 V during the oxidation reaction, since all bands decrease in intensity as shown in Fig.3.15a. Color changes of the TiOPc in solution during the redox processes were recorded with *in-situ* electrocolorimetric measurements and given in Fig. 3.15b.

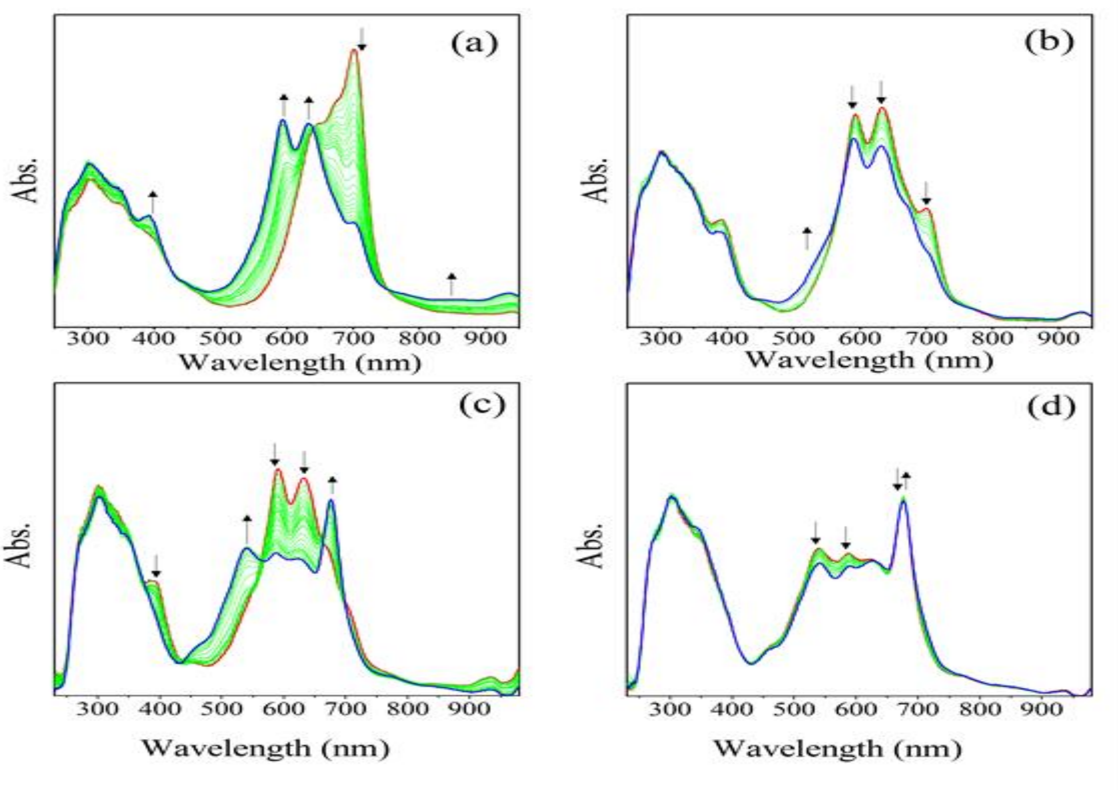

Figure 3.14 *In-situ* UV-Vis spectral changes of **TiOPc** in DMSO. **a**) E_{app}= -0.55 V. **b**)E_{app}= -0.70 V. **c**) E_{app}= = -0.90 V. **d**) E_{app}= = -1.30 V.

When we collect the responses of CV, SWV and spectroelectrochemical measurements and the data from the literature, we can propose the mechanism the following mechanism for the electrochemical responses of TiOPc.

$$[Ti^{IV}OPc^{-1}]^{1+} \xleftrightarrow{E_{1/2}=0.80\,V} [Ti^{IV}OPc^{-2}] \xleftrightarrow{E_{1/2}=-0.48\,V} [Ti^{III}OPc^{-2}]^{1-} \xleftrightarrow{E_{1/2}=-0.63\,V} [Ti^{III}OPc^{-3}]^{2-}$$

$$[Ti^{III}OPc^{-3}]^{2-} \xleftrightarrow{E_{1/2}=-0.83\,V} [Ti^{II}OPc^{-3}]^{3-} \xleftrightarrow{E_{1/2}=-0.99\,V} [Ti^{II}OPc^{-4}]^{4-} \xleftrightarrow{E_{1/2}=-1.70\,V} [Ti^{II}OPc^{-5}]^{5-}$$

[3.3]

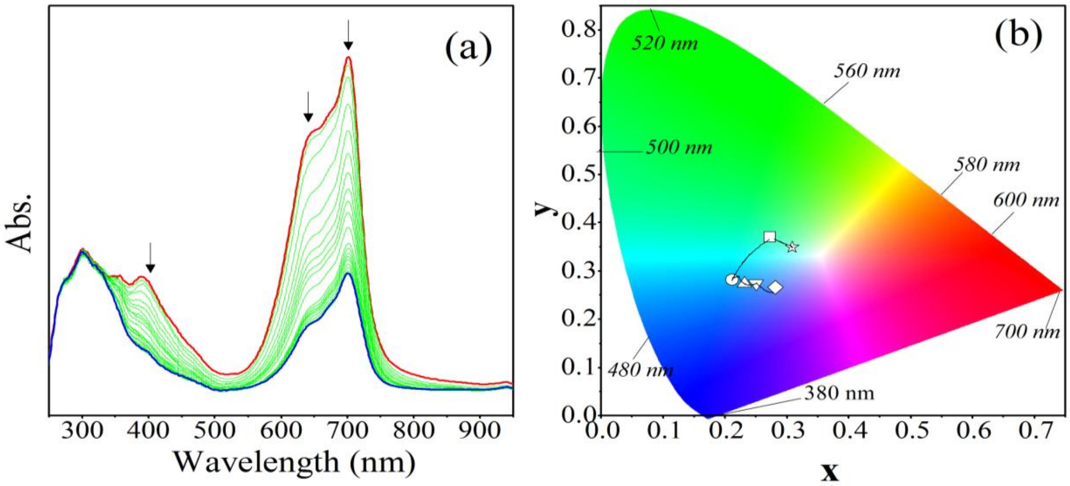

Figure 3.15. *In-situ* UV-Vis spectral changes of TiOPc in DMSO. **a**) = 1.00 V. **b**)Chromaticity diagram (each symbol represents the color of electro-generated species; □: $[Ti^{IV}OPc^{-2}]$, ○:$[Ti^{III}OPc^{-2}]^{-1}$△: $[Ti^{III}OPc^{-3}]^{-2}$, $[Ti^{III}OPc^{-3}]^{-2}$; △ : $[Ti^{II}OPc^{-3}]^{-3}$; ◇: $[Ti^{II}OPc^{-4}]^{-4}$; ☆ : $[Ti^{IV}OPc^{-2}]^{+1}$.

3.2.1.5 Langmuir Blodgett Film Preparation and Sensor Measurements

It is well known that some MPc complexes can be used as sensors for various targets such as gas sensor for O_2, O_3, NH_3 and NO_2 sensing and metal ion sensor for Ag^{+}, Hg^{2+}, Pd^{2+}. Voltammetric and spectroelectrochemical analysis of TiOPc complexes studies here indicate possible usage as sensors for different target species. It is well documented that a redox active species having reversible multi-electron transfer properties at low potentials (potentials near to zero) are candidates for electrochemical sensors. Another desired property of a complex for sensor application is the presence of an electroactive group and a binding side on the structure of the complex behaving as an antenna and receiver for the sensing species. TiOPcs studied here are unique molecular materials carrying both binding sites (substituents) and attractive functional antennas (metal center and Pc ring). It is known that the substituents of MPcs carrying O, N and S atoms behave as binding sites and form stable complexes with soft transition metal ions, such as Ag^{+}, Hg^{2+}, Pd^{2+}. Consequently, we investigated the interaction of the TiOPcs studied here with Ag^{+} and Pd^{2+} ions.

To investigate the interaction of MPcs with the metal ions, TiOPcs solution is titrated with metal ions. Results of these titrations indicate that all of three complexes behave as a sensor for both of Ag^{+} and Pd^{2+} ions in solution.

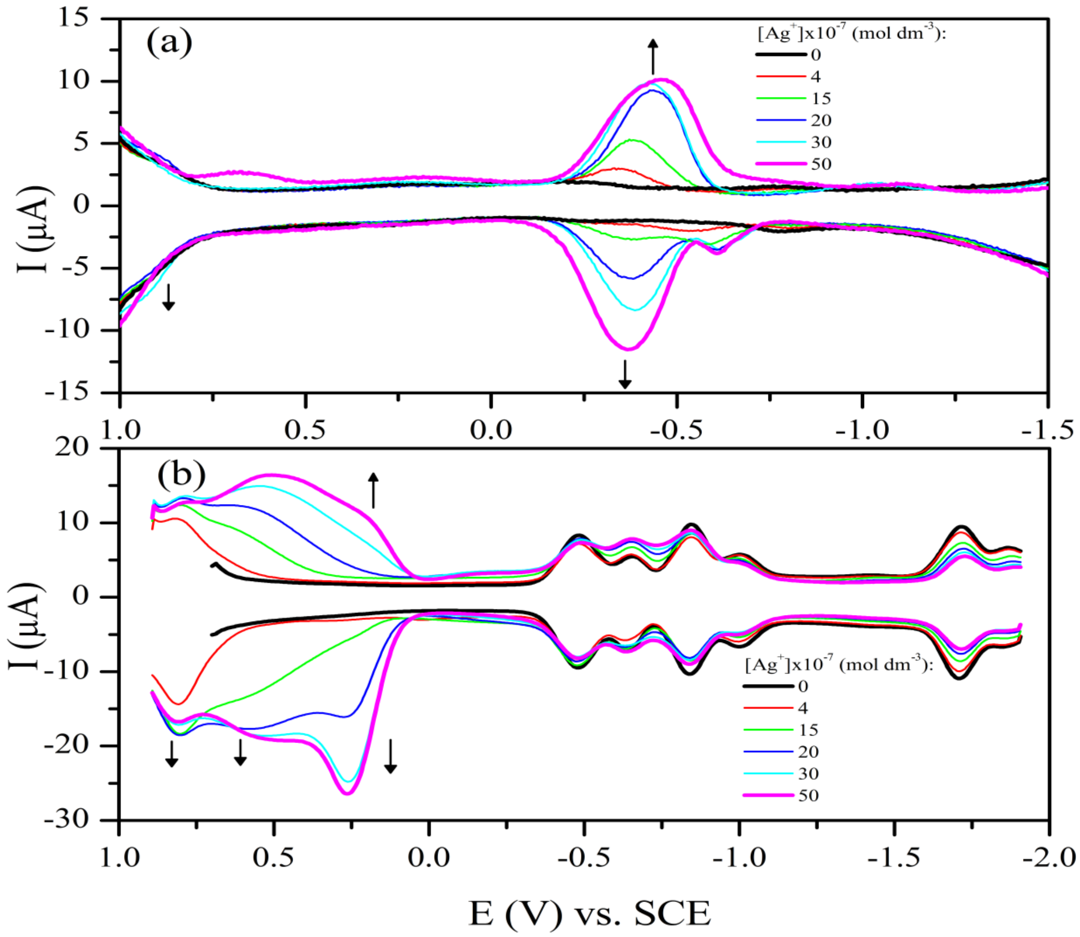

Figure 3.16. a) (Blank test) SWV responses of bare Pt electrode in DMSO/TBAP electrolyte system during titration with Ag^{+}. b) SWV responses of β-TiOPc in DMSO/TBAP electrolyte system on a Pt electrode during titration with Ag^{+}. (Black arrows show the direction of change of SWV responses with respect to Ag^{+} addition.)

Fig. 3.16 represents the SWV responses of the interaction of β-TiOPc with the Ag+ ion in DMSO/$LiClO_4$ electrolyte system on a Pt working electrode as a representative of the sensing measurements in solution. Blank titration of DMSO/LiClO4 electrolyte system without β-TiOPc on a Pt working electrode is also performed (Fig. 3.16a). As shown in Fig. 3.16a, Ag^{+} ions give a reduction/oxidation couple at -0.35 V with the negative potential shift with respect to increasing Ag+ concentration during the SWV scans.

When β-TiOPc presents in solution, voltammetric responses of the system change completely (Fig. 3.16b).

While the reduction couples of decreases slightly in current intensity, new waves are recorded at around 0.27, 0.60 and 0.81 V as a function of the increasing Ag^+ concentration. These data indicate that Ag^+ ions interact with β-TiOPc and the products of this interaction give the redox processes.

The mechanism of the interaction of Ag^+ with β-TiOPc could not be derived from the voltammetric study. However it is well known that soft transition metal ions coordinate with the electron donating groups, O, N and S atoms of ligands. Most probably in this study Ag^+ ions coordinates with the O atoms of β-TiOPc and this coordination cause to the aggregation of β-TiOPc monomers. This aggregate ion decreases the peak current of the redox couples due to the decreasing of the concentration of the redox active species.

For practical applications, a sensing material should be coated on a substrate, thus we coat β-TiOPc on ITO electrode with Langmuir Blodgett technique.

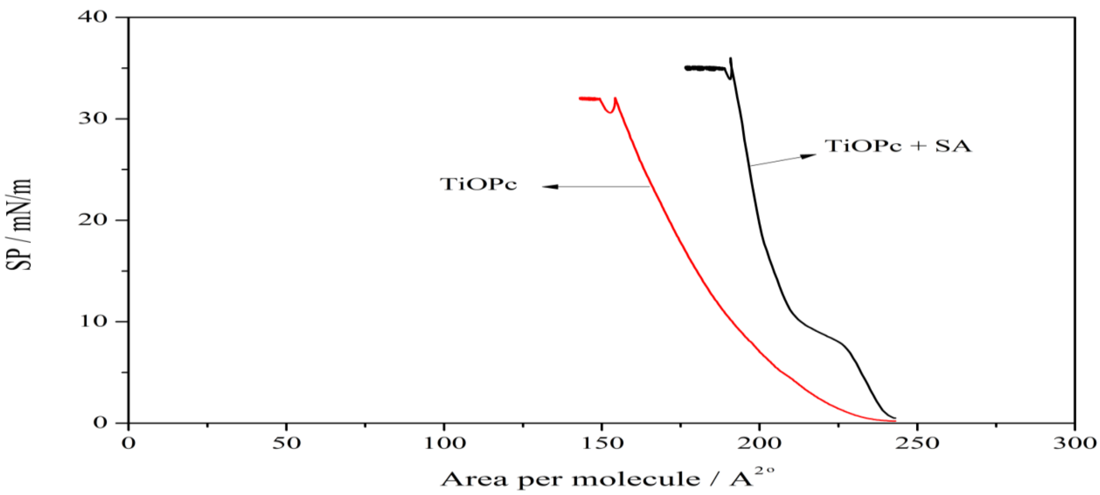

Figure 3.17. π-A isotherms of β-TiOPc and 1:1 mixture of SA and β-TiOPc.

Fig. 3.17 represents the isotherm recorded for β-TiOPc and β-TiOPc-SA mixture (1:1). The limiting area calculated from the slope of the curve indicates the area per β-TiOPc molecule. The area of β-TiOPc is 190 Å2 which is slightly larger than that observed for unsubstituted bisphthalocyanines , but it is similar with the limiting areas of reported substituted phthalocyanines (eight C_4 groups or phenyl per ring). Limiting areas of β-TiOPc (190 Å2) suggests edge-on orientations of the complex on the water subphase. Presence of SA in β-TiOPc just increases the limiting area to 210 Å2. Without SA, β-TiOPc could not be transferred on the ITO substrate as monolayer.

While the transfer rate for the first up stroke is one, this transfer rate decreases during the further up stroke transfers. Transfer rates for all down strokes are recorded as approximately zero. This means that β-TiOPc is transferred on ITO surface as Z types transfer without SA. However when 1:1 mixture of SA and β-TiOPc is used all transfer rated during both up stroke and down stroke are recorded as one, which indicates a Y types transfer. β-TiOPc-SA mixture is coated on the ITO surface for sensing studies.

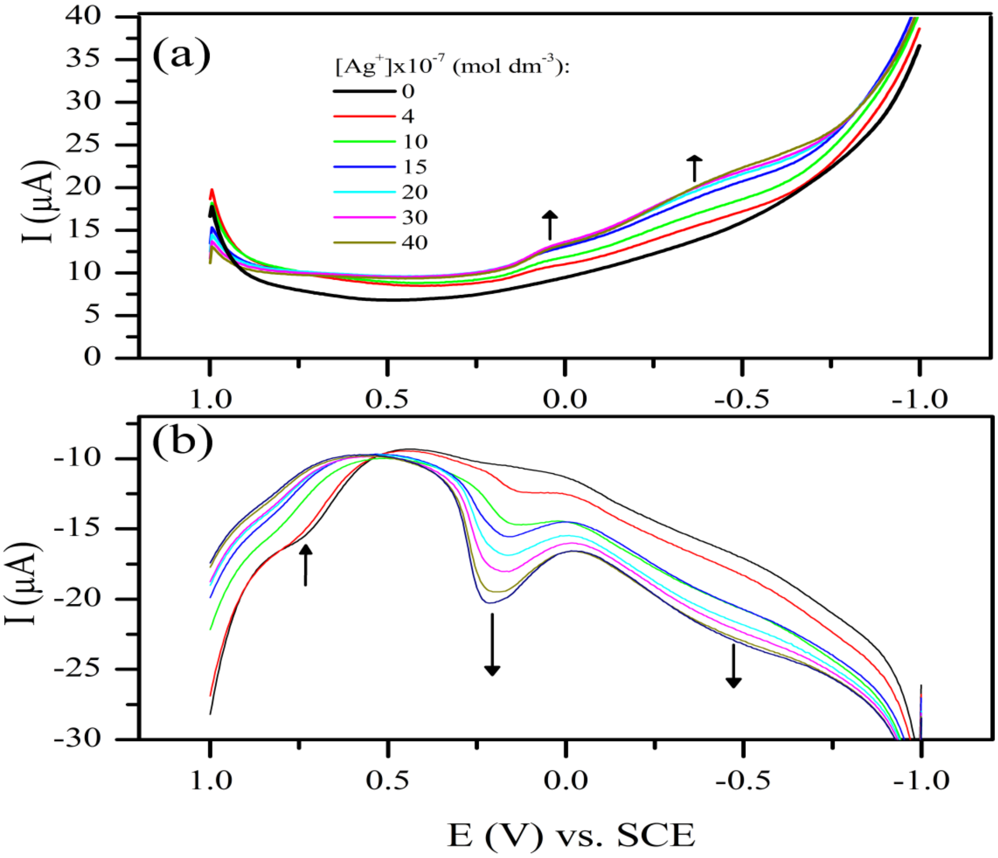

Figure 3.18. SWV responses of ITO/ β-TiOPc+SA(LB) electrode in H2O/LiClO4 electrolyte system during titration with Ag+. a) Cathodic potential scans; Ei = +1.0 V and Ef = -1.0 V. b) anodic potential scans; Ei = -1.0 V and Ef = +1.0 V. (Black arrows show the direction of change of SWV responses with respect to Ag+ addition.)

SWV responses of the interaction of ITO/ β-TiOPc+SA(LB) electrode with the Ag+ ion in $H_2O/LiClO_4$ electrolyte system are represented in Fig. 3.18. As shown in the SWV (Fig. 3.16) responses of the system, β -TiOPc gives an irreversible reduction process at -0.80 V and an oxidation process at 0.80 V without Ag^+.

When Ag^{+} is added gradually, a new reduction wave is recorded at -0.23 V during the cathodic potential scan and an anodic wave is recorded at 0.17 V with positive potential shift as a function of increasing Ag+ concentration. Moreover, the oxidation wave at 0.80 V shifts to positive potentials with decreasing in current intensity. These voltammetric behaviors indicate the interaction of ITO/ β-TiOPc+SA(LB) electrode with the Ag+ ion.

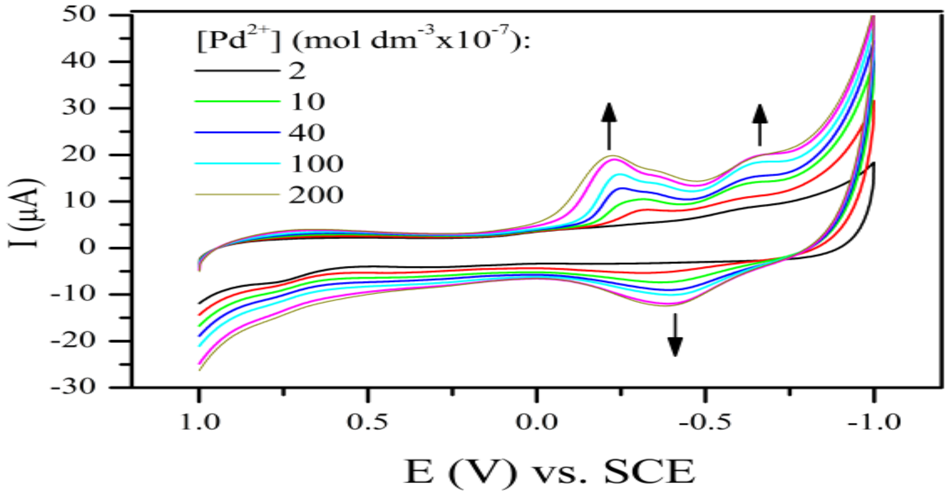

Figure 3.19. CV responses of ITO/ β-TiOPc+SA(LB) electrode in $H_2O/LiClO_4$ electrolyte system during titration with Pd^{+2}.

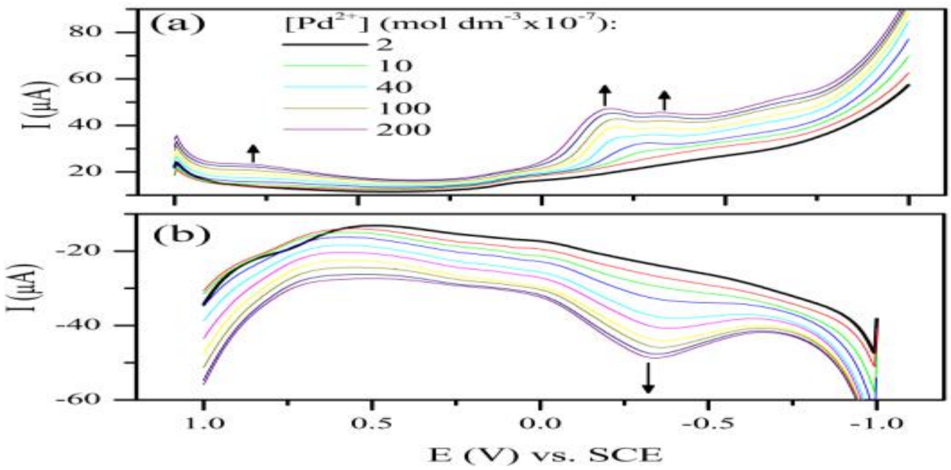

Figure 3.20. SWV responses of ITO/ β-TiOPc+SA(LB) electrode in H2O/LiClO4 electrolyte system during titration with Pd+2+. a) Cathodic potential scans; Ei = +1.0 V and Ef = -1.0 V. b) Anodic potential scans; Ei = -1.0 V and Ef = +1.0 V. (Black arrows show the direction of change of SWV responses with respect to Pd+2 addition.)

Fig. 3.19 and Fig. 3.20 represents the CV and SWV responses of the interaction of ITO/ β-TiOPc+SA(LB) electrode with the Pd^{2+} ion in $H_2O/LiClO_4$ electrolyte system. Redox responses of ITO/ β-TiOPc+SA(LB) electrode to the Ag^+ and Pd^{2+} ion are different than each other. As shown in Fig. 3.19 and 3.20, two reduction wave during the cathodic scan and an anodic wave during the reverse scan at cathodic potentials are observed as a function of gradual increasing of the Pd^{2+} ion concentration. These data indicate the interaction of Pd^{2+} ion with β -TiOPc. Since ITO electrode did not give any response to the addition of Pd^{2+} ion during the blank test, we may easily assign all changes on the redox responses of ITO/ β-TiOPc+SA(LB) electrode to the interaction of Pd^{2+} ion with β-TiOPc.

3.2.1.6. Electrocatalytic oxygen reduction reaction (ORR) measurements

We aim to use these complexes as electrocatalysts for oxygen reduction reaction as a sequel of our energy based studies. Redox responses of all TiOPcs were recorded with and without O_2 to investigate the interaction of molecular oxygen with the complexes and effects of these interactions to the redox responses of TiOPcs and O_2. These measurements indicated that all complex interact with O_2. While these interactions have a general trend for all complexes, some specific differences are recorded with respect to different structure of the complexes. Comparative CV and SWV responses of octa-TiOPc recorded in *"case 3"* (both of TiOPc and O_2 are present in electrolyte) are given in Fig. 3.21 and 3.22 for comparison with the responses of octa-TiOPc in "*case 1*" (only TiOPc is present in electrolyte) and responses of O_2 in "*case 2" (only O_2 is present in electrolyte)* (Fig. 3.21 inset). Inset graph in Fig. 3.21 shows the CV responses of O_2, which is dissolved in DCM/TBAP electrolyte system without octa-TiOPc (*case 2*). It is shown in the literature that that molecular O_2 reduces to superoxide in the non-aqueous environment at around -1.0 V vs. SCE depending on the electrolyte system and type of the working electrode. Similarly oxygen/superoxide (O_2/O_2^-) reduction couple is recorded at -1.12 V (E_{pc}) in DCM at 0.10 mVs^{-1} scan rate ant this process shifts up to -1.46 V with increasing of O_2 concentration.

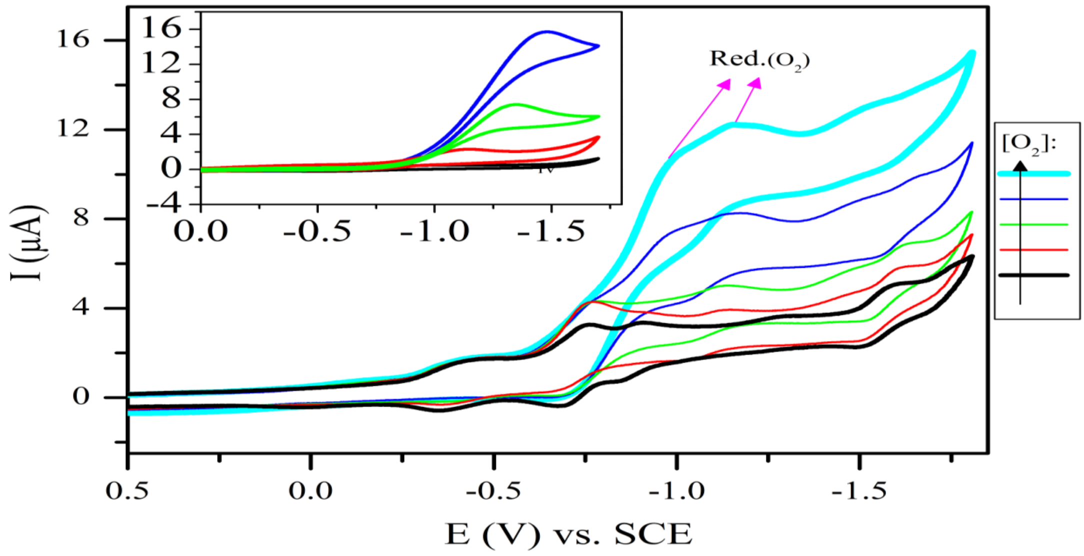

Fig. 3.21. CVs of **octa-TiPc** recorded at 0.100 Vs^{-1} scan rate with increasing amounts of O_2 in DCM/TBAP electrolyte system on Pt working electrode. (Inset: oxygen reduction reaction on a Pt electrode at 0.100 Vs^{-1} scan rate with increasing amounts of O_2 in DCM/TBAP electrolyte system).

The voltammetric responses of octa-TiOPc in the O_2 dissolved DCM/TBAP electrolyte system (*case 3*) were recorded to monitor the interaction of octa-TiOPc with O_2 (Fig. 3.21 and 3.22). Without O_2, octa-TiOPc gives five redox couples sequentially Ic/Ia at -0.40 V, IIc/IIa at -0.72 V, IIIc/IIIa at -0.87 V, IVc/IVa at -1.24 V, and Vc/Va at -1.55 V in DCM/TBAP electrolyte without O_2 (in *case 1)*. These redox responses change considerable with increasing O_2 concentration (in *case 3*). These redox responses are recorded more clearly with SWV measurements given in Fig. 3.22 During the forward SWV scans (E_i=1.0 V and E_f=-1.80 V) and because of the increasing O_2 concentration (Fig. 3.22a), these are the changes of octa-TiOPc responses: first, IVc peak disappears immediately while the others decrease in current intensity. Then II c, Ic and IIIc peak disappears sequentially, while Vc peak shifts to negative potentials. During this process two new waves are also recorded at -0.94 V and -1.13 V.While the second peak at -1.13 V is immediately recorded and stay approximately constant in current intensity during the initial bubbles of oxygen addition, the wave at around 0.94 V increases in current intensity continuously with the negative potential shifts as a function of the increasing O_2 concentration.

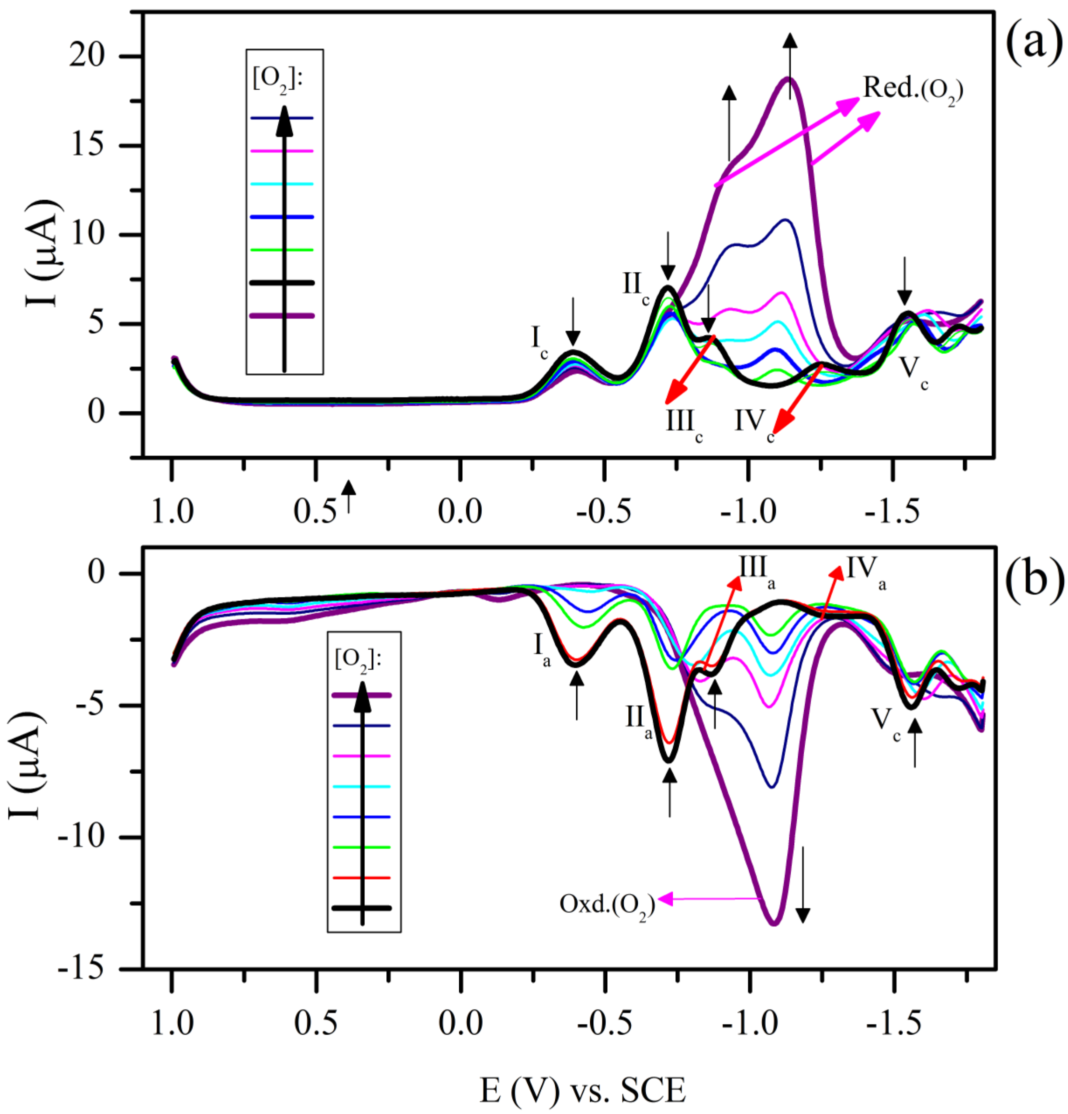

Fig. 3.22. SWVs of **octa-TiPc** recorded at 0.100 Vs^{-1} scan rate with increasing amounts of O_2 in DCM/TBAP electrolyte system on Pt working electrode. (**a**) Forward SWV: Initial potential E_i = 1.0 V and final potential E_f = -1.80 V. (**b**) Backward SWV: E_i = -1.80 V and E_f = 1.0 V.

These new waves can be easily assigned to the reduction of the interaction products of **octa-TiOPc** and O_2 to the superoxide or peroxide species. During the reverse SWV scans (Initial potential (E_i) = -1.80 V and final potential (E_f) = 1.0 V), similar voltammetric responses are recorded. Initially IIIa and IVa peaks, and then Ia peak disappears completely due to the interaction with oxygen and a new anodic peak (Oxd (O_2)) is recorded at -1.01 V.

When octa-TiOPc responses in “*case 3*” is compared with the redox responses of O_2 in “*case 2*”, it is clear that ORR splits into two waves in “*case 3*”, while only one wave is recorded in “*case 2*”.

This voltammetric difference indicates the catalytic effects of octa-TiOPc and this catalytic effect decreases the ORR at about 0.50 V and changes the products of the ORR. Moreover, redox response of ORR gets more reversible in “*case 3*”.

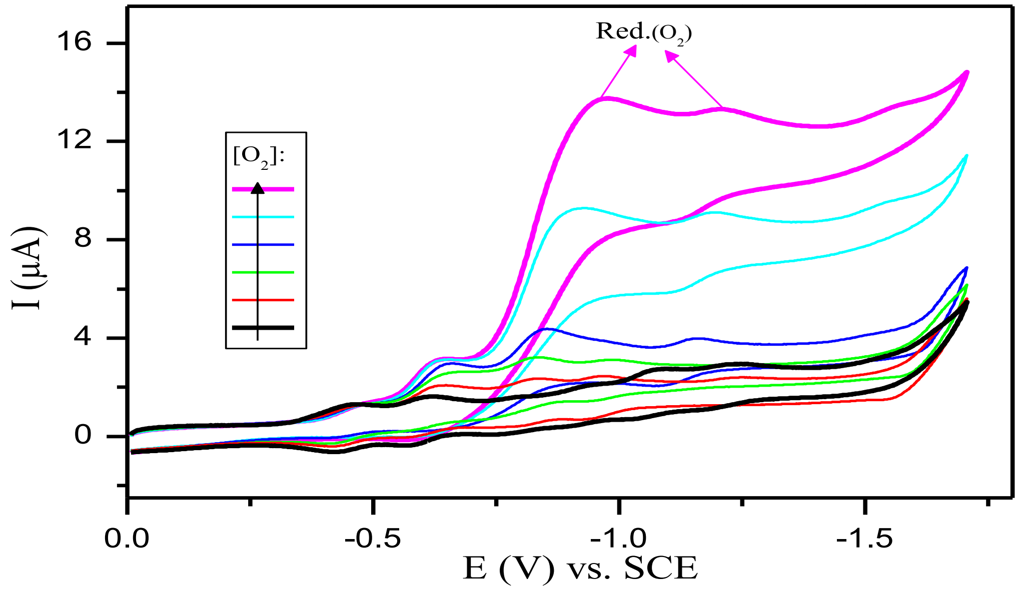

Fig. 3.23. CVs of **α -TiPc** recorded at 0.100 Vs^{-1} scan rate with increasing amounts of O_2 in DCM/TBAP electrolyte system on Pt working electrode.

α-TiOPc (CVs are in Fig. 3.23) and β-TiOPc (CVs are in Fig. 3.24) exhibit similar redox responses with those of octa-TiOPc in “*case 3*”.

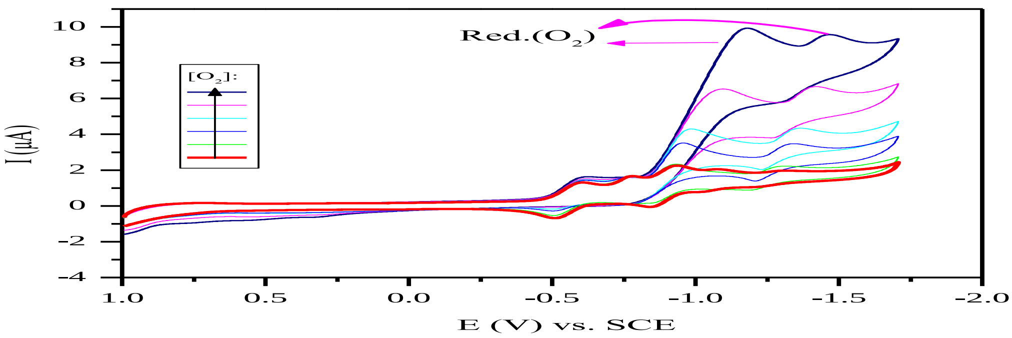

Fig. 3.24. CVs of **β-TiPc** recorded at 0.100 Vs^{-1} scan rate with increasing amounts of O_2 in DCM/TBAP electrolyte system on Pt working electrode.

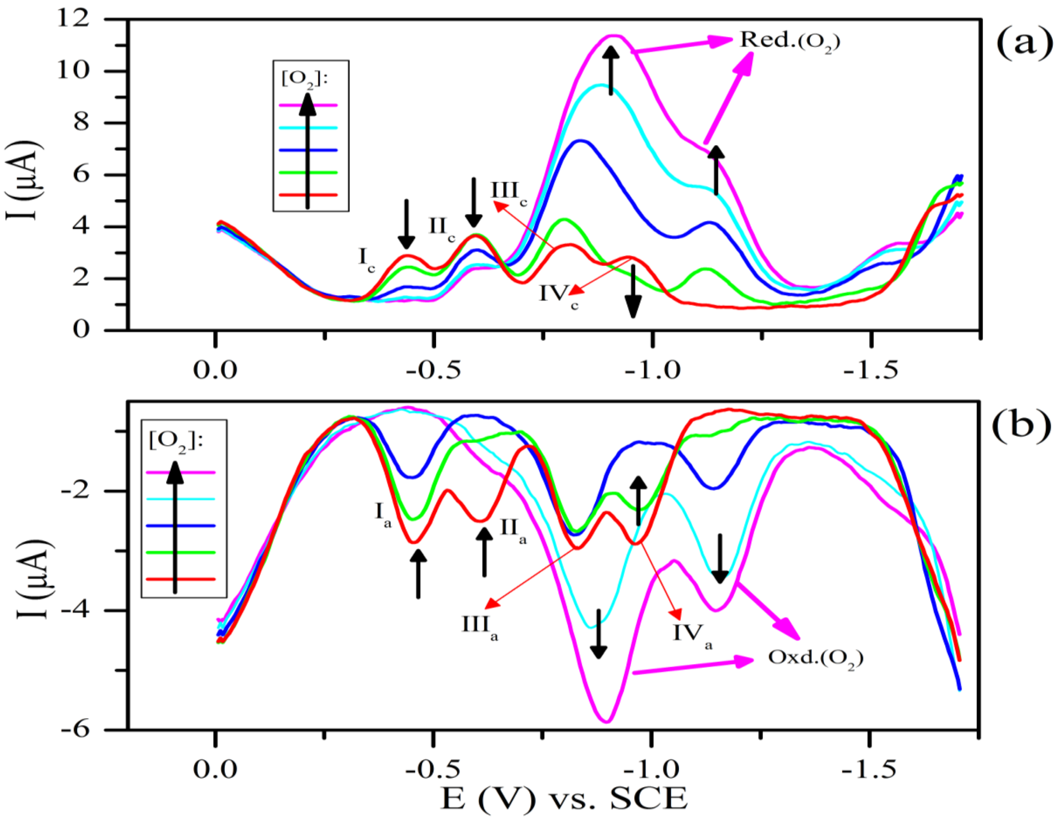

Fig. 3.25. SWVs of **α-TiPc** recorded at 0.100 Vs^{-1} scan rate with increasing amounts of O_2 in DCM/TBAP electrolyte system on Pt working electrode. (**a**) Forward SWV: E_i = 0.0 V and E_f = -1.80 V. (**b**) Backward SWV: E_i = -1.80 V and E_f = 0.0 V.

During the reaction of α-TiOPc with O_2, II_c and IV_c peaks during the forward SWV scans (Fig. 3.25a) and Ia, IIa and IVa peaks during the reverse SWV scans (Fig. 3.25a) disappear completely while the others decreases in current intensity. At the same times, new cathodic waves (Red O_2) are recorded at -0.83 V (shift to -0.93 V) and -1.13 V due to the ORR. While octa-TiOPc gives only one anodic wave, α-TiOPc gives two anodic waves (labeled as Oxd.(O_2)) at -0.89 V and -1.15 V. Same ORR responses are also recorded with **β-TiOPc**. Differences between these complexes are the behaviors of ORR. The cathodic waves assigned to ORR are recorded at the more negative potentials (-0.98 V and -1.29 V) and shift to the more negative potentials (-1.14 V and -1.46 V) with increasing oxygen concentration, when **β-TiOPc** is used as the electrocatalyst. Similar redox trends are recorded during the reverse SWV scans.

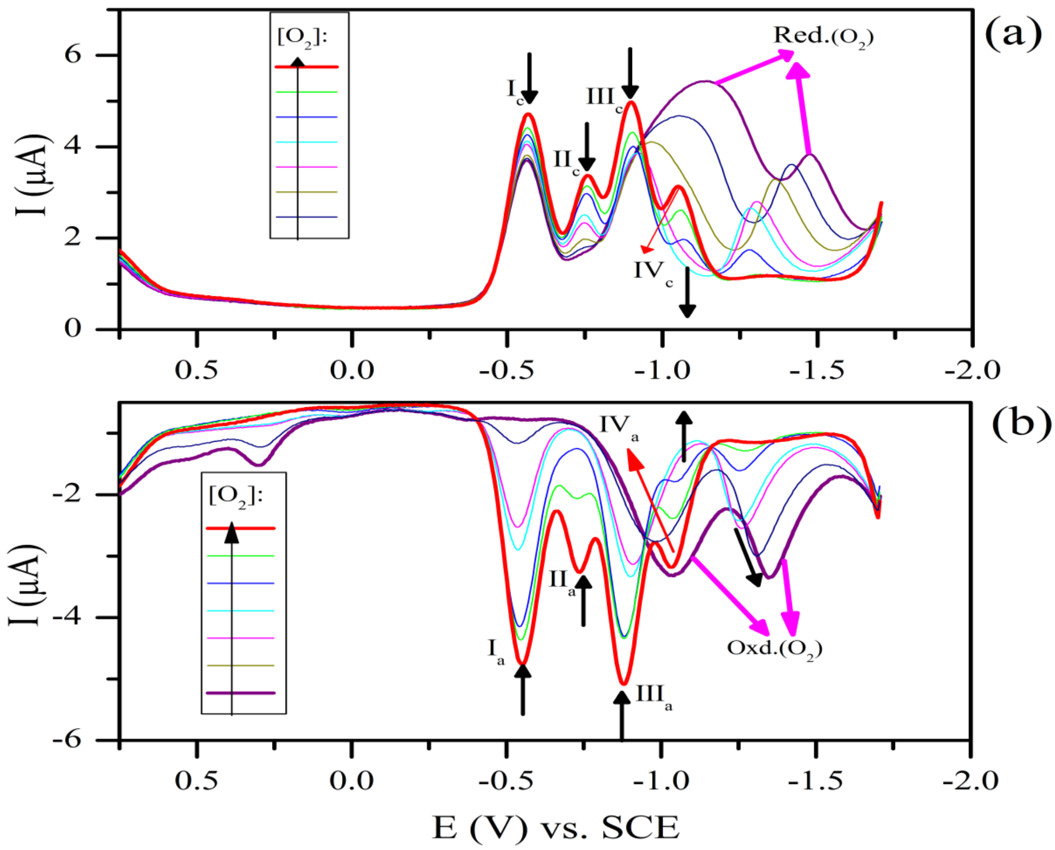

Fig. 3.26. SWVs of **β-TiPc** recorded at 0.100 Vs^{-1} scan rate with increasing amounts of O_2 in DCM/TBAP electrolyte system on Pt working electrode. (**a**) Forward SWV: E_i = 0.70 V and E_f = -1.80 V. (**b**) Backward SWV: E_i = -1.80 V and E_f = 0.70 V.

When the redox responses illustrated in Fig. 3.26 (β-TiOPc) are compared with those in Fig. 3.21 (octa-TiOPc) and Fig. 3.22 (α-TiOPc), it is clearly drawn that electro catalytic ORR activity of β-TiOPc is less than those of α-TiOPc and octa-TiOPc. Highest catalytic activity is recorded with α-TiOPc with respect to the decreasing of the ORR potentials. These catalytic activity differences are most probably resulted from the different degrees of the effects of the electron releasing 3,4-(methylendioxy)-phenoxy substituent to the Pc ring electron density. Since it is well known that the substituents present at α position of Pc ring is more effective than the β- position to the electrochemical and spectral response of Pc ring. Increasing the electron density of the Pc ring also effect the electron transfer properties, especially reduction and /or oxidation potentials of the metal centers. These effects also alter the electrocatalytic activities of the complexes.

To investigate the effect of the solvent to the catalytic activities of the complexes for ORR, similar measurements were also performed in DMSO, which is a polar coordinating solvent.

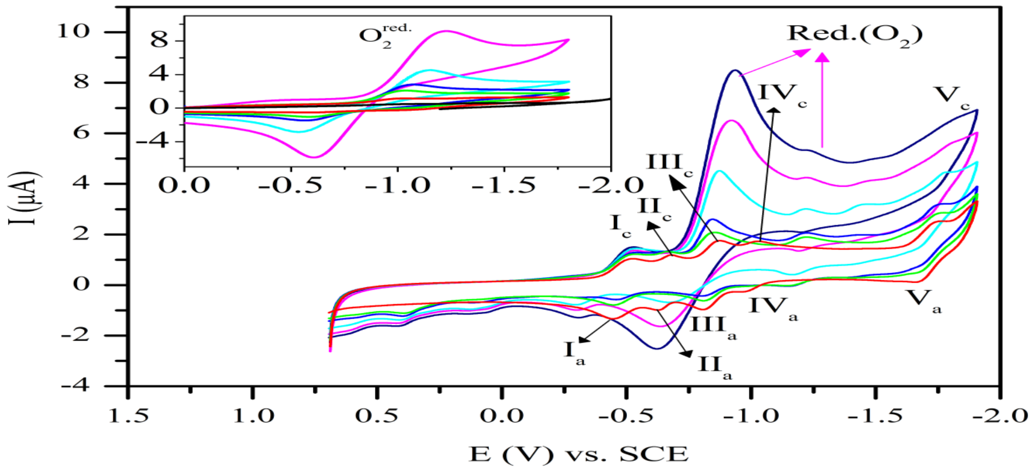

Fig. 3.27. CVs of **β-TiPc** recorded at 0.100 Vs^{-1} scan rate with increasing amounts of O_2 in DMSO/TBAP electrolyte system on Pt working electrode. (Inset: oxygen reduction reaction on a Pt electrode at 0.100 Vs^{-1} scan rate with increasing amounts of O_2 in DMSO/TBAP electrolyte system).

Fig. 3.27 and 3.28 represents CV and SWV outcomes of β-TiOPc in "*case 3*" and responses of O2 in "*case 2*". Fig. 3.27 (inset) gives CV responses of O_2 dissolved in DMSO (*case 2*). Quasi-reversible oxygen/superoxide (O_2/O_2^-) couple is recorded at -1.00 V in DMSO at 0.100 Vs^{-1} scan rate, which shifts up to -1.25 V with increasing oxygen concentration. This ORR wave is recorded at -0.83 V and shifts up to -0.93 V in "case 3" (Fig. 3.27). when β-TiOPc is present in the electrolyte system (Fig. 7). These data indicate that presence of β-TiOPc in the DMSO electrolyte system catalyzes ORR and as a result of this catalytic reduction ORR process is recorded at less negative potential (about 0.20 V) than those recorded in in "*case 2*". SWV responses of the interaction reaction of β-TiOPc with O_2 are represented in Fig. 3.26. Interaction reaction of β-TiOPc with O_2 gives generally similar SWV responses in both DCM and DMSO. Two main differences are observed; Oxd (O_2) peak shifts up to -0.67 V in DMSO, while this wave is recorded at -1.00 V in DCM. Red(O_2) waves are also recorded at less negative potentials (at-0.90 V and -1.23 V) without any shifting in DMSO.

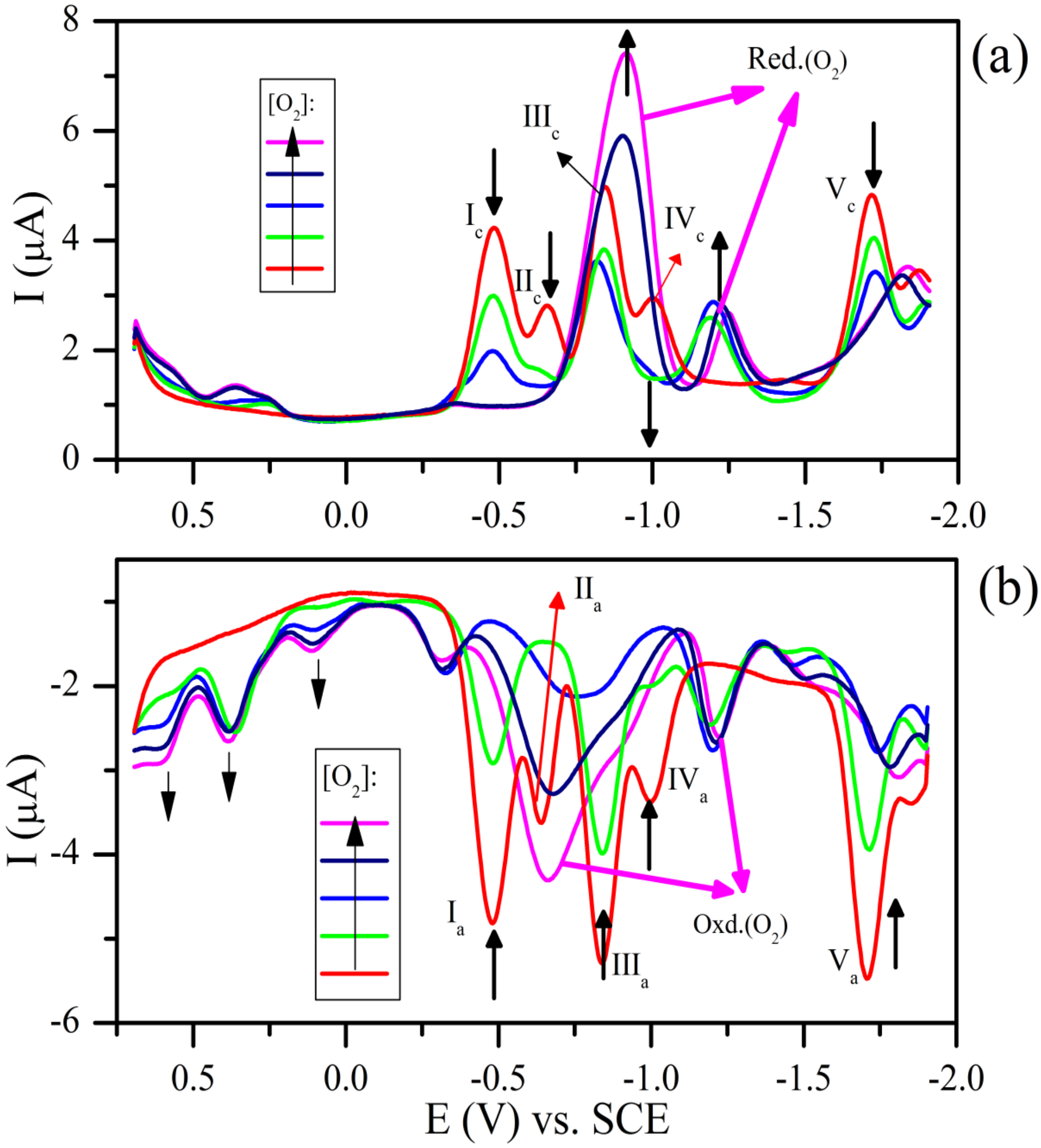

Fig. 3.28. SWVs of **β-TiPc** recorded at 0.100 Vs^{-1} scan rate with increasing amounts of O_2 in DMSO/TBAP electrolyte system on Pt working electrode. (**a**) Forward SWV: E_i = 0.70 V and E_f = -1.80 V. (**b**) Backward SWV: E_i = -1.80 V and E_f = 0.70 V.

These waves are recorded at approximately 0.10 V higher potentials and shifts in high extend in DCM. These voltammetric responses indicate higher electro catalytic activity of β-TiOPc in DMSO than those in DCM.

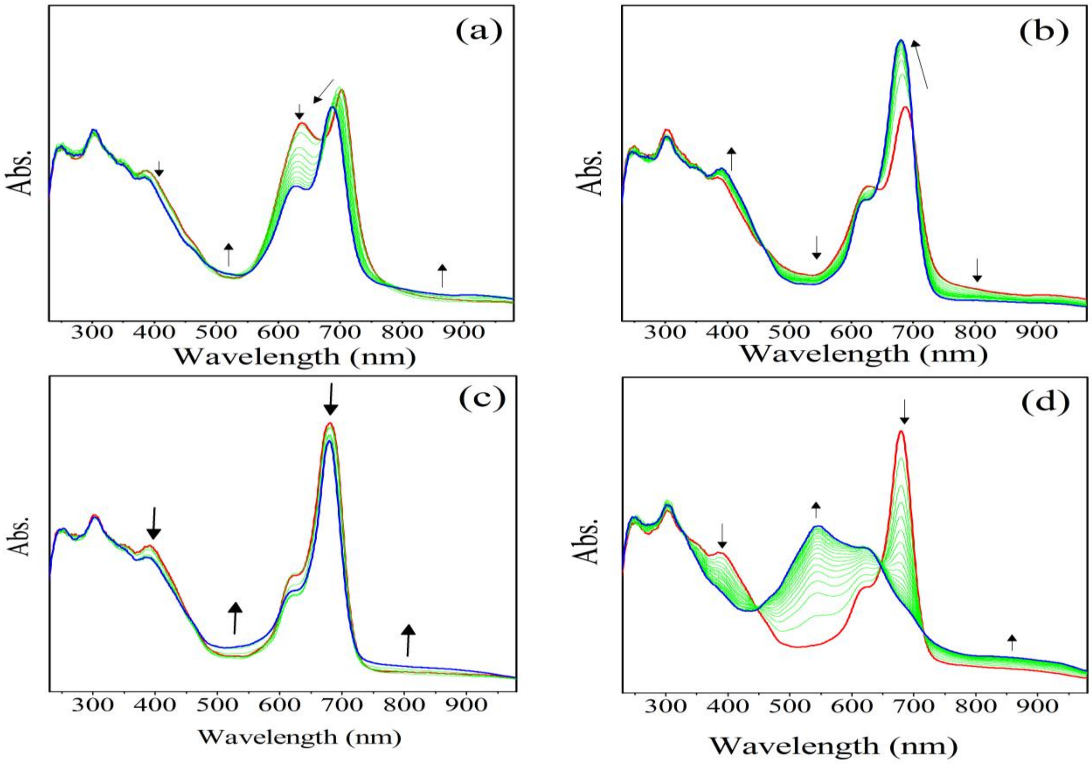

Fig. 3.29. *In-situ* UV-vis spectral changes of **octa-TiPc** in DCM/TBAP electrolyte without molecular oxygen (purged with N_2) **a**) E_{app}= -0.50 V. **b**) E_{app}= -0.75 V. **c**) E_{app}= -1.20 V. **d**) E_{app}= -1.50 V

In-situ spectroelectrochemical studies were applied to support the interaction between TiOPcs and O_2. All TiOPcs showed very similar in situ spectroelectrochemical responses in solutions saturated with molecular oxygen, although their responses were different in oxygen-removed solutions. Fig. 3.29 and 3.30 illustrate in-situ UV-vis spectral changes of octa-TiOPc in "*case 1* and *3"* respectively in DCM/TBAP electrolyte system the applied constant potential (E_{app}) at the potentials of the redox processes as a representative of TiOPcs.

To illustrate the spectral changes of octa-TiOPc without molecular oxygen in situ spectroelectrochemical responses of octa-TiOPc is recorded in oxygen-removed DCM/TBAP electrolyte system (*case 1*) and these responses were compared with those recorded in oxygen-saturated system (*case 3*). As illustrated in Fig. 3.29a, the Q band of octa-TiOPc shifts from 701 nm to 689 nm with slight decreasing under the applied potential of -0.50 V. This spectral change is characteristic changes for a metal based reduction of the complex, $[Ti^{IV}OPc^{-2}]$ / $[Ti^{III}OPc^{-2}]^{-1}$ process.

During the second reduction reaction under -0.85 V, the band at 689 nm shift to 680 nm with increasing in intensity (Fig. 3.29b), which is assigned to, $[Ti^{III}OPc^{-2}]^{-1}$ / $[Ti^{II}OPc^{-2}]^{-2}$ process. As shown in Fig 3.29c the Q band decreases slightly without shifting and a band increases at around 600 nm under the-1.20 V potential application. These spectral changes are assigned to $[Ti^{II}OPc^{-2}]^{-2}$/ $[Ti^{II}OPc^{-3}]^{-3}$. During the fourth reduction process, the Q band disappears completely and a new huge band is recorded at 547 with a shoulder at 623 nm, which are also characteristic spectral changes of $[Ti^{II}OPc^{-3}]^{-3}$/ $[Ti^{II}OPc^{-4}]^{-4}$ reaction (Fig 3.29d).

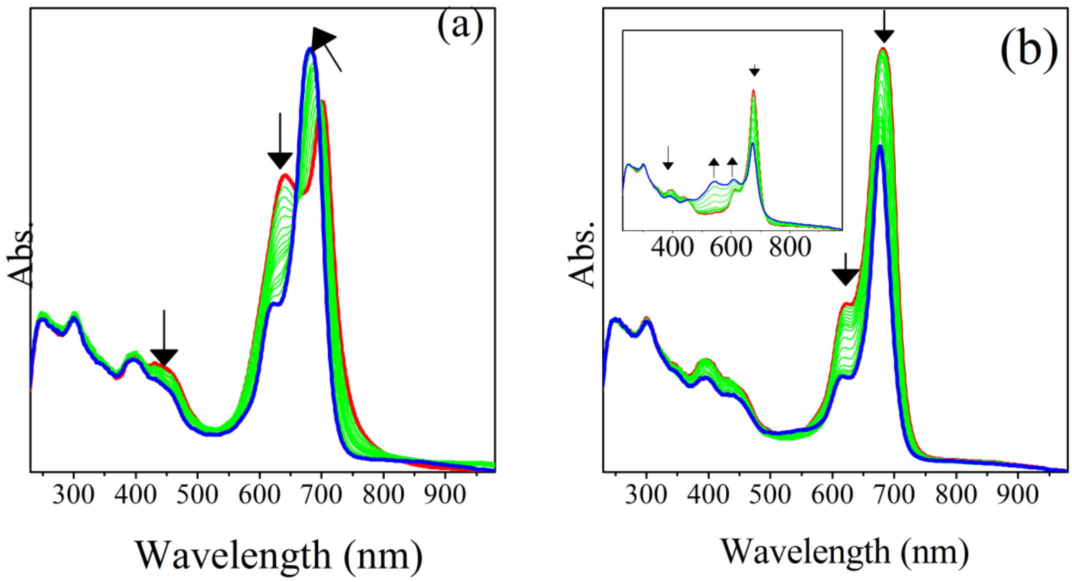

Fig. 3.30. *In-situ* UV-vis spectral changes of octa-TiPc in DCM/TBAP electrolyte saturated with O_2. a) E_{app}=-0.50 V. b) E_{app}= -1.25 V (inset: E_{app}= 0.00 V.).

For comparison, same in-situ spectroelectrochemical measurements of octa-TiOPc were performed in oxygen saturated DCM/TBAP electrolyte (Fig 3.30). Under the open circuit potential, spectra of octa-TiOPc did not change with time both in "*case 1* and in *"case 3"*. This indicates that $[Ti^{II}Pc^{-2}]$ do not interact with O_2. During the first reduction process at -0.50 V, same spectral changes are recorded both in "*case 1*" (Fig 9a) and in "*case 3*" assigned to $[Ti^{IV}OPc^{-2}]$ / $[Ti^{III}OPc^{-2}]^{-1}$. These spectral changes indicate that $[Ti^{IV}OPc^{-2}]$ species do not interact with O_2. When -1.25 V was applied to the working electrode, all bands decrease continuously in the spectra of the complex in "*case 3*" .These spectral changes are different than those for the second reduction of **octa-TiOPc** recorded in "*case 1*".

This behavior indicates interaction of reduced form of the complex, $[Ti^{III}OPc^{-2}]^{-1}$ species, with O_2. This interaction reaction is not a reversible process. Because, 0.0 V application does not change the spectrum to those of the previous form of the complex as shown in (Fig 3.30b inset).

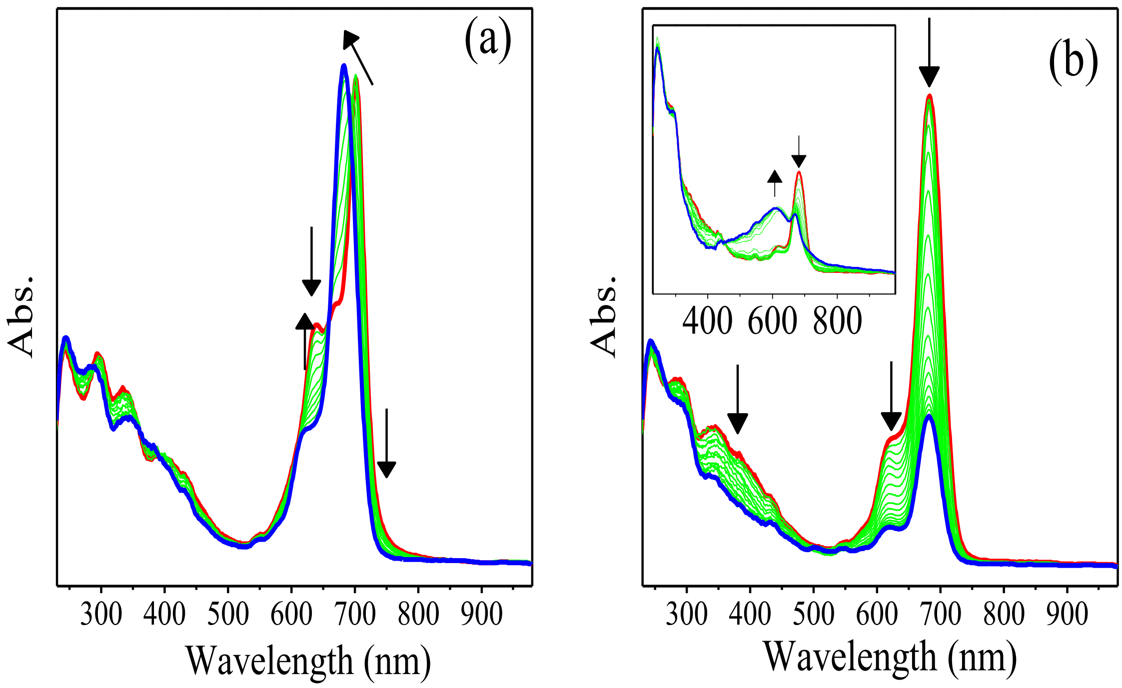

Fig. 3.31. *In-situ* UV-vis spectral changes of β-TiPc in DCM/TBAP electrolyte saturated with O_2. a) E_{app}=-0.60 V. b) E_{app}= -1.25 V (inset: E_{app}= 0.00 V).

α-TiOPc and β-TiOPc (Fig. 3.31.) represent similar spectral changes in "case 3", which indicate interaction of all TiOPcs with molecular oxygen and this interaction reaction alters the spectrum of the complexes.

In summary, voltammetric and spectroelectrochemical results of this study indicate that TiOPcs behaves as homogeneous electrocatalysts for ORR in aprotic solvents, DCM and DMSO. To investigate the heterogeneous electro catalytic activity of TiOPcs for ORR in aqueous electrolyte, LB films of TiOPcs are coated on ITO electrodes and these modified electrodes (ITO/TiOPc (LB)) were testes as heterogeneous electro catalyst for ORR in aqueous solution. For practical applications, a catalyst should be coated on a substrate, thus we coat octa-TiOPc on ITO electrode with Langmuir Blodgett technique.

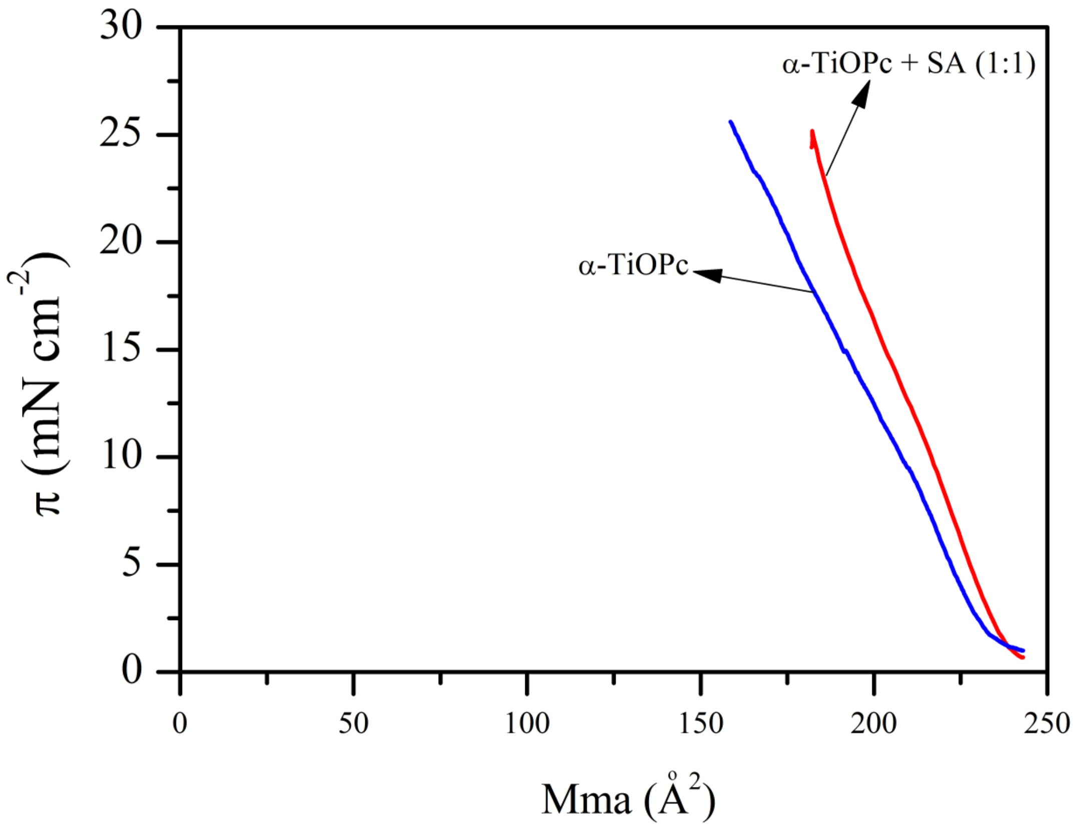

Fig. 3.32. π-A isotherms of α -TiPc and 1:1 mixture of SA and α -TiPc.

Fig 3.32 represents the π-area isotherm of α -TiOPc-SA mixture (1:1). The area per α -TiOPc molecule is calculated from the slope of the curve as 230 Å^2 which is in harmony with those observed for similar phthalocyanine [33,34] Limiting areas of α -TiOPc (230 Å^2) suggests face-on orientations of the complex on the water subphase [33,34]. Presence of SA in octa-TiOPc just increases the limiting area to 235 Å^2. Without SA, α -TiOPc could not be transferred on the ITO substrate as monolayer. Thus SA was used to facilitate transfer of octa-TiOPc on ITO surface.

When 1:1 mixture of SA and α -TiOPc is used all transfer rated during both up stroke and down stroke are recorded as one, which indicates a Y type transfer. 20 LB monolayers could be coated on ITO surface with all α -TiOPc sprayed on the tray of the LB instrument in one trial.

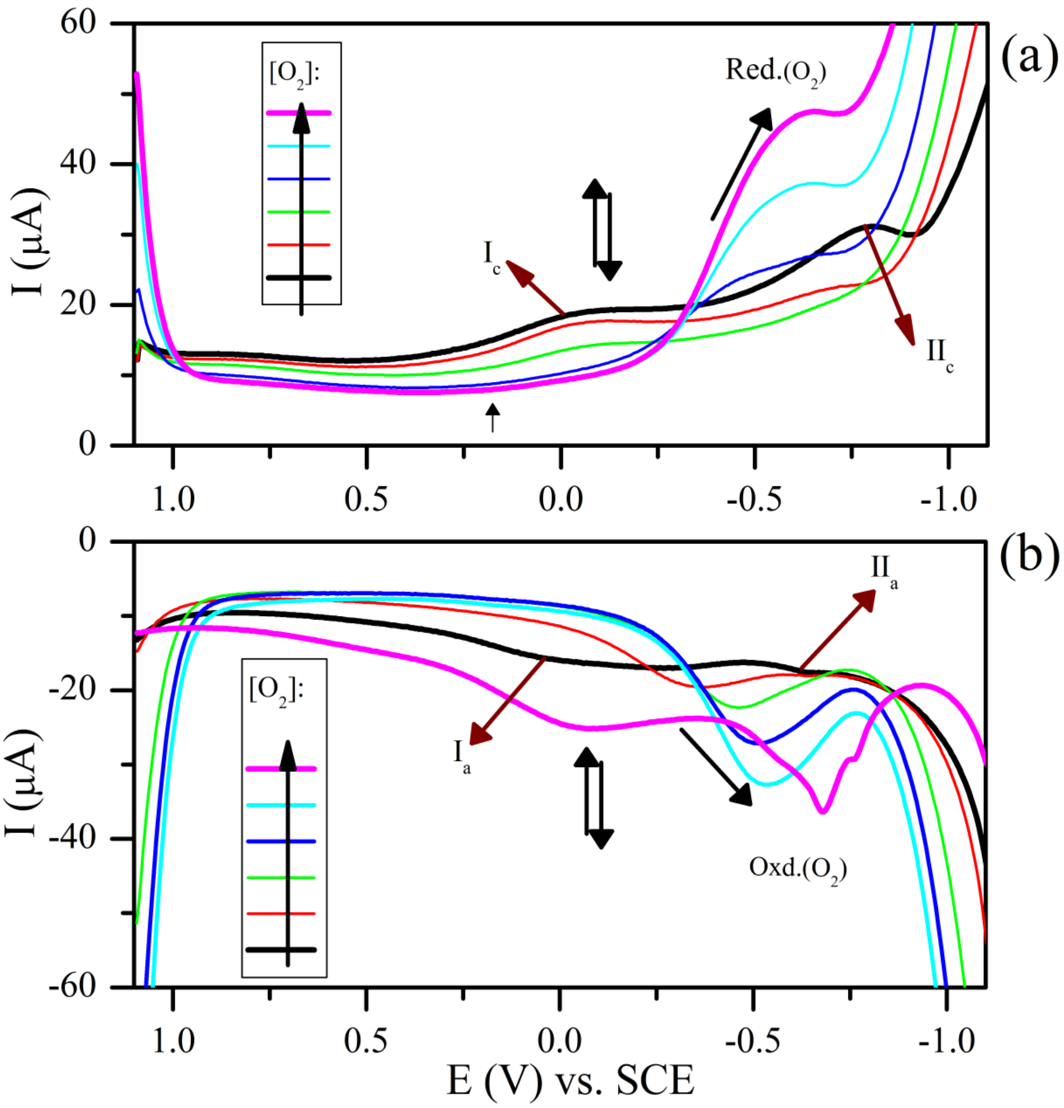

Fig. 3.33 SWVs of **ITO/ α -TiPc** LB film recorded at 0.100 Vs^{-1} scan rate with increasing amounts of O_2 in $LiClO_4$ aqueous electrolyte system on Pt working electrode. (**a**) Forward SWV: E_i = 1.10 V and E_f = -1.10 V. (**b**) Backward SWV: E_i = -1.10 V and E_f = 1.10 V.

LB film of all complexes indicates similar voltammetric responses for the ORR in $LiClO_4$ aqueous solution bubbled with molecular oxygen gradually (*case 3*). Fig. 3.33 represents SWV outcomes of ITO/octa-TiOPc(LB) as a representative of TiOPcs. ITO/ α -TiOPc(LB) give two reduction reactions at -0.07 and -0.77 V without O_2.

As a result of increasing O_2 concentration, while the redox processes of ITO/ α -TiOPc(LB) decreases, a new wave is recorded at -0.47 V.

This new wave shifts until -0.59 V with increasing O_2 concentration. These voltammetric responses indicate catalytic activity of ITO/ α -TiOPc(LB) for ORR. Because O_2 reduced at -0.65 V with negative shifting up to -0.77 V on unmodified ITO electrode in $LiClO_4$ aqueous solution.

3.2.2 Dimethylamine (DMA) derivatised Phthalocyanines (H_2Pc,NiPc, CuPc and CoPc)

Electrochemical analyses of the complex(shown in Figure 3.34) were investigated in solution to propose possible applications of the complexes in different fields of electrochemical technologies. Thus, CV and SWV analysis of the complexes were performed in deaerated DCM and/or DMSO/TBAP electrolyte system on a Pt working electrode.

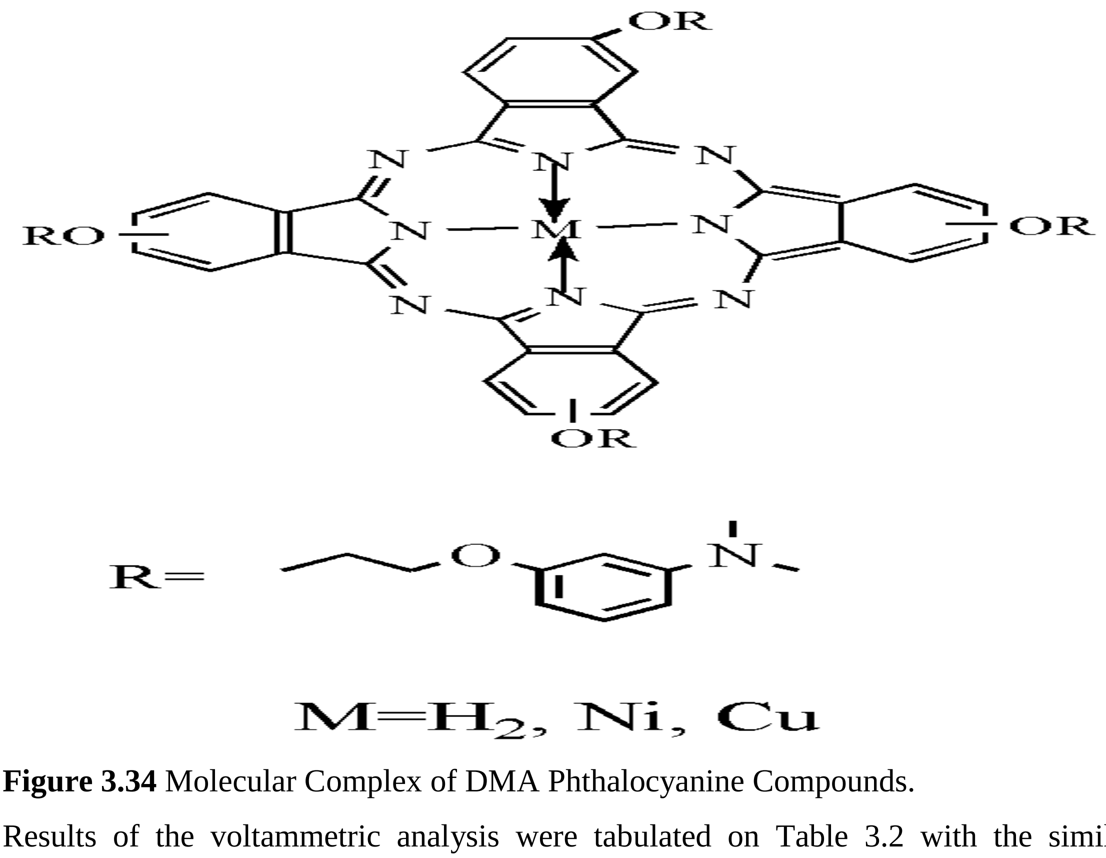

Figure 3.34 Molecular Complex of DMA Phthalocyanine Compounds.

Results of the voltammetric analysis were tabulated on Table 3.2 with the similar complexes in the literature for comparison. As shown in Table 1 $E_{1/2}$ and $\Delta E_{1/2}$ values of the complexes are in agreements with the similar complexes in the literature.

Generally while H_2Pc, CuPc and NiPc complexes give two common ring-based reduction processes, CoPc gives a metal-based and a ring based reduction processes during the cathodic potential scans.

General similarities of the complexes are the aggregation of the complexes. Because of the aggregation of the complexes, the first reduction couples are complicated with a chemical reaction, aggregation-disaggregation equilibrium. Due to the aggregation, the peak current of the first couples of the complexes generally smaller than those of the second reduction couples. All redox couples are far from the reversible character due to the aggregation. Concentration, and scan rate effects to the peak characters support the aggregation behaviors of the complexes. During the oxidation processes, all complexes are electro polymerized on the working electrode. Applied potential ranges and metal center of the complexes affect the polymerization mechanism. Electropolymerization processes increases the possible usage of the complexes in different areas. Since for practical applications, a functional species should be coated on a substrate. It is well documented that electrode modification with electropolymerization process is of the most preferred method for the electrode coating processes. Because, it is very easy to control the film thickness and film type and morphology on an electrode with electrochemical polymerization technique.

H_2Pc, CuPc and NiPc complexes illustrate very similar electrochemical responses, thus the CV and SWV responses of CuPc are represented in Fig. 3.32. CuPc displays two reduction couples (R_1 at -0.84 V and R_2 at -1.12 V). SWVs clearly show these redox processes (Fig. 3.32b). ΔE_p's of these couples are 100 and 90 mV respectively at 0.10 Vs^{-1}. ΔE_p values of these redox couples are bigger than that of reversible ferrocene whose ΔE_p is 70 mV at 0.10 Vs^{-1}. Thus these couples are in electrochemical quasi-reversible character.

Table 3.2 Voltammetric data of the dimethyl amine phthalocyanine complexes. All voltammetric data were given versus SCE.

Complex		Ring Oxidations		M^{III}/M^{II}	M^{II}/M^{I}	Ring Reductions			$^{d}\Delta E_{1/2}$
H_2Pc	$^{a}E_{1/2}$	-	0.81^{e}	-	-	-0.83	-1.13	-	1.17
	$^{b}\Delta E_p$ (mV)	-	-	-	-	89	86	-	
	$^{c}I_{p,a}/I_{p,c}$	-	-	-	-	0.95	0.96	-	
NiPc	$^{a}E_{1/2}$	-	0.75^{e}	-	-	-0.97	-1.26	-	1.00
	$^{b}\Delta E_p$ (mV)	-	-	-	-	110	96	-	
	$^{c}I_{p,a}/I_{p,c}$	-	-	-	-	0.92	0.97	-	
CuPc	$^{a}E_{1/2}$	-	0.78^{e}	-	-	-0.92	-1.22	-	0.98
	$^{b}\Delta E_p$ (mV)	-	-	-	-	100	110	-	
	$^{c}I_{p,a}/I_{p,c}$	-	-	-	-	0.96	0.91	-	
CoPc	$^{a}E_{1/2}$	1.44	0.87^{e}	0.41	-0.20	-1.44	-	-	0.77
	$^{b}\Delta E_p$ (mV)	-	-	64	95	83	-	-	
	$^{c}I_{p,a}/I_{p,c}$	-	-	0.93	0.73	0.96	-	-	

a: $E_{1/2}$ values ((E_{pa}+E_{pc})/2) were given versus SCE and Fc/Fc^{+} (in parenthesis) at 0.100 Vs^{-1} scan rate. **b:** $\Delta E_p = E_{pa} - E_{pc}$. **c**: $I_{p,a}/I_{p,c}$ for reduction, $I_{p,c}/I_{p,a}$ for oxidation processes. **d**: $\Delta E_{1/2} = E_{1/2}$ (first oxidation)- $E_{1/2}$ (first reduction). **e**: Recorded by SWV. **g**: the solvent is DMSO/Cl^{-}. **h**: the solvent is DMF. **i**: the solvent is DCM. (Ferrocene gives a redox couple at 0.30 V in DMF, at 0.28 V in DMSO, and at 0.50 V in DCM versus SCE at 0.100 Vs^{-1} scan rate). **tw**: This work.

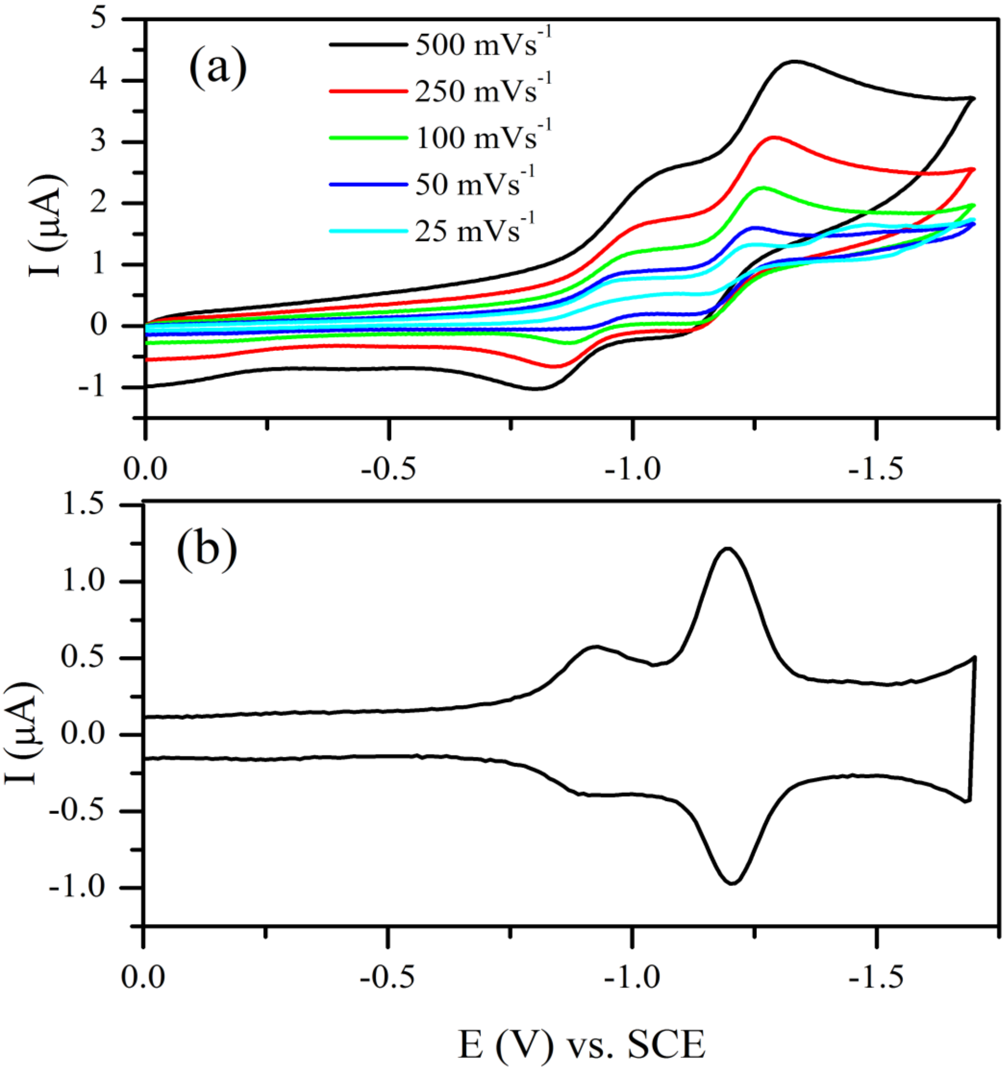

Figure 3.35. (a) CVs of CuPc recorded at cathodic potentials at various scan rates on a Pt working electrode in DCM/TBAP and (b) SWV of CuPc recorded with SWV parameters: step size = 5 mV; pulse size = 100 mV; Frequency = 25 Hz.

Moreover reversibility of these couples can be concluded with respect to symmetry and peak current ratios of the waves recorded during the forward and reverse SWV scans (Fig. 3.35b). During the anodic scans, CuPc is electro polymerized on the working electrode.

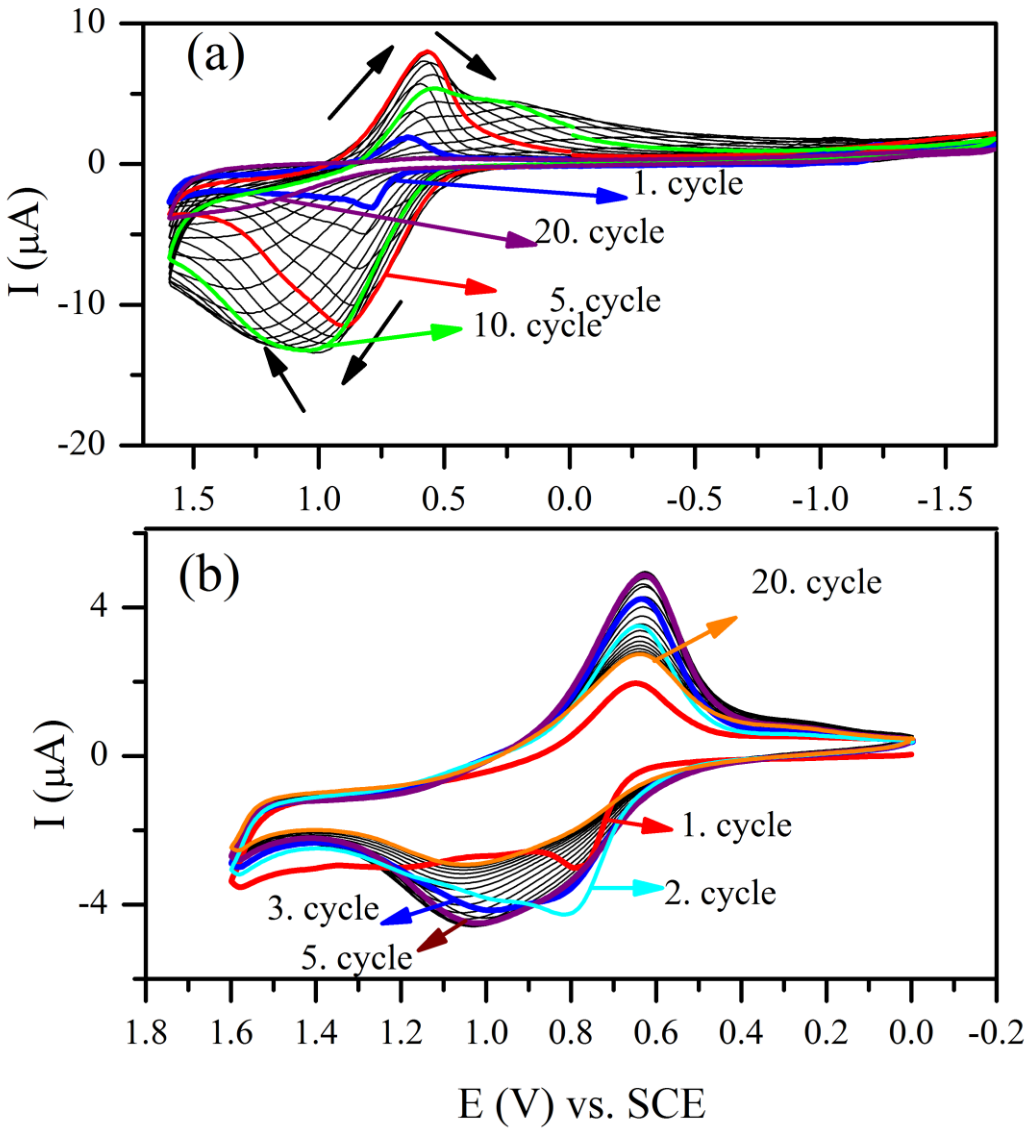

Figure 3.36. (a) Repetitive CVs of CuPc recorded with in the whole potential windows of DCM/TBAP electrolyte system at 0.100 Vs^{-1} scan rate on a Pt working electrode (b) Repetitive CVs of CuPc recorded at anodic potential windows of DCM/TBAP electrolyte system at 0.100 Vs^{-1} scan rate on a Pt working electrode.

As shown in Fig. 3.36, when the reverse applied potentials are changed, polymerization process also changes. Fig. 3.36a illustrates the repetitive CV scans within the whole potential windows of DCM/TBAP (between -1.70 and +1.60 V). When only the anodic potentials are scanned responses of the electropolymerization process get different than the previous one.

During the first anodic scan an anodic wave at 0.78 V and its reverse couple is recorded at 0.64 V. During the continuous CV scans, anodic wave increases in current intensity with positive potential shift up to 1.02 V until the 10. CV scan. However the cathodic couple increases in current intensity with negative shift from 0.64 V to 0.57 V until the 5. scan. A new wave is recorded at 0.23 V between the 5. and 10. scans. After this point these couples stars to decrease in current intensity with the same potential shifts. These voltammetric behaviors indicate the electropolymerization of the complex on the working electrode. When only anodic potentials are scanned (from 0.0 V to 1.70 V), polymerization process of the complex changes. As shown in Fig. 3.36b, an anodic wave was recorded at 0.77 V and its reverse couple is recorded at 0.64 V during the first CV cycle. the anodic wave increases during the second CV cycle, however it immediately shifts to 1.00 V during the third CV cycle and increases in current intensity until the 5. cycle. However after this point, it decreases in current intensity until the 20. cycle. During these anodic changes the cathodic wave increases until the 5. Cycle and decreases until the 20. cycle. As we compare the CV responses given in Fig. 3.36a with Fig. 3.36b, it is clearly shown that changing the potential range of CV cycles, alter the polymerization process considerable.

To analyze the effects of redox active metal center to the electropolymerization and reduction processes of MPcs, CV and SWV responses of CoPc are also performed and compared with those of CuPc. Fig. 3.37 illustrates the CV and SWV responses of CoPc in DCM/TBAP electrolyte system. CoPc gives two common reduction processes, first one is a metal based reduction at -0.20 V and the second one is a Pc ring based reduction at -1.30 V during the cathodic scan.

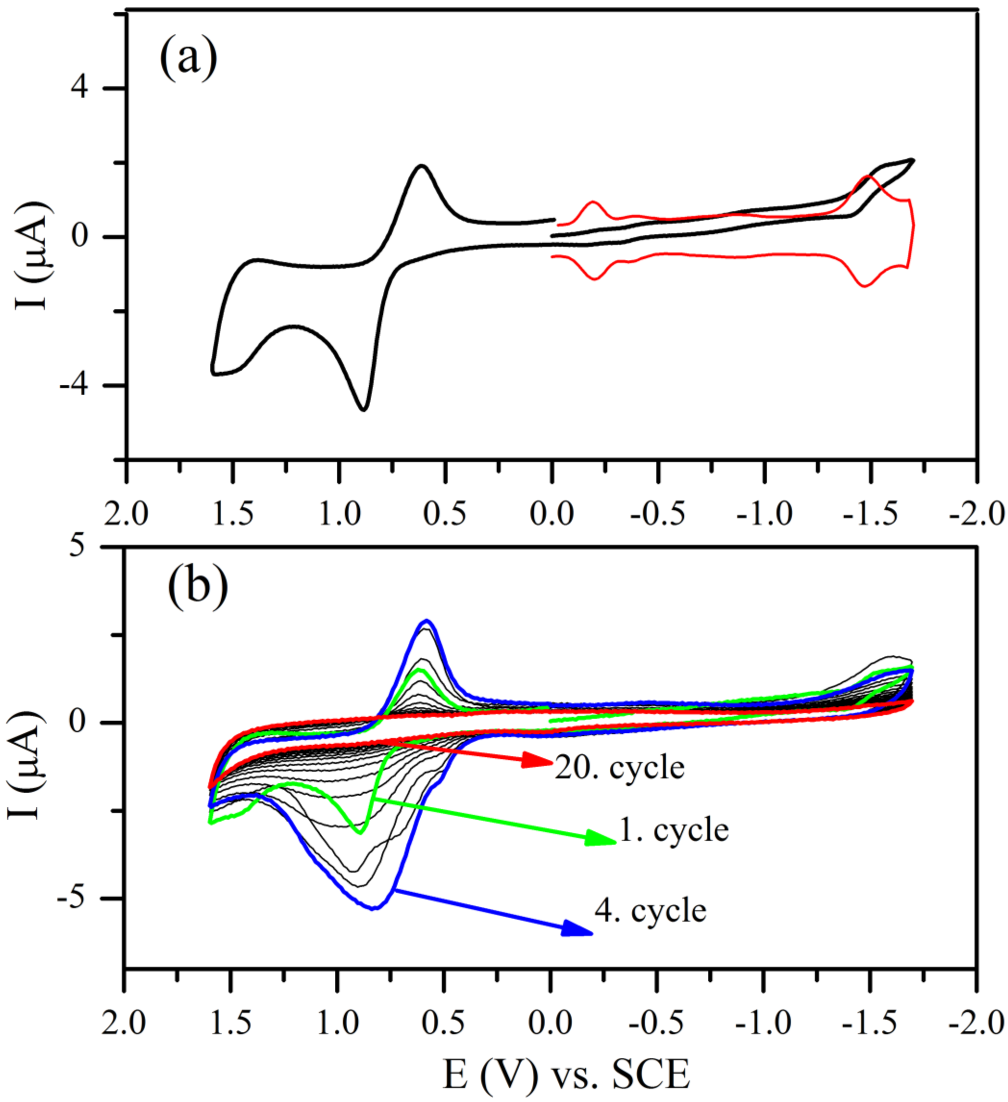

Figure 3.37. (a) CV and SWV of CoPc recorded at 0.100 Vs^{-1} scan rate on a Pt working electrode in DCM/TBAP (b) Repetitive CVs of CoPc recorded with in the whole potential windows of DCM/TBAP electrolyte system at 0.100 Vs^{-1} scan rate on a Pt working electrode.

CoPc is also electro polymerized on the working electrode. During the first CV, it gives an anodic peak at 0.87 V and its reverse cathodic couple at 0.60 V and these waves increase in current intensity until the fourth CV cycle. Moreover a small anodic wave is also recorded at 1.45 V during the first CV cycle and it disappeared just after the second CV cycle.

In addition to the previous wave, an anodic wave is recorded at 0.50 V during the second CV cycle, and then it shifts to the positive potentials and mixes with the wave at 0.87 V with increasing CV cycles. It is clearly shown in Fig. 5 and 6 that CV responses of CoPc is completely different than those of CuPc, which indicates that changing the metal center of MPcs alters the electropolymerization process.

In situ spectroelectrochemical studies were employed to perform assignments of the electron transfer reactions recorded with CV and SWV measurements. It is well documented that H_2Pc, CuPc and NiPc complexes have redox inactive metal centers, thus these complexes show spectral changes assigned to the electron transfer of Pc rings during the reduction reactions. Spectral changes, decreasing the Q bands in intensity without shift and observation of new bands in the LMCT regions, are characteristic changes for the MPcs having redox inactive metal centers. During the oxidation reactions, all bands of these complexes decreased in intensity, which support the electropolymerization of the complexes. Because concentration of MPcs decreases due to the polymerization, thus the bands decrease in intensity. CoPc has redox active metal center thus its spectral changes are different than those of Pcs having redox inactive metal center.

Fig. 3.38 represents in situ UV-Vis spectral changes and in situ recorded chromaticity diagram of CoPc in DCM/TBAP during the electron transfer processes. Shifting of the Q band and observation of a new band at 450 nm during the first reduction reaction indicates reduction of $[Co^{II}Pc^{-2}]$ to $[Co^{I}Pc^{-2}]^{1-}$ (Fig. 3.35a) [19-24]. Well defined isobestic points at 382, 575, and 700 nm and a color changes from bluish green ($x = 0.270$ and $y = 0.351$) to light green ($x = 0.3368$ and $y = 0.4108$) are recorded during the first reduction reaction (Fig. 3.38d). Spectral changes given in Fig. 3.38b indicate the ring-based reduction character of the second reduction reaction. Since while the Q band at 706 nm and its shoulder at 674 nm decrease, a new broad band is recorded at 537 nm. All bands decreases in intensity due to the electropolymerization of the complexes during the oxidation reaction at 1.10 V potential application (Fig. 3.38c from red to pink spectrum). However, when more positive potential is applied, absorption intensity of the ligand to metal charge transfer regions (MLCT) (around 600 nm and 800 nm) increases, while the intensity of the Q band and its shoulder decreases in intensity (Fig. 3.38c from pink to blue spectrum).

These spectral changes indicate a ring based oxidation process of the complex.

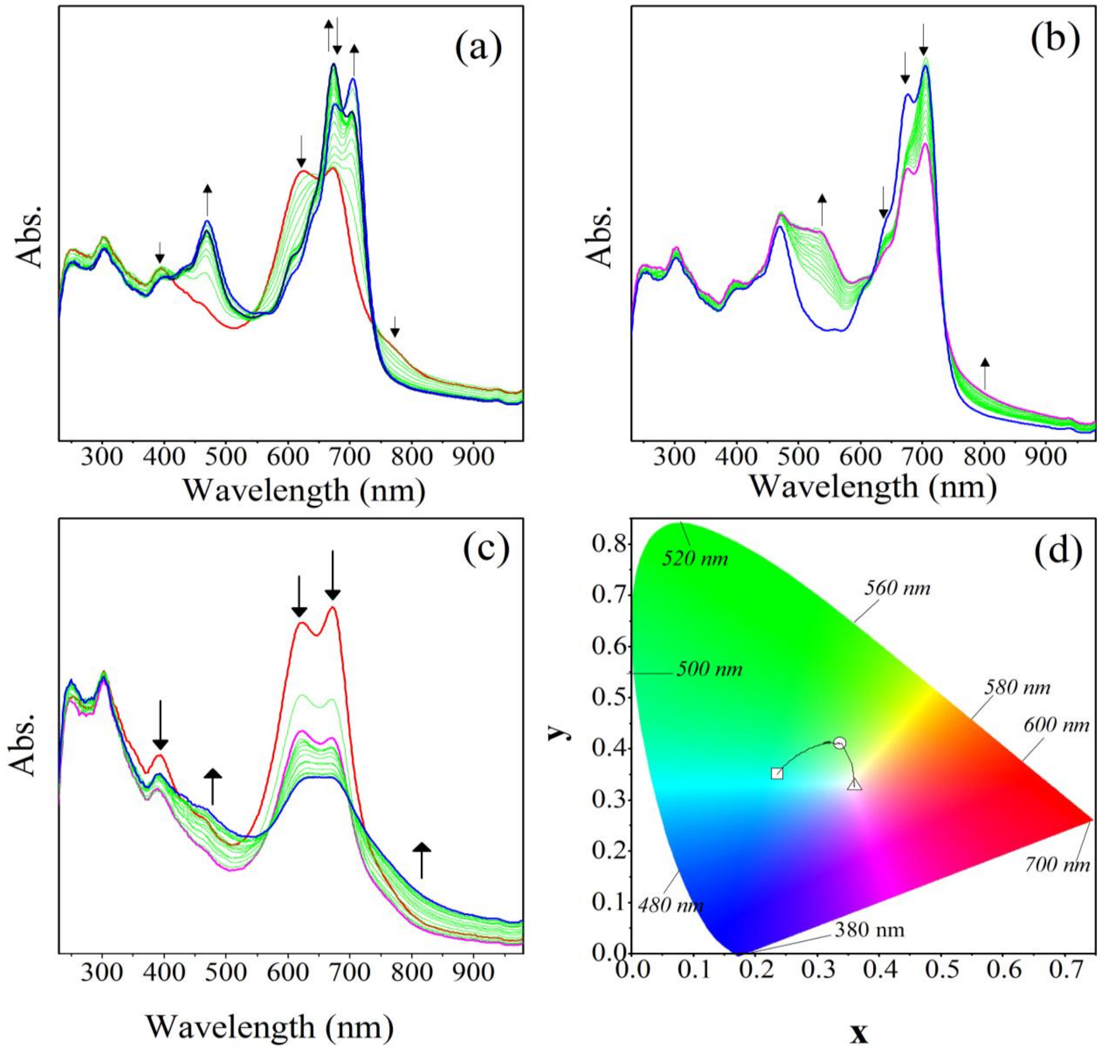

Figure 3.38. In-situ UV-Vis spectral changes of CoPc in DCM/TBAP. a) E_{app}= -0.50 V. b) E_{app}= = -1.50 V. b) E_{app}= = 1.50 V. d) Chromaticity diagram (each symbol represents the color of electro-generated species; □: $[Co^{II}Pc^{-2}]$, ○:$[Co^{I}Pc^{-2}]^{-1}$ △: $[Co^{I}Pc^{-3}]^{-2}$.

Well defined isosbestic points at 382, 575, and 700 nm and a color changes from bluish green (x = 0.270 and y = 0.351) to light green (x = 0.3368 and y = 0.4108) are recorded during the first reduction reaction (Fig. 3.38d). Spectral changes given in Fig. 3.38b indicate the ring-based reduction character of the second reduction reaction.

Since while the Q band at 706 nm and its shoulder at 674 nm decrease, a new broad band is recorded at 537 nm.

All bands decreases in intensity due to the electropolymerization of the complexes during the oxidation reaction at 1.10 V potential application (Fig. 3.38c from red to pink spectrum). However, when more positive potential is applied, absorption intensity of the ligand to metal charge transfer regions (MLCT) (around 600 nm and 800 nm) increases, while the intensity of the Q band and its shoulder decreases in intensity (Fig. 3.38c from pink to blue spectrum). These spectral changes indicate a ring based oxidation process of the complex.

3.2.3 Diethylamine (DEA) Derivatised Phthalocyanines (H_2Pc,NiPc,and CuPc)

Electrochemical analyses of the complex(shown in Figure 3.39) were investigated in solution to propose possible applications of the complexes in different fields of electrochemical technologies. Thus, CV and SWV analysis of the complexes were performed in deaerated DCM and/or DMSO/TBAP electrolyte system on a Pt working electrode.

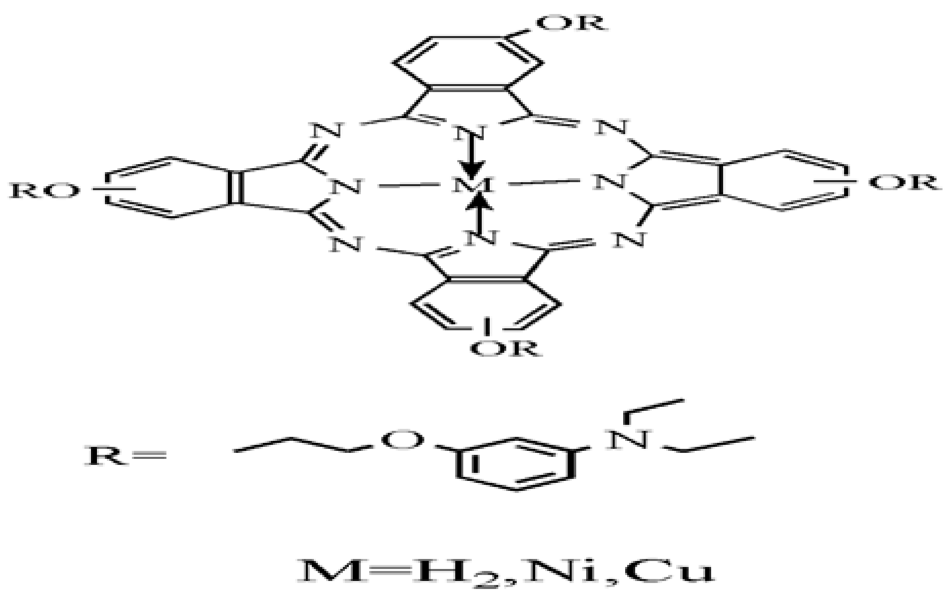

Figure 3.39. Molecular Complex of DEA Phthalocyanine Compounds.

Voltammetric analyses were tabulated on Table 3 with the similar complexes in the literature for comparison.

As shown in Table 3 fundamental voltammetric parameters, especially $E_{1/2}$ and $\Delta E_{1/2}$ values of the complexes are in agreements with the similar complexes in the literature [9-12], which support the proposed structures of the complexes. It is well documented in the literature that, phthalocyanines bearing $2H^+$, Cu^{+2}, and Cu^{+2} ions in the core and redox inactive substituents give only ring-based reduction and oxidation processes which have $\Delta E_{1/2}$ values at around 1.50 V.

Table 3.3 Voltammetric data of the complexes. All voltammetric data were given versus SCE.

Complex		Polymerization Waves		Ring Reductions	
H_2Pc	$^aE_{1/2}$	-	0.76^d $(0.65)^e$	-0.76	-1.08
	$^b\Delta E_p$ (mV)	-	-	75	84
	$^cI_{p,a}/I_{p,c}$	-	-	0.96	0.92
NiPc	$^aE_{1/2}$	-	0.86^d $(0.62)^e$	-0.97	-1.26
	$^b\Delta E_p$ (mV)	-	-	110	96
	$^cI_{p,a}/I_{p,c}$	-	-	0.92	0.97
CuPc	$^aE_{1/2}$	-	0.85^d $(0.61)^e$	-0.96	-1.22
	$^b\Delta E_p$ (mV)	-	-	100	110
	$^cI_{p,a}/I_{p,c}$	-	-	0.96	0.91

a: $E_{1/2}$ values $((E_{pa}+E_{pc})/2)$ were given versus SCE and Fc/Fc^+ (in parenthesis) at 0.100 Vs^{-1} scan rate. **b:** $\Delta E_p = E_{pa}-E_{pc}$. **c**: $I_{p,a}/I_{p,c}$ for reduction, $I_{p,c}/I_{p,a}$ for oxidation processes. **d**: E_{pa} of first CV cycle; **e**: E_{pc} of first CV cycle;

H_2Pc, CuPc and NiPc complexes studied here obey this behavior. General similarities of the complexes are the aggregation of the complexes. Especially the first reduction couples of the complexes deviates from reversibility due to the aggregation. All complexes are oxidative electro polymerized on the working electrode. Applied potential ranges and metal center of the complexes affect the polymerization mechanism.

Fig.3.40 illustrates CV responses of H_2Pc. It displays two quasi-reversible couples (R_1 at -0.76 V and R_2 at -1.08 V) during the cathodic potential scans. During the first anodic scans, it gives an anodic wave at 0.74 V and its reverse cathodic wave at 0.65 V. During the repetitive potential scans, a new huge anodic wave is recorded at 0.63 V, which increases with positive potential shift up to 5. CV cycles and collapsed the wave at 0.74 V (Fig.3.40).

At the same time new wave is observed at -1.12 V with increasing in current intensity. After the 5. CV cycles, these waves starts to decrease with potential shifts.

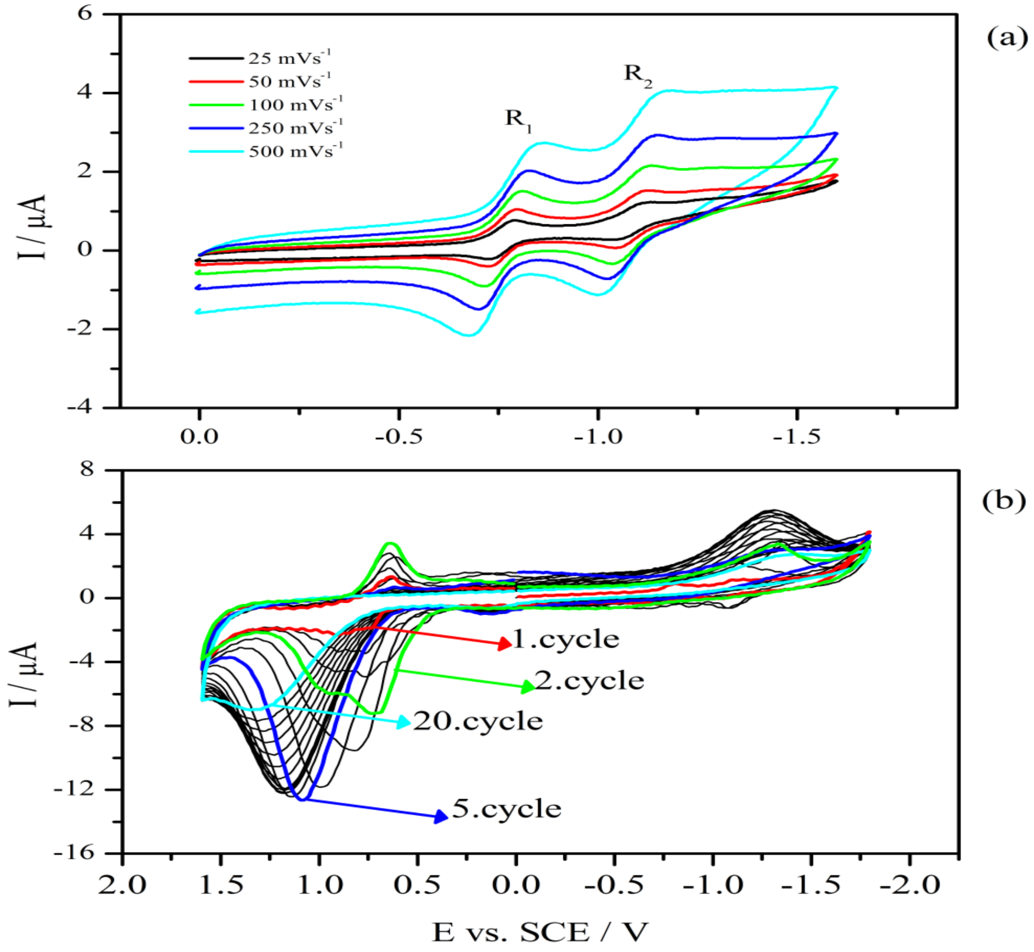

Figure 3.40 (a) Repetitive CVs of H_2Pc recorded with in the whole potential windows of DCM/TBAP electrolyte system at 0.100 Vs^{-1} scan rate on a Pt working electrode (b) Repetitive CVs of H_2Pc recorded at anodic potential windows of DCM/TBAP electrolyte system at 0.100 Vs^{-1} scan rate on a Pt working electrode.

These voltammetric data indicate electropolymerization of the complex on the working electrode. While H_2Pc dissolves in DCM very well, electro polymerized H_2Pc is insoluble in the same solvent. CuPc and NiPc also give two reduction reactions and electropolymerized during the oxidation reactions. Main differences of the voltammetric responses are the aggregation of CuPc and NiPc.

Due to the aggregation, the first reduction reactions of these complexes have irreversible characters. Electropolymerization behaviors of the complexes also differ due to the different metal center of the complexes.

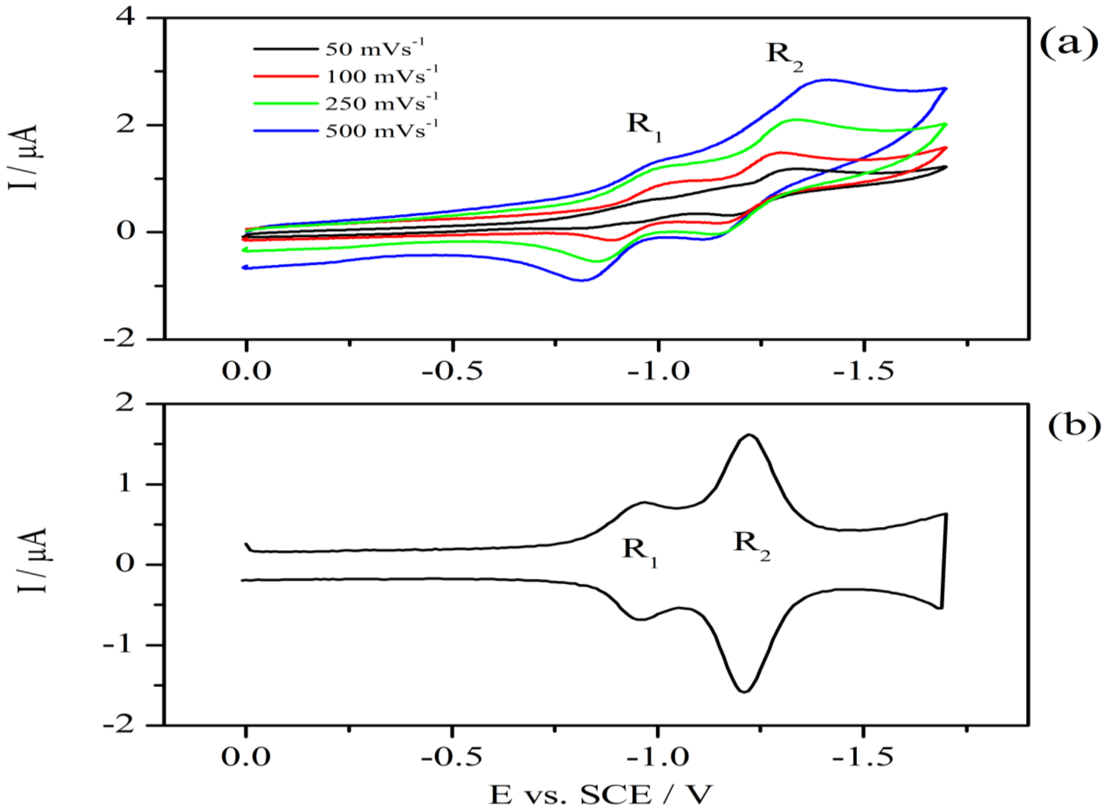

Figure 3.41. (a) CVs of CuPc recorded at cathodic potentials at various scan rates on a Pt working electrode in DCM/TBAP and (b) SWV of CuPc recorded with SWV parameters: step size = 5 mV; pulse size = 100 mV; Frequency = 25 Hz.

As shown in Fig. 3.41, CuPc gives an irreversible reduction (R_1 at -0.96 V) followed with a reversible one (R_2 at -1.22 V) during the cathodic scans.

However when anodic potentials are scanned after the cathodic potentials continuously, CuPc is electro polymerized on the working electrode (Fig. 3.42a). Electropolymerized waves increase up to 11. CV cycles with a potential shift. During electropolymerization reaction, redox wave of CuPc disappears completely and new waves attributed to the electro polymerized film are recorded.

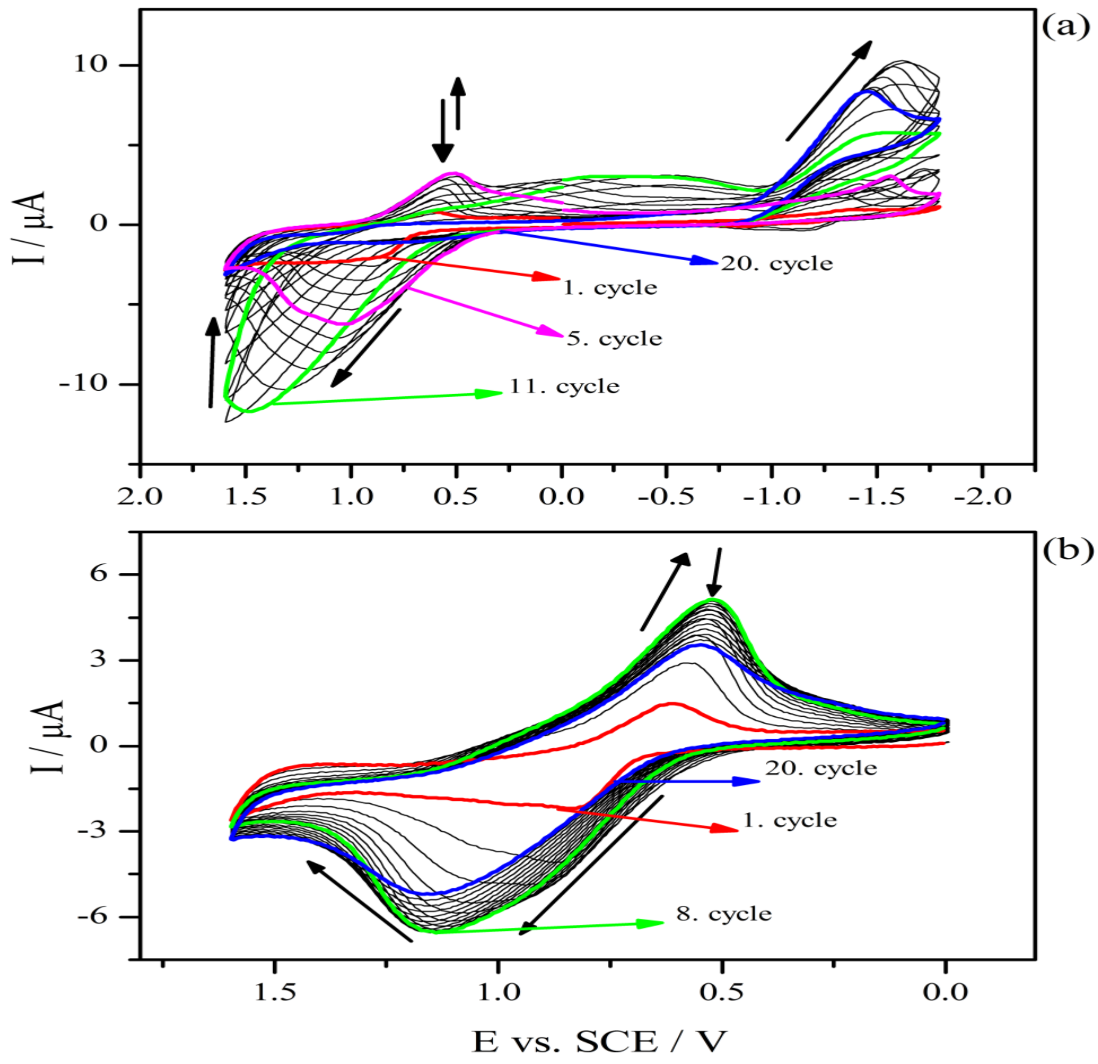

Figure 3.42. (a) Repetitive CVs of CuPc recorded with in the whole potential windows of DCM/TBAP electrolyte system at 0.100 Vs^{-1} scan rate on a Pt working electrode (b) Repetitive CVs of CuPc recorded at anodic potential windows of DCM/TBAP electrolyte system at 0.100 Vs^{-1} scan rate on a Pt working electrode.

Electropolymerized film of CuPc is insoluble in DCM like H_2Pc. When the positive potentials are scanned instead of the whole potential window of the electrolyte system, polymerization mechanism changes as shown in Fig. 3.42b. Shifting of the redox wave of CuPc is smaller and the redox process of the polymerization reaction is more reversible when only anodic potentials are scanned.

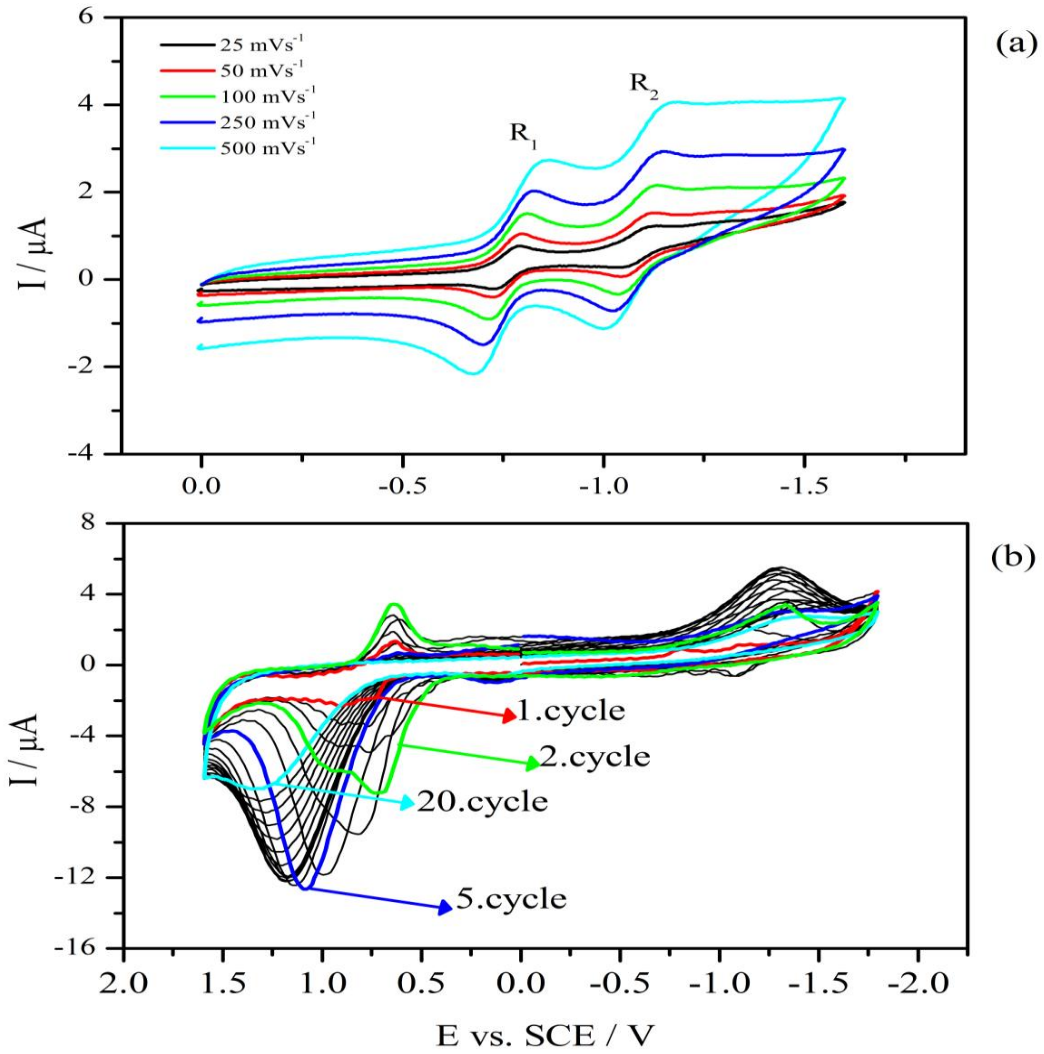

Figure 3.43. (a) Repetitive CVs of NiPc recorded with in the whole potential windows of DCM/TBAP electrolyte system at 0.100 Vs^{-1} scan rate on a Pt working electrode (b) Repetitive CVs of NiPc recorded at anodic potential windows of DCM/TBAP electrolyte system at 0.100 Vs^{-1} scan rate on a Pt working electrode.

Fig. 3.43 shows the voltammetric responses of NiPc. Reduction processes of NiPc are more reversible than CuPc, but less reversible than those of H_2Pc. It gives the first reduction reaction (R_1) at -0.97 V with ΔE_p of 110 mV and the second reduction reaction (R_2) at -1.26 V with ΔE_p of 90 mV. Easy of reduction order of these complex is H_2Pc > CuPc > NiPc. During the anodic potential scans, NiPc gives a huge oxidation wave, which increases in current intensity with repetitive CV cycles (Fig. 3.43b).

Changing the potential window of the potential scan changes the polymerization mechanism of NiPc, like those of H_2Pc and CuPc. Although monomeric NiPc is soluble in DCM, polymerized film on the working electrode is insoluble in the same solvent.

In situ spectroelectrochemical studies were employed to perform assignments of the electron transfer reactions recorded with CV and SWV measurements. It is well documented that H_2Pc, CuPc and NiPc complexes.

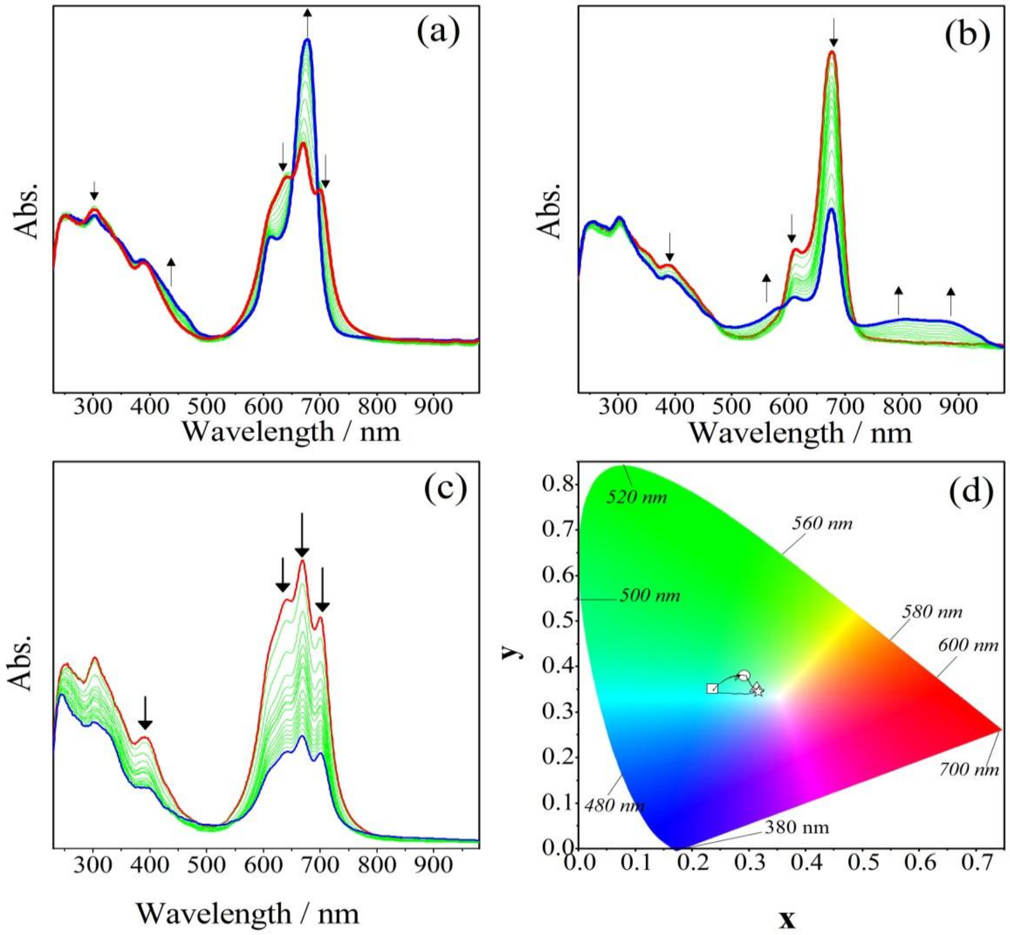

Figure 3.44. In-situ UV-Vis spectral changes of H_2Pc in DCM/TBAP. a) E_{app}= -1.10 V. b) E_{app}= = -1.50 V. b) E_{app}= = 1.50 V. d) Chromaticity diagram (each symbol represents the color of electro-generated species; □: $[H_2Pc^{-2}]$, ○:$[H_2Pc^{-2}]^{-1}$; ☆ :$[H_2Pc^{-3}]^{-2}$; △: $[H_2Pc^{-1}]^{+1}$.

In situ UV-Vis spectral changes and in situ recorded chromaticity diagram of H_2Pc was represented in Fig. 3.44.Without any potential application, H_2Pc shows a split Q band at 670 and 70 nm with a shoulder at 637 nm.

During the first reduction reaction at -1.00 V, Q band the split Q band turn to a single band due to increasing a sharp band at 677 nm. These spectral changes are characteristic changes for the first reduction reaction of metal free phthalocyanines (Fig. 3.44a). Upon applied potential of -1.40 V, while the Q band at 677 nm decreases in intensity, new bands are recorded at 675, 800, and 880 nm. Spectral changes given in Fig. 3.44b are easily assigned to the reduction of dianionic H_2Pc species. All bands decreases in intensity due to the electropolymerization of the H_2Pc during the oxidation reaction at 1.10 V potential application (Fig. 3.44c). Color changes due to the electron transfer reactions of H_2Pc are illustrated in the chromaticity diagram (Fig. 3.44d).

CuPc and NiPc complexes gave very similar spectral changes during in-situ spectroelectrochemical measurements. Both complexes electro polymerized during the oxidation processes and all bands in the spectra of these complexes decrease in intensity due to the polymerization. During the reduction reactions both complexes gave spectral changes assigned to the Pc ring reduction reactions.

In-situ spectroelectrochemical results of CuPc are given as a representative of these complexes in Fig. 3.45. Before any potential application, CuPc gives the Q band at 678 nm and a shoulder at 621 nm. Due to the aggregation of the complex intensity of the band at 621 nm is higher than the Q band of the monomeric species. This spectral behavior supports aggregation effects to the CV responses of the complex.

During the first reduction reaction, while the Q band at 678 nm and the band at 621 nm decrease in intensity a new band is recorded at 582 nm. Moreover, two new bands are observed at 887 and 951 nm.

These spectral changes indicated reduction of both aggregated and monomeric $Cu^{II}Pc^{-2}$ species to the monomeric $Cu^{II}Pc^{-3}$ (Fig. 3.45a) . During the second reduction reaction, while the Q band and its shoulder decrease, two new bands increase at 800 and 890 nm. At the same time the bands at 582 and 951 nm decreases in intensity (Fig. 3.45b). These are the characteristic changes for the reduction of monoanionic $Cu^{II}Pc^{-3}$ to dianionic $Cu^{II}Pc^{-3}$ species.

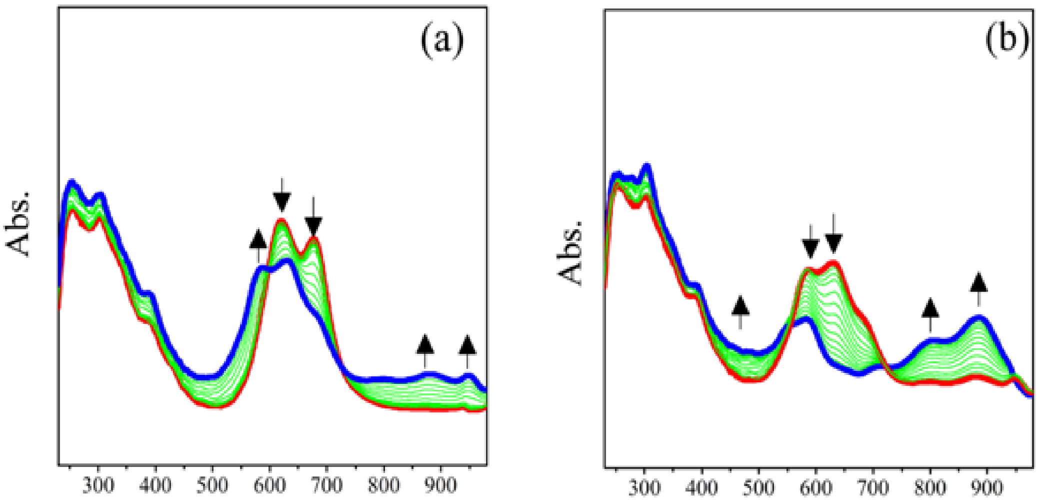

Figure 3.45. In-situ UV-Vis spectral changes of **CuPc** in DCM/TBAP. **a**) E_{app}= -1.00 V. **b**) E_{app}= = -1.50 V.

3.2.4 Electrochromic Measurements of Diethylamine (DEA) Derivatised Phthalocyanines (H_2Pc,NiPc,and CuPc)

The film coated on the working electrode with electropolymerization (ITO/DEA-Pc (ep)) gets insoluble in DCM, while monomeric(H_2Pc, NiPc, CuPc) is highly soluble. Thus the film gives stable and reproducible CV responses in different solvents such as H_2O, AN, and DCM without dissolving. During the CV measurements in these solvents, color changes of the film on the electrode were easily observed with naked eyes due to the electrochromic feature of the film. Different color of the oxidized and reduced form of (ITO/DEA-Pcs(ep)) indicate possible application in the display technologies, e.g. electrochromic and data storage application.

3.2.4.1 Film Thickness Effect

ITO/H_2Pc, NiPc, and CuPc(ep) films were prepared with different film thickness adjusted with the CV cycle numbers and their in situ spectrochronocoulometric (SCC) analyses were carried out to derive the basic electrochromic parameters of the complexes.

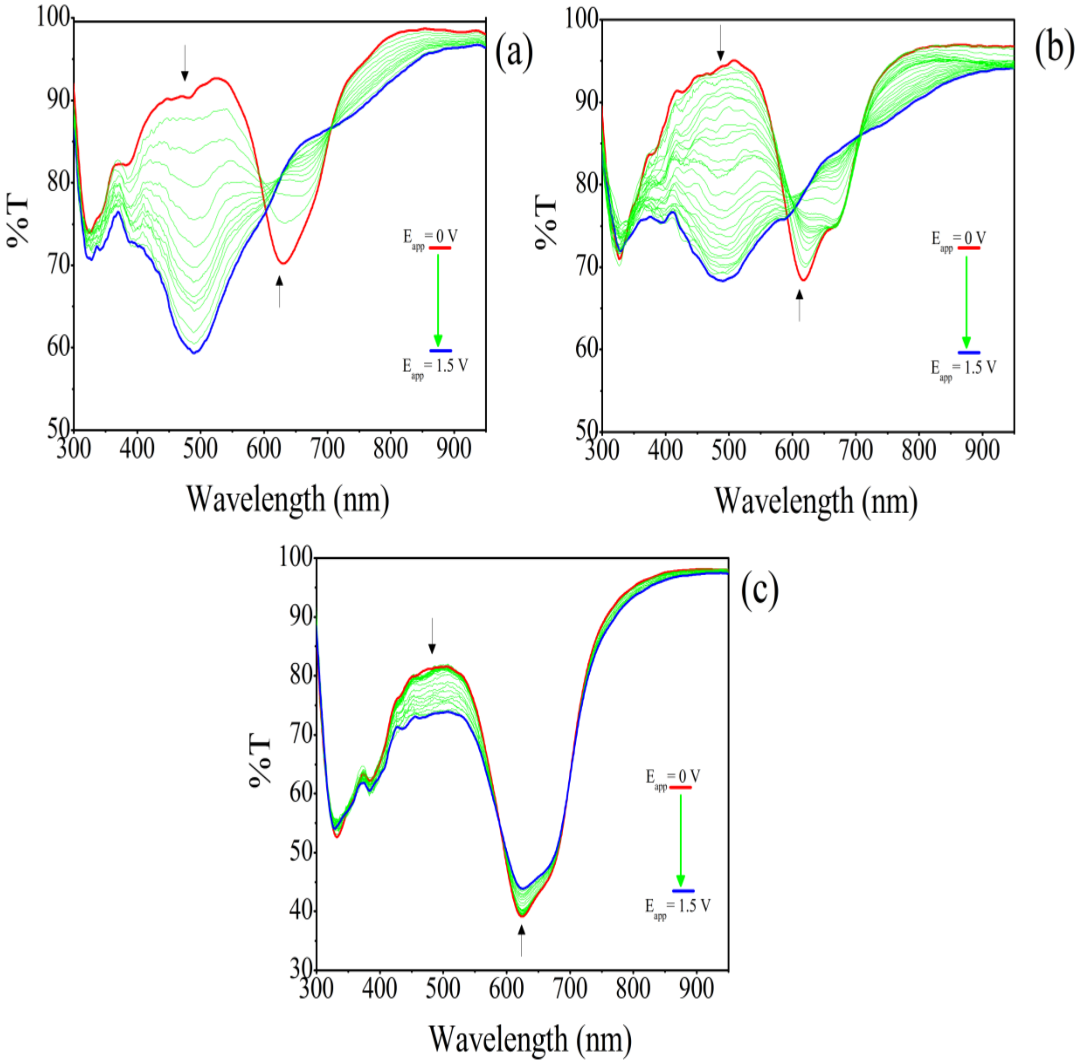

Figure 3.46 %T changes of **ITO/NiPc(ep)** film in DCM/TBAP electrolyte system in different film thickness. **a)** 5 cycle **b)** 10 cycle **c)** 20 cycle**.**

Fig. 3.46 indicates %T changes of ITO/NiPc(ep) film in different film thickness. As it is seen in the figure that the optimum electrochromic responses were recorded with the ITO/NiPc(ep**)** film prepared with 5 CV cycles. For this reason all electrochromic measurements the films prepared with 5 cycles were used.

3.2.4.2 Supporting Electrolyte Effect

To explore ideal supporting electrolytes, in situ spectrochronocoulometric analysis were repeated in different electrolyte systems consisting different anions.

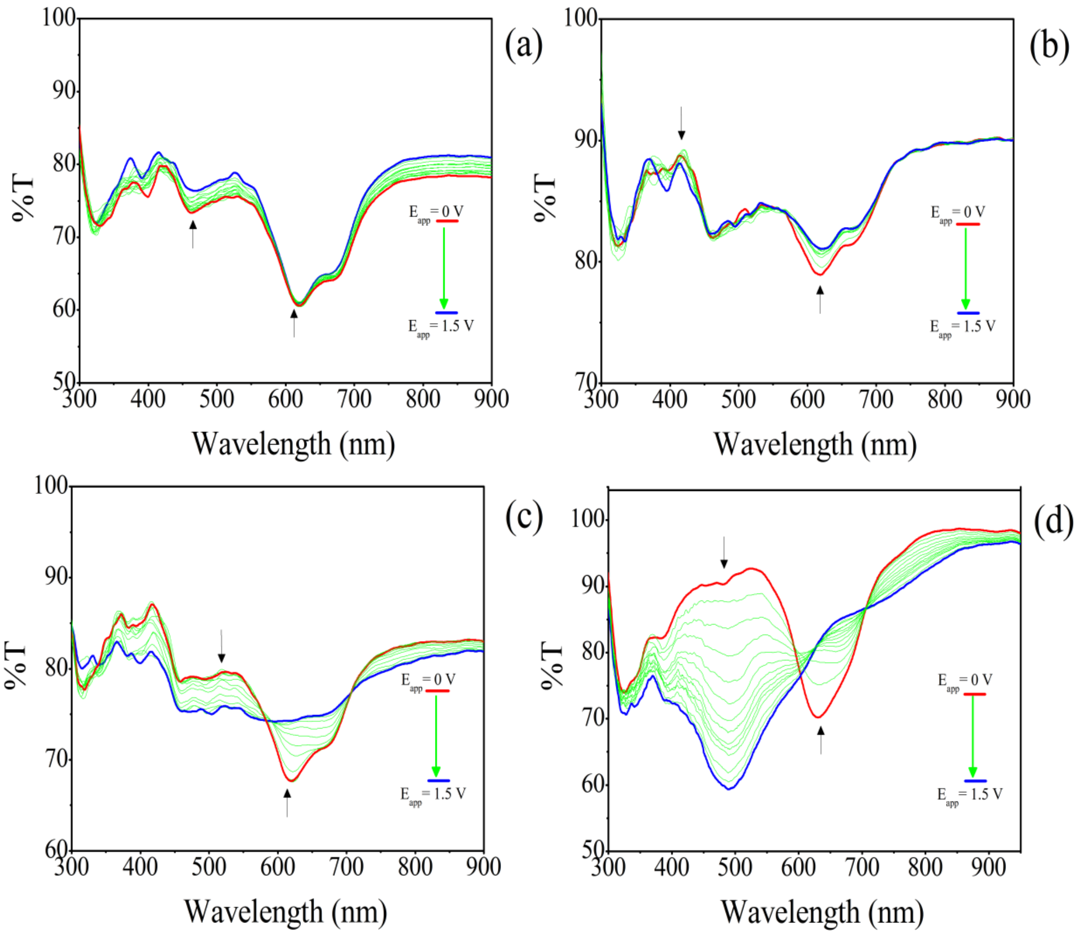

Figure 3.47 %T changes of ITO/NiPc(ep) film in DCM at different electrolyte system **a)** Tetrabutylammonium fluoride **b)** Tetrabutylammonium chloride **c)** Tetrabutylammonium tetrafluoroborate **d)** Tetrabutylammonium perchlorate

Fig. 3.47 represents in situ % transmitans change of **ITO/NiPc(ep)** film in DCM consisting different supporting electrolyte. When ion size of the supporting electrode decreases, % transmittance change also diminishes. This means that size of the anion should be fitted to porosity of the film. If the anion is too smaller than pore of the film, anion could not easily hold on the film or If the anion is too larger than pore of the film, it could not penetrate in to the film. Perchloride is found as the optimal anion for **ITO/NiPc(ep)** film in DCM. For this reason, all measurements were carried out in TBAP electrolyte system.

3.2.4.3 Solvent Effect

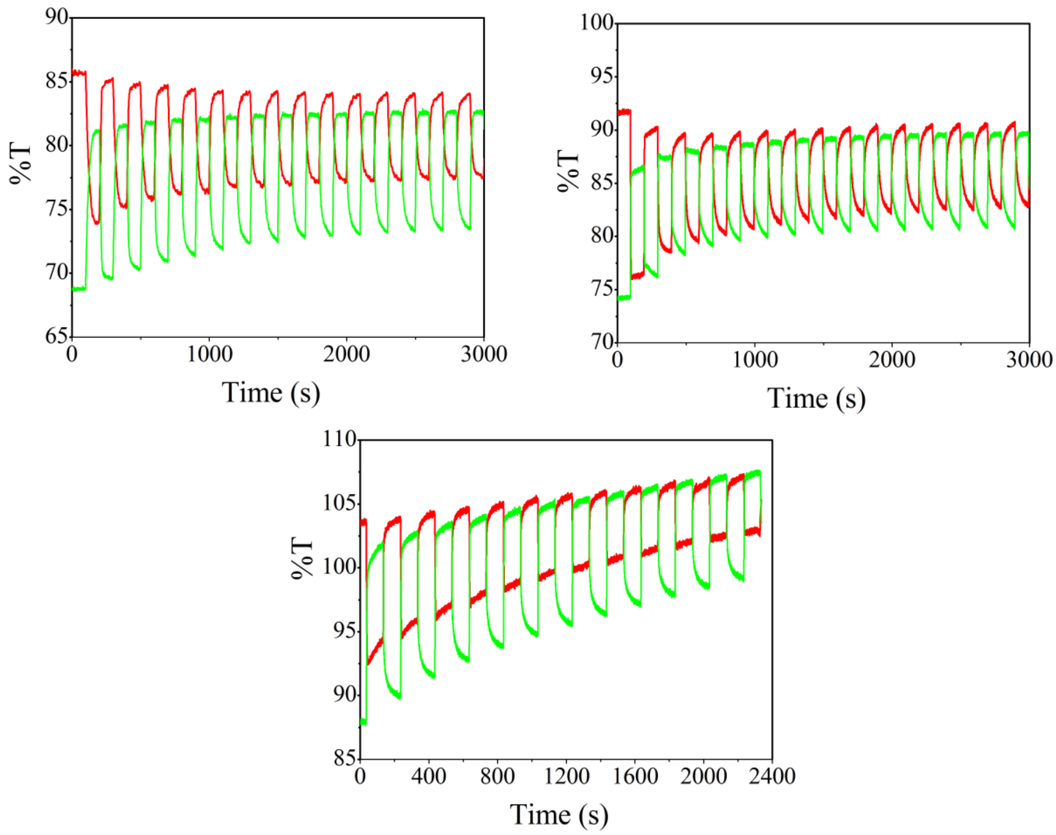

Figure 3.48 %T changes of ITO/CuPc(ep) film at 500nm (red) and 620 nm (green) versus time in different solvents during the repetitive chronocoulometric measurements. **a)** Dichloromethane(DCM/TBAP) **b)** Acetonitrile(AN/TBAP) **c)** Distilled water ($H_2O/LiClO_4$).

To analyze the effect of solvent to color change of the system, ITO/ CuPc(ep) were analyzed with respect to the redox responses and spectral changes under the applied potentials in different media, e.g. DCM/TBAP, AN/TBAP, and $H_2O/LiClO_4$. Fig.3.48 shows %T versus time response of the film was recorded at 500 nm and 620 nm in different solvents. ITO/CuPc(ep) illustrates excellent electrochemical responses in AN/TBAP electrolyte system. While the basic electrochromic parameters of the film in DCM/TBAP was also stable and acceptable, $H_2O/LiClO_4$ results were not satisfying.

It is obvious that such a definition of solvent effect cannot be expressed by an individual physical quantity .

These results show that the solvent effect on UV/vis absorption spectra of CuPc film was variable strongly depend on the nature of the substituent on the phthalocyanines

3.2.4.4 Central Metal Effect

After all parameters were measured, to investigate the central metal effect on the electrochromic responses ITO/H_2Pc,NiPc,CuPc(ep) films were analyzed in AN/TBAP media.

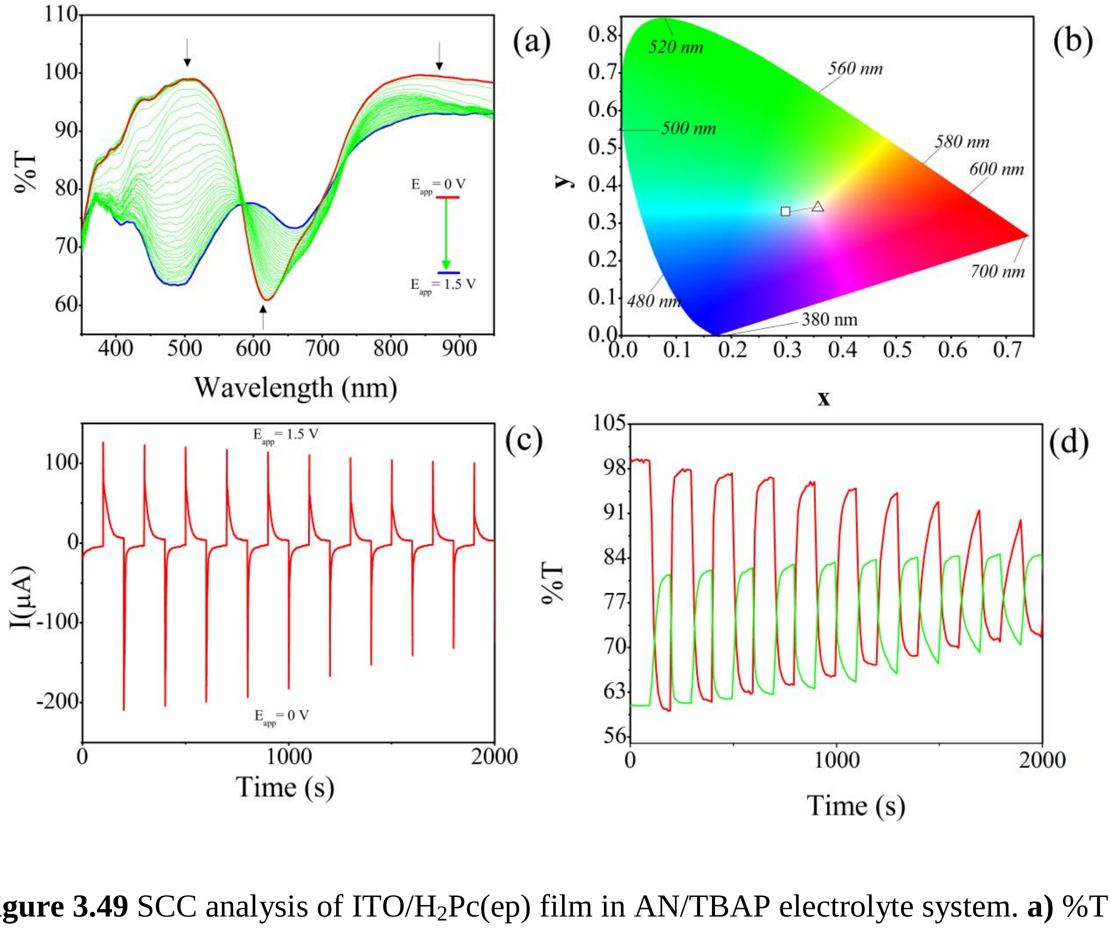

Figure 3.49 SCC analysis of ITO/H_2Pc(ep) film in AN/TBAP electrolyte system. **a)** %T changes recorded during in situ spectroelectrochemical measurement under 1.50 V potential application. **b)** Chromaticity diagram of ITO/H_2Pc(ep) film. **c)** Repetitive chronoamperometric responses between $E_{app.}$=0.0 V and $E_{app.}$= 1.50 V within 100 s time interval. **d)** %T changes at 500nm (red) and 620 nm (green) versus time.

Fig. 3.49 represents in situ spectrochronocoulometric analysis (SCC) analysis of ITO/ H_2Pc(ep) film in AN/TBAP electrolyte system.

In situ spectroelectrochemical analysis of the ITO/ H_2Pc(ep) is given in Fig. 3.49a to represent the optic responses of the film under potential stress. Without any potential application, the Q band of NiPc film is recorded at 621 nm (red spectrum).

When 1.50 V was applied to the working electrode, spectrum of the film changes immediately. First of all, the Q band decreases slightly in intensity and two new bands are recorded at 410 and 500 nm. These two different spectral changes indicate presence of at least two electron transfer reaction. This spectral changes cause a color changes from cyan to uncolored. Color changes during the redox processes are represented in the chromaticity diagram in Fig. 3.49b. Under 0.0 V potential application, film has green color (x: 0.301 and y: 0.329, point □). When 1.50 V was applied, color changes to uncolored immediately (x: 0.360 and y:0.343, point △). To derive basic electrochromic parameters of the ITO/ H_2Pc(ep) film, repetitive chronocoulometric measurements were performed with the spectral measurements (in situ spectrochronocoulometric analysis, SCC). Fig. 3.49c illustrate the current responses of the ITO/ H_2Pc(ep) film under the constant potential application which was switched between 0.0 and 1.50 V. A stable current-time response is recorded until the 10 cycles as shown in Fig. 3.49c during the repetitive potential application, which indicate the columbic stability of the film. %T versus time response of the film was recorded at 500 nm and 620 nm to determine the response time, optic stability, and columbic efficiency of the film (3.49d).At 500 nm, while %T is %99 under 0.00 V potential application, it decreases to %59 when 1.50 V was applied thus illustrate a %40 optic contrast. However this change was not stable after a copule of cycles. At 620 nm, while %T is %60 under 0.00 V potential application, it increases to %81 when 1.50 V was applied thus illustrate a %21 optic contrast These %T responses of the film changes very too much during the 10 cycles, which indicates unsatisfactory optic stability of ITO/ H_2Pc(ep) film.

Fig. 3.50 illustrates in situ spectrochronocoulometric analysis (SCC) analysis of ITO/NiPc(ep) film in AN/TBAP electrolyte system.

In situ spectroelectrochemical analysis of the ITO/NiPc(ep) is given in Fig. 3.50a to represent the optic responses of the film under potential stress. Without any potential application, the Q band of NiPc film is recorded at 634 nm (red spectrum). When 1.50 V was applied to the working electrode, spectrum of the film changes immediately.

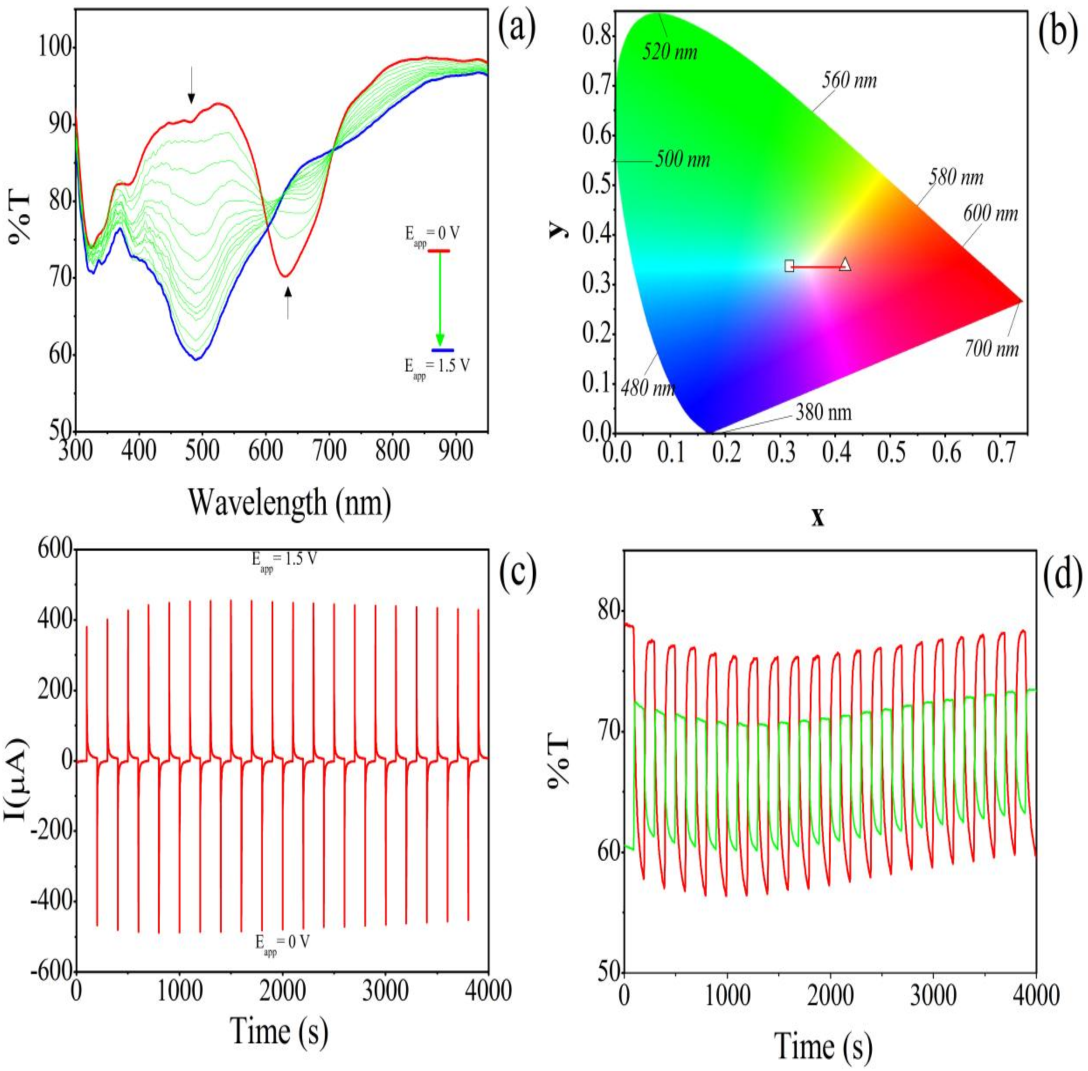

Figure 3.50 SCC analysis of ITO/NiPc(ep) film in AN/TBAP electrolyte system. **a)** %T changes recorded during in situ spectroelectrochemical measurement under 1.50 V potential application. **b)** Chromaticity diagram of ITO/NiPc(ep) film. **c)** Repetitive chronoamperometric responses between $E_{app.}$=0.0 V and $E_{app.}$= 1.50 V within 100 s time interval. **d)** %T changes at 500nm (red) and 620 nm (green) versus time.

When 1.50 V was applied to the working electrode, spectrum of the film changes immediately. First of all, the Q band decreases slightly in intensity and new band is recorded at 500 nm. This spectral changes cause a color changes from cyan to red. Color changes during the redox processes are represented in the chromaticity diagram in Fig. 3.50b. Under 0.0 V potential application, film has green color (x: 0.324 and y: 0.335, point □). When 1.50 V was applied, color changes to cyan immediately (x: 0.418 and y:0.338, point △). To derive basic electrochromic parameters of the ITO/NiPc(ep) film, repetitive chronocoulometric measurements were performed with the spectral measurements (in situ spectrochronocoulometric analysis, SCC). Fig. 3.50c illustrate the current responses of the ITO/NiPc(ep) film under the constant potential application which was switched between 0.0 and 1.50 V. A stable current-time response is recorded until the 20 cycles as shown in Fig. 3.50c during the repetitive potential application, which indicate the columbic stability of the film. %T versus time response of the film was recorded at 500 nm and 620 nm to determine the response time, optic stability, and columbic efficiency of the film (3.50d).At 500 nm, while %T is %79 under 0.00 V potential application, it decreases to %57 when 1.50 V was applied thus illustrate a %22 optic contrast. At 620 nm, while %T is %60 under 0.00 V potential application, it increases to %73 when 1.50 V was applied thus illustrate a %13 optic contrast These %T responses of the film changes very little during the 20 cycles, which indicates excellent optic stability of ITO/NiPc(ep) film. Responses times are 1 and 1.2 s for anodic response (changing from cyan to red) these responses stay stable during 20 cycles. Anodic and cathodic efficiencies of the films (slope of %T versus charge density) are found as 250 and 160 cm^2/mC.

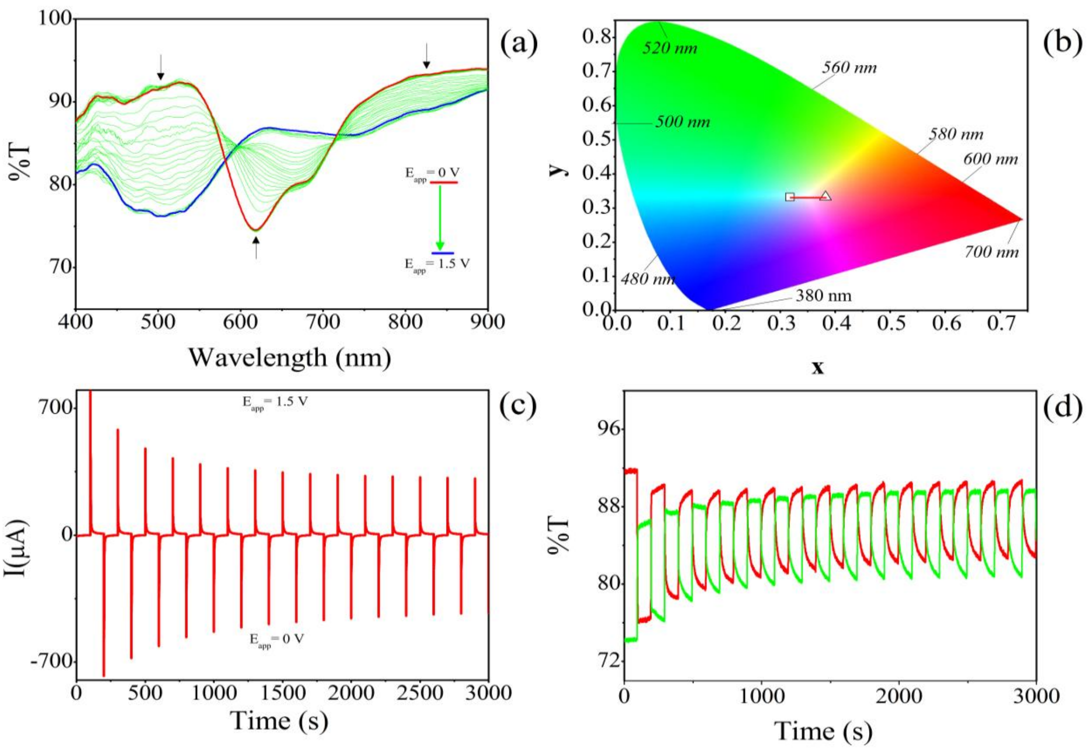

Figure 3.51 SCC analysis of ITO/CuPc(ep) film in AN/TBAP electrolyte system. **a)** %T changes recorded during in situ spectroelectrochemical measurement under 1.50 V potential application. **b)** Chromaticity diagram of ITO/CuPc(ep) film. **c)** Repetitive chronoamperometric responses between $E_{app.}$=0.0 V and $E_{app.}$= 1.50 V within 100 s time interval. **d)** %T changes at 500nm (red) and 620 nm (green) versus time.

Finally, spectrochronocoulometric measurements of ITO/CuPc(ep) film in AN/TBAP electrolyte system were analyzed. The color of the film was also changed cyan to red. At 500 and 620 nm films illustrate respectively %12 and %11 optic contrast. These %T responses of the film changes very few during the 15 cycles, which indicates good optic stability of ITO/ CuPc (ep) film. Anodic and cathodic efficiencies of the films (slope of %T versus charge density) are found as 180 and 120 cm^2/ mC. All measurements indicate that electrochromic properties are affected a couple of paremeters. Metals on the center of the complexes are also directly related of the characteristic properties.

4. CONCLUSIONS

Voltammetric and in-situ spectroelectrochemical studies show that TiOPc complexes give both metal and ligand-based, multi-electron reduction processes, which were affected from number and position of the substituents. Substituent variation of the complexes affects the peak potential and assignment of the redox processes. Electrochemical and spectroelectrochemical measurement of TiOPc complexes indicated that incorporation redox active metal centers, TiO into the phthalocyanine core extend the redox richness of the Pc ring with the reversible metal-based reduction couples in addition to the common Pc ring-based electron transfer processes. This expanded redox behavior of the complexes are the desired properties of the electrochemical applications, especially, electro catalytic, electrochromic and electro sensing applications. In situ electro colorimetric measurements of the new complexes allow quantification of color coordinates of the each electro generated anionic and cationic redox species. Different color of the electro generated species indicates their possible application in the display technologies, e.g. electrochromic and data storage application. All TiOPc complexes coated on ITO electrode with LB technique sense Ag^{+} and Pd^{+2} ions. Presence of Ag^{+} and Pd^{+2} ions in the electrolyte system influences the redox couples of the complexes due to the interaction between metal ions and TiOPc. All complexes behave as homogeneous electro catalyst for ORR and catalytic activities varies with substituent environments of the complexes. According to the voltammetric and spectroelectrochemical response of the systems with or without O_2, the electro catalytic activity of the complexes depends on the substituents and solvent of the system. Since, catalytic activity of α-TiOPc increases in DMSO with respect to the activity in DCM. Moreover, Langmuir Blodgett films of the complexes can be used as heterogeneous ORR electrocatalysts in aqueous solution. These catalytic data indicated possible usage of the complexes in fuel cell technology as a cathode active material, in the non-aqueous metal-air batteries, as electrocatalysts for the production of superoxide from molecular oxygen in the aprotic solvents, and as electrochemical sensors.

Electrochemical and spectroelectrochemical measurement revealed that incorporation redox active metal centers, Co^{II}, $Ti^{IV}O$, and $Mn^{III}OAc$ into the phthalocyanine core extend the redox richness of the Pc ring with the reversible metal-based reduction and oxidation couples in addition to the common Pc ring-based electron transfer processes. This expanded redox behavior of the complexes are the desired properties of the electrochemical applications, especially, electro catalytic, electrochromic and electro sensing applications. Solvent of the electrolyte affects the redox properties of the complexes which have redox active metal center due to the coordination ability differences of the solvents. *In-situ* electro colorimetric measurements of the new complexes allow quantification of color coordinates of the each electro generated anionic and cationic redox species. Different color of the electro generated species indicates their possible application in the display technologies, e.g. electrochromic and data storage application. Presence of O_2 in the electrolyte system influences the redox couples of the complexes due to the interaction between O_2 and MPcs having redox active metal center, which is the desired properties for the fuel cell applications of the complexes as cathode active material.

Electrochemical and spectroelectrochemical measurement indicates that substitution of the complexes with dimethylamine and diethylamine groups supply electropolymerization of the complexes on the working electrode. Coating of the complexes on a substrate (e.g. an electrode) with electropolymerization is a desired property for preparation of composite electrode, which has potentials for the usage in different electrochemical technologies such as, electrocatalytic, electrochromic and electro sensing applications. Since a functional material should be coated on a substrate with a techniques (e.g. electropolymerization), with which film thickness, morphology, roughness, and conductivity could be controlled easily.

Electron transfer reactions of diethyl amine substituted phthalocyanine complexes alter the optical responses of the complex in solution as well as in solid state due to the disappearance of the Q band of the complex and observation of new bands in the visible region of the light spectrum. Optical changing’s in the visible light spectrum are the desired properties for a material for the usage in the display technologies.

In situ spectrochronocoulometric measurements indicate that electro polymerized Pc films illustrate excellent electrochromic properties with fast response time, high efficiency, high columbic and optic stability, and high optical contrast.

REFERENCES

[1] Falke, M., Graehlert, X., Falke, U., Schulze, S., & Hietschold, M. (1995). Structural imaging of lanthanoide diphthalocyanines by transmission electron microscopy. *Physica status solid (a)*, *150*(1), 359-369.

[2] De Diesbach, H., & von der Weid, E. (1927). Quelques sels complexes des o-dinitriles avec le cuivre et la pyridine. *Helvetica Chimica Acta*, *10*(1), 886-888.

[3] Bard, A.J.; Faulkner, L.R. (2001), *Electrochemical Methods: fundamentals and applications*, 2nd Edition, John Wiley & Sons, Inc., 1-430 New York, USA.

[4] Gregory P., (2000), Industrial applications of phthalocyanines, J. Porphyrins Phthalocyanines, 4, 432.

[5] Linstead R. P. (1934), An unusual isomeric change in the three-carbon system, Journal of Chemical. Society, 57, 1016-1024.

[6] Robertson J. M., (1935), An X-ray study of the structure of phthalocyanines, J. Chem. Soc. 615.

[7] Paul, I. C., Sim, G. A., Hamor, T. A., & Robertson, J. M. (1962). 802. The structure of clerodin: X-ray analysis of clerodin bromo-lactone. *Journal of the Chemical Society (Resumed)*, 4133-4145.

[8] Gregory, P. (1999). Steamrollers, sports cars and security: phthalocyanine progress through the ages. *Journal of Porphyrins and Phthalocyanines*, *3*(06), 468-476.

[9] Reddy, K. R. V. and J. Keshavayya (2002) Synthesis of symmmetrically substituted octabromophthalocyanine pigments and their characterisation, Dyes and Pigments 53(3), 187-194.

[10] Hanack, M., & Lang, M. (1994). Conducting stacked metallophthalocyanines and related compounds. *Advanced Materials*, *6*(11), 819-833.

[11] Linstead, R. P. (1936), An unusual isomeric change in the three-carbon system, Journal of Chemical. Society, 57, 1016-1024

[12] Byrne, G. T., Linstead, R. P., & Lowe, A. R. (1934). 213. Phthalocyanines. Part II. The preparation of phthalocyanine and some metallic derivatives from o-cyanobenzamide and phthalimide. *Journal of the Chemical Society (Resumed)*, 1017-1022.

[13] Bottomley L. A., Gorce J.-N., Goedken V. L. and Ercolani C., (1985), *Inorg. Chem.*, 24, 3733–3737.

[14] Wilson, M. S., (2005), Electrochemical immunosensors for the simultaneous detection of two tumor markers, Analytical Chemistry 77(5), 1496–1502.

[15] Davis, S. B., W. E. Doering, P. Levine and R. P. Linstead (1950) The Stereochemistry of Catalytic Hydrogenation .8. Pyrolysis of the 6 Perhydrodiphenic Acids - Limitations of Blanc Rule, Journal of the Chemical Society(Jun), 1423-1425.

[16] Linstead, R. P., & Lowe, A. R. (1934). 216. Phthalocyanines. Part V. The molecular weight of magnesium phthalocyanine. *Journal of the Chemical Society (Resumed)*, 1031-1033.

[17] Linstead, R. P. and F. T. Weiss (1950) Phthalocyanines and Related Compounds .20. Further Investigations on Tetrabenzporphin and Allied Substances, Journal of the Chemical Society(Nov), 2975-2981.

[18] Ukei, K., (1973), 'Lead Phthalocyanine', *Acta Cryst. B*, B29 2290-2297

[19] Iyechika, Y., Yakushi K., Ikemoto I., Kuroda H., (1982), Structure of Lead Phthalocyanine *Acta Cryst. B*, 38 766-770.

[20] Day, P.N., Wang, Z.Q., Pachter, R., (1998), Ab-initio study of the ring-opening reactions of pyran, nitrochromene, and spiropyran, *J. Mol. Struct. (Theochem)*, 455, 33-38.

[21] Kubiak, R., Janczak, J., (1992), A simple, novel method for the preparation of metallophthalocyanines, *J. Alloy Compd.*, 189, 107-111.

[22] Friedel, M.K., Hoskins, B.F., Martin, R.L., Mason, S.A., (1970), Lead Phthalocyanine: A one-dimensional conductor, *J. Chem. Soc., Chem*, 18, 400-401 .

[23] Zhang, Y., Zhang, X., Liu, Z., Xu, H., Jiang, J., (2006), Comparative density functional theory study of the structures and properties of metallophthalocyanines of group IV B, *Vib. Spectrosc.*, 40, 289-294.

[24] Barrett, P.A., Dent, C.E., Linstead, R.P., (1936), Phthalocyanine as a co-ordinating group. A general investigation of the metallic derivatives, *J. Chem. Soc.*, 1719-1725.

[25] Ziolo R.F., Günther W.H.H., Troup J.J., (1981), Planar, pleated, and saddle-shaped structures of the phthalocyanine dianion in two novel multidentate oxygen-donor complexes of dipotassium phthalocyanine, *J. Am. Chem. Soc.*, 103, 4629-4633.

[26] Ziolo, R.F., Extine, M., (1981), New alkali metal phthalocyanine (Pc) complexes. Structure of the quasi-multimacrocycle K2Pc (DMF) 4 and the KPcK template, *Inorg. Chem.*, 20 2709-2712.

[27] Guyon, F., Pondaven, A., Guenot, P., & L'Her, M. (1994). Bis (2, 3-NiPchthalocyaninato) lutetium (III) and (2, 3-NiPchthalocyaninato)(phthalocyaninato) lutetium (III) Complexes: Synthesis, Spectroscopic Characterization, and Electrochemistry, *Inorganic Chemistry*, *33*(21), 4787-4793.

[28] Jiang, J., Liu, W., Law, W. F., Lin, J., & Ng, D. K. (1998). A new synthetic route to unsymmetrical bis (phthalocyaninato) europium (III) complexes.*Inorganica chimica acta*, *268*(1), 141-144.

[29] McKeown, N. B., Chambrier, I., & Cook, M. J. (1990). Synthesis and characterisation of some 1, 4, 8, 11, 15, 18, 22, 25-octa-alkyl-and 1, 4, 8, 11, 15, 18-hexa-alkyl-22, 25-bis (carboxypropyl) phthalocyanines. *J. Chem. Soc., Perkin Trans. 1*, (4), 1169-1177.

[30] Lebedeva, N. S., Pavlycheva, N. A., Petrova, O. V., Vyugin, A. I., Kinchin, A. N., Parfenyuk, E. V., Shaposhnikov, G. P. (2003). Determination of the dimerization constants of water soluble metallophthalocyanines by calorimetric titration using electron-donating ligands. *Mendeleev Communications*, *13*(5), 237-238.

[31] Chen, Y., Doyle, J., Liu, Y., Strevens, A., Lin, Y., Ei-Khouly, M. E., ... & Ito, O. (2007). Optoelectronic and nonlinear optical properties of< i> t</i> Bu< sub> 4</sub> PcTiO/polymer composite materials. *Journal of Photochemistry and Photobiology A: Chemistry*, *185*(2), 263-270.

[32] Goedken, V. L., Dessy, G., Ercolani, C., & Fares, V. (1985). Synthesis, reactivity, and X-ray crystal structure of dichloro (phthalocyaninato) titanium (IV). *Inorganic Chemistry*, *24*(7), 991-995.

[33] Gingl, F., & Strahle, J. (1990). Structure of bicyclophthalocyaninatochloroniobium (IV). *Acta Crystallographica Section C: Crystal Structure Communications*, *46*(10), 1841-1843.

[34] Wang, X., Chen, Y., Liu, H., & Jiang, J. (2006). Spectroscopic and structural characteristics of Langmuir–Blodgett films of bis [2, 3, 9, 10, 16, 17, 24, 25-octakis (octyloxy) phthalocyaninato] rare earth complexes. *Thin solid films*,*496*(2), 619-625.
[35] Bilgiçli, A. T., Günsel, A., Kandaz, M., & Özkaya, A. R. (2012). Highly selective thioalcohol modified phthalocyanine sensors for Ag (i) and Pd (ii) based on target induced J-and H-type aggregations: synthesis, electrochemistry and peripheral metal ion binding studies. *Dalton Transactions*,*41*(23), 7047-7056.
[36] Kadish, K. M., Smith, K. M., & Guilard, R. (2003). The Porphyrin Handbook: Applications of Phthalocyanines (Vol. 19). Elsevier.
[37] McKeown, N. B. (1998). *Phthalocyanine materials: synthesis, structure, and function* (Vol. 6). Cambridge University Press.
[38] Rawson, F. J., Purcell, W. M., Xu, J., Cowell, D. C., Fielden, P. R., Biddle, N., & Hart, J. P. (2007). Fabrication and characterisation of novel screen-printed tubular microband electrodes, and their application to the measurement of hydrogen peroxide. *Electrochimica acta*, *52*(25), 7248-7253.
[39] McKeown, N. B. (1998). *Phthalocyanine materials: synthesis, structure, and function* (Vol. 6). Cambridge University Press.
[40] Maree, S., & Nyokong, T. (2000). Electrocatalytic behavior of substituted cobalt phthalocyanines towards the oxidation of cysteine. *Journal of Electroanalytical Chemistry*, *492*(2), 120-127.
[41] Nombona, N., Tau, P., Sehlotho, N., & Nyokong, T. (2008). Electrochemical and electrocatalytic properties of α-substituted manganese and titanium phthalocyanines. *Electrochimica Acta*, *53*(7), 3139-3148.
[42] Lever, A. B. P. (1999). The Phthalocyanines—Molecules of Enduring Value; a Two-dimensional Analysis of Redox Potentials. *Journal of Porphyrins and Phthalocyanines*, *3*(06), 488-499.
[43] Ozoemena, K. I., Pillay, J., & Nyokong, T. (2006). Preferential electrosorption of cobalt (II) tetra-aminophthalocyanine at single-wall carbon nanotubes immobilized on a basal plane pyrolytic graphite electrode. *Electrochemistry communications, 8*(8), 1391-1396**.**

[44] Siswana, M. P., Ozoemena, K. I., & Nyokong, T. (2006). Electrocatalysis of asulam on cobalt phthalocyanine modified multi-walled carbon nanotubes immobilized on a basal plane pyrolytic graphite electrode. *Electrochimica acta*,*52*(1), 114-122.
[45] Ramírez, G., Trollund, E., Canales, J. C., Canales, M. J., Armijo, F., & Aguirre, M. J. (2001). Effect of the conditions of electropolymerization on the electrocatalytic response of non-metalled-poly-tetraaminophthalocyanine-modified electrodes toward the reduction of oxygen.*Boletin de la sociedad chilena de quimica*, *46*(3), 247-255.
[46] Nkosi, D., & Ozoemena, K. I. (2008). Interrogating the electrocatalytic properties of coordination self-assembled nanostructures of single-walled carbon nanotube–octa (hydroxyethylthio) phthalocyaninatoiron (II) using thiocyanate as an analytical probe. *Journal of Electroanalytical Chemistry*,*621*(2), 304-313.
[47] Chicharro, M., Zapardiel, A., Bermejo, E., Moreno, M., & Madrid, E. (2002). Electrocatalytic amperometric determination of amitrole using a cobalt-phthalocyanine-modified carbon paste electrode. *Analytical and bioanalytical chemistry*, *373*(4-5), 277-283.
[48] Agboola, B. O., Ozoemena, K. I., & Nyokong, T. (2006). Electrochemical properties of benzylmercapto and dodecylmercapto tetra substituted nickel phthalocyanine complexes: electrocatalytic oxidation of nitrite. *Electrochimica acta*, *51*(28), 6470-6478.
[49] Koca, A., Dinçer, H. A., Koçak, M. B., & Gül, A. (2006). Electrochemical characterization of Co (II) and Pd (II) phthalocyanines carrying diethoxymalonyl and carboxymethyl substituents. *Russian Journal of Electrochemistry*, *42*(1), 31-37.
[50] Lever, A. B. P., & Minor, P. C. (1981). Electrochemistry of main-group phthalocyanines. *Inorganic Chemistry*, *20*(11), 4015-4017.
[51] Lever, A. B. P. (1965). The phthalocyanines. *Adv. Inorg. Chem. Radiochem*, *7*, 27-114.
[52] Schlettwein, D., & Yoshida, T. (1998). Electrochemical reduction of substituted cobalt phthalocyanines adsorbed on graphite. *Journal of Electroanalytical Chemistry*, *441*(1), 139-146.
[53] Lever, A. B. P., Pickens, S. R., Minor, P. C., Licoccia, S., Ramaswamy, B. S., & Magnell, K. (1981). Charge-transfer spectra of metallophthalocyanines: correlation with electrode potentials. *Journal of the American Chemical Society*,*103*(23), 6800-6806.

[54] Zagal, J. H., Gulppi, M. A., & Cárdenas-Jirón, G. (2000). Metal-centered redox chemistry of substituted cobalt phthalocyanines adsorbed on graphite and correlations with MO calculations and Hammett parameters. Electrocatalytic reduction of a disulfide. *Polyhedron*, *19*(22), 2255-2260.

[55] Ureta-Zañartu, M. S., Bravo, P., & Zagal, J. H. (1992). Methanol oxidation on modified iridium electrodes. *Journal of Electroanalytical Chemistry*, *337*(1), 241-251.

[56] Chen, Y., Fujitsuka, M., O'Flaherty, S. M., Hanack, M., Ito, O., & Blau, W. J. (2003). Strong optical limiting of soluble axially substituted gallium and indium phthalocyanines. *Advanced Materials*, *15*(11), 899-902.

[57] Wöhrle, D. (2001). Phthalocyanines in macromolecular phases–methods of synthesis and properties of the materials. *Macromolecular rapid communications*, *22*(2), 68-97.

[58] Zagal, J. H., M. A. Gulppi and G. Cardenas-Jiron (2000) Metal-centered redox chemistry of substituted cobalt phthalocyanines adsorbed on graphite and correlations with MO calculations and Hammett parameters. Electrocatalytic reduction of a disulfide, Polyhedron 19(22-23), 2255-2260.

[59] Koca, A., Özkaya, A. R., Arslanoğlu, Y., & Hamuryudan, E. (2007). Electrochemistry, spectroelectrochemistry and electrochemical polymerization of titanylphthalocyanines. *Electrochimica acta*, *52*(9), 3216-3221.

[60] Alpatova, N. M., Ovsyannikova, E. V., Tomilova, L. G., Korenchenko, O. V., & Kondrashov, Y. V. (2001). Anodic doping of electropolymerized copper 2, 9, 16, 23-tetraaminophthalocyanine. *Russian journal of electrochemistry*, *37*(10), 1012-1016.

[61] Neustroeva, N. R., Bazanov, M. I., & Vorob'ev, Y. G. (2001). Electrochemical properties of a binuclear cobalt-containing macroheterocycle with an enlarged coordination cavity. *Russian journal of electrochemistry*, *37*(2), 205-207.

[62] Özer, M., Altındal, A., Özkaya, A. R., Bulut, M., & Bekaroğlu, Ö. (2006). Synthesis, characterization and some properties of novel bis (pentafluorophenyl) methoxyl substituted metal free and metallophthalocyanines. *Polyhedron*, *25*(18), 3593-3602.

[63] Ozoemena, K. I., Nyokong, T., & Westbroek, P. (2003). Self-Assembled Monolayers of Cobalt and Iron Phthalocyanine Complexes on Gold Electrodes: Comparative Surface Electrochemistry and Electrocatalytic Interaction with Thiols and Thiocyanate. *Electroanalysis*, *15*(22), 1762-1770.

[64] Li, Z., Lieberman, M., & Hill, W. (2001). XPS and SERS study of silicon phthalocyanine monolayers: umbrella vs octopus design strategies for formation of oriented SAMs. *Langmuir*, *17*(16), 4887-4894.

[65] Lever, A. B. P., & Wilshire, J. P. (1978). Electrochemistry of iron phthalocyanine complexes in nonaqueous solvents and the identification of five-coordinate iron (I) phthalocyanine derivatives. *Inorganic Chemistry*, *17*(5), 1145-1151.

[66] Liao, M. S., Watts, J. D., Huang, M. J., Gorun, S. M., Kar, T., & Scheiner, S. (2005). Effects of Peripheral Substituents on the Electronic Structure and Properties of Unligated and Ligated Metal Phthalocyanines, Metal= Fe, Co, Zn.*Journal of Chemical Theory and Computation*, *1*(6), 1201-1210.

[67] Bard, A. J. (1982). Design of semiconductor photoelectrochemical systems for solar energy conversion. *The Journal of Physical Chemistry*, *86*(2), 172-177.

[68] Lever, A. B. P., Minor, P. C., & Wilshire, J. P. (1981). Electrochemistry of manganese phthalocyanine in nonaqueous media. *Inorganic Chemistry*, *20*(8), 2550-2553.

[69] Lever, A. B. P. (1965). The phthalocyanines. *Adv. Inorg. Chem. Radiochem*, *7*, 27-114.

[70] Bekaroğlu, Ö. (1996). Phthalocyanines containing macrocycles. *Applied organometallic chemistry*, *10*(8), 605-622

[71] Lever, A. B. P., & Minor, P. C. (1981). Electrochemistry of main-group phthalocyanines. *Inorganic Chemistry*, *20*(11), 4015-4017.

[72] Roberge, P. R., Beaudoin, R., & Berthiaume, J. F. (1988). Fabrication and characterization of an activated carbon for electrochemical applications.*Carbon*, *26*(2), 173-182.

[73] Gouterman, M. (1961). Spectra of porphyrins. *Journal of Molecular Spectroscopy*, *6*, 138-163.

[74] Weiss, C., Kobayashi, H., & Gouterman, M. (1965). Spectra of porphyrins: part III. Self-consistent molecular orbital calculations of porphyrin and related ring systems. *Journal of Molecular Spectroscopy*, *16*(2), 415-450.

[75] Boucher, B., Buhl, R., & Perrin, M. (1971). Proprietes et structure magnetique de Mn< sub> 3</sub> O< sub> 4</sub>. *Journal of Physics and Chemistry of Solids*, *32*(10), 2429-2437.

[76] Cook, M. J., Dunn, A. J., Howe, S. D., Thomson, A. J., & Harrison, K. J. (1988). Octa-alkoxy phthalocyanine and NiPchthalocyanine derivatives: dyes with Q-band absorption in the far red or near infrared. *J. Chem. Soc., Perkin Trans. 1*, (8), 2453-2458.

[77] Christie, R. M. (1995). Colour and constitution relationships in organic pigments. Part 5: The influence of solvents, the central metal atom and substituents on the electronic spectra of phthalocyanines. *Dyes and pigments*,*27*(1), 35-43.

[78] Chauke, V., Ogunsipe, A., Durmuş, M., & Nyokong, T. (2007). Novel gallium (III) phthalocyanine derivatives–Synthesis, photophysics and photochemistry.*Polyhedron*, *26*(12), 2663-2671.

[79] Yilmaz, I., Gürek, A., & Ahsen, V. (2005). Synthesis, electrochemical, and spectroelectrochemical properties of tetrakis (13, 17-dioxa nonacosane-15-sulphanyl) phthalocyaninato zinc (II). *Polyhedron*, *24*(7), 791-798.

[80] Mbambisa, G. (2009). Synthesis and electrochemistry of octapentylthio phthalocyanine complexes of manganese, titanium and vanadium (Doctoral dissertation, Rhodes University).

[81] Kobayashi, N., Ogata, H., Nonaka, N., & Luk'yanets, E. A. (2003). Effect of Peripheral Substitution on the Electronic Absorption and Fluorescence Spectra of Metal-Free and Zinc Phthalocyanines. *Chemistry-A European Journal*, *9*(20), 5123-5134.

[82] Guo, L., Ellis, D. E., Hoffman, B. M., & Ishikawa, Y. (1996). Ligand substitution effect on electronic structure and optical properties of nickel porphyrazines.*Inorganic Chemistry*, *35*(18), 5304-5312.

[83] Chidawanyika, W., Ogunsipe, A., & Nyokong, T. (2007). Syntheses and photophysics of new phthalocyanine derivatives of zinc, cadmium and mercury.*New Journal of Chemistry*, *31*(3), 377-384.

[84] Obirai, J., & Nyokong, T. (2005). Synthesis, spectral and electrochemical characterization of mercaptopyrimidine-substituted cobalt, manganese and Zn (II) phthalocyanine complexes. *Electrochimica acta*, *50*(16), 3296-3304.

[85] Stillman, M. J., & Thomson, A. J. (1974). Orbital reduction factors in the lowest excited state of the phthalocyanine ring and their measurement by magnetic circular dichroism spectroscopy. *J. Chem. Soc., Faraday Trans. 2*, *70*, 805-814.

[86] Lever, A. B. P., Pickens, S. R., Minor, P. C., Licoccia, S., Ramaswamy, B. S., & Magnell, K. (1981). Charge-transfer spectra of metallophthalocyanines: correlation with electrode potentials. *Journal of the American Chemical Society*,*103*(23), 6800-6806.

[87] Donner, S., Li, H. W., Yeung, E. S., & Porter, M. D. (2006). Fabrication of optically transparent carbon electrodes by the pyrolysis of photoresist films: approach to single-molecule spectroelectrochemistry. *Analytical chemistry*,*78*(8), 2816-2822.

[88] Keizer, S. P., Mack, J., Bench, B. A., Gorun, S. M., & Stillman, M. J. (2003). Spectroscopy and electronic structure of electron deficient zinc phthalocyanines. *Journal of the American Chemical Society*, *125*(23), 7067-7085.

[89] Khene, S., Geraldo, D. A., Togo, C. A., Limson, J., & Nyokong, T. (2008). Synthesis, electrochemical characterization of tetra-and octa-substituted dodecyl-mercapto tin phthalocyanines in solution and as self-assembled monolayers. *Electrochimica Acta*, *54*(2), 183-191.

[90] Nyokong, T., & Isago, H. (2004). The renaissance in optical spectroscopy of phthalocyanines and other tetraazaporphyrins. *Journal of Porphyrins and Phthalocyanines*, *8*(09), 1083-1090.

[91] Kobayashi, N. (1991). A rigid, laterally bridged binuclear subphthalocyanine: the first dimer of aromatic macrocyclic complexes containing boron. *J. Chem. Soc., Chem. Commun.*, (17), 1203-1205.

[92] Rauschnabel, J., & Hanack, M. (1995). New derivatives and homologues of subphthalocyanine. *Tetrahedron letters*, *36*(10), 1629-1632.

[93] Wiederkehr, N. A. (1999). A model for specific interactions of manganese-phthalocyanine in protic media. *Eclética Química*, *24*, 45-59.

[94] George, R. D., Snow, A. W., Shirk, J. S., & Barger, W. R. (1998). The alpha substitution effect on phthalocyanine aggregation. *Journal of Porphyrins and Phthalocyanines*, *2*(1), 1-7.

[95] Cook, M. J., McMurdo, J., Miles, D. A., Poynter, R. H., Simmons, J. M., Haslam, S. D., ... & Welford, K. (1994). Monolayer behaviour and Langmuir–Blodgett film properties of some amphiphilic phthalocyanines: factors influencing molecular organisation within the film assembly. *J. Mater. Chem.*,*4*(8), 1205-1213.

[96] Somashekarappa, M. P., Keshavayya, J., & Sampath, S. (2002). Self-assembled molecular films of tetraamino metal (Co, Cu, Fe) phthalocyanines on gold and silver. Electrochemical and spectroscopic characterization. *Pure and Applied Chemistry*, *74*(9), 1609-1620.

[97] Dabak, S., Gümüs, G., Gül, A., & Bekaroglu, Ö. (1996). Synthesis and properties of new phthalocyanines with tertiary or quaternarized aminoethylsulfanyl substituents. *Journal of coordination chemistry*, *38*(4), 287-293.

[98] Stillman, M. J., & Thomson, A. J. (1974). Orbital reduction factors in the lowest excited state of the phthalocyanine ring and their measurement by magnetic circular dichroism spectroscopy. *J. Chem. Soc., Faraday Trans. 2*, *70*, 805-814.

[99] Lever, A. B., Hempstead, M. R., Leznoff, C. C., Liu, W., Melnik, M., Nevin, W. A., & Seymour, P. (1986). *Recent studies in phthalocyanine chemistry*. Defense Technical Information Center.

[100] Schultz, H., Lehmann, H., Rein, M., & Hanack, M. (1991). Phthalocyaninatometal and related complexes with special electrical and optical properties. In *Metal Complexes with Tetrapyrrole Ligands II* (pp. 41-146). Springer Berlin Heidelberg.

[101] Zhou, S., Jin, X., Hu, W., Liu, Y., & Liu, S. (1999). An interesting phenomenon of impurity sulfur in phthalocyanine photoreceptor device. *Solid state communications*, *112*(5), 269-273.

[102] Pai, D. M., & Springett, B. E. (1993). Physics of electrophotography. *Reviews of modern physics*, *65*(1), 163.

[103] Bao, Z. (2000). Materials and fabrication needs for low-cost organic transistor circuits. *Advanced Materials*, *12*(3), 227-230.

[104] Yuen, C. W. M., Ku, S. K. A., Kan, C. W., & Choi, P. S. R. (2007). Enhancing textile ink-jet printing with chitosan. *Coloration technology*, *123*(4), 267-270.

[105] Law, K. Y. (1993). Organic photoconductive materials: recent trends and developments. *Chemical reviews*, *93*(1), 449-486.

[106] Kaji, H., & Shimoyama, Y. (2002). An electron paramagnetic resonance study of vacuum-deposited films of titanyl phthalocyanine. *Thin solid films*, *408*(1), 245-251.

[107] Gregory, Peter, and Ronald W. Kenyon. "Phthalocyanine colorants and their use in ink jet printing." U.S. Patent No. 5,296,023. 22 Mar. 1994.

[108] Schlebusch, C., Morenzin, J., Kessler, B., & Eberhardt, W. (1999). Organic photoconductors with C< sub> 60</sub> for xerography. *Carbon*, *37*(5), 717-720.

[109] Sies, H. (1986). Biochemistry of oxidative stress. *Angewandte Chemie International Edition in English*, *25*(12), 1058-1071.

[110] Soncin, M., Busetti, A., Biola, R., Jori, G., Kwag, G., Li, Y. S., ... & Rodgers, M. A. (1998). Photoinactivation of amelanotic and melanotic melanoma cells sensitized by axially substituted Si-NiPchthalocyanines. *Journal of Photochemistry and Photobiology B: Biology*, *42*(3), 202-210.

[111] Bonnett, R., & Martınez, G. (2001). Photobleaching of sensitisers used in photodynamic therapy. *Tetrahedron*, *57*(47), 9513-9547.

[112] Dougherty, T. J. (1989). Photodynamic therapy: status and potential. *Oncology (Williston Park, NY)*, *3*(7), 67.

[113] Henderson, B. W., & Dougherty, T. J. (1992). How does photodynamic therapy work?. *Photochemistry and photobiology*, *55*(1), 145-157.

[114] Bonnett, R. (1995). Photosensitizers of the porphyrin and phthalocyanine series for photodynamic therapy. *Chemical Society Reviews*, *24*(1), 19-33.

[115] Shirk, J. S., Pong, R. G., Bartoli, F. J., & Snow, A. W. (1993). Optical limiter using a lead phthalocyanine. *Applied physics letters*, *63*(14), 1880-1882.

[116] Perry, J. W., Mansour, K., Lee, I. Y., Wu, X. L., Bedworth, P. V., Chen, C. T., ... & Sasabe, H. (1996). Organic optical limiter with a strong nonlinear absorptive response. *Science*, *273*(5281), 1533-1536.

[117] Kaliya, O. L., Lukyanets, E. A., & Vorozhtsov, G. N. (1999). Catalysis and photocatalysis by phthalocyanines for technology, ecology and medicine.*Journal of Porphyrins and Phthalocyanines*, *3*(07), 592-610.

[118] Neys, P. E. F., Vankelecom, I. F. J., Parton, R. F., Dehaen, W., L'abbe, G., & Jacobs, P. A. (1997). The oxidation of cyclic alcohols from an aqueous solution by manganese porphyrins embedded in a polydimethylsiloxane membrane.*Journal of Molecular Catalysis A: Chemical*, *126*(1), L9-L12.

[119] Miyasaka, H., Campos-Fernández, C. S., Clérac, R., & Dunbar, K. R. (2000). Hexagonal layered materials composed of [M2 (O2CCF3) 4](M= Ru and Rh) donors and TCNQ acceptors. *Angewandte Chemie*, *112*(21), 3989-3993.

[120] Zagal, J. H., Gulppi, M. A., Caro, C. A., & Cárdenas-Jirón, G. I. (1999). Paradoxical effect of the redox potential of adsorbed metallophthalocyanines on their activity for the oxidation of 2-mercaptoethanol. Inner versus outer sphere electrocatalysis. *Electrochemistry communications*, *1*(9), 389-393.

[121] Kobayashi, N., Lam, H., Nevin, W. A., Janda, P., Leznoff, C. C., & Lever, A. B. P. (1990). Electrochemistry and spectroelectrochemistry of 1, 8-NiPchthalene-and 1, 8-anthracene-linked cofacial binuclear metallophthalocyanines. New mixed-valence metallophthalocyanines. *Inorganic Chemistry, 29*(18), 3415-3425.

[122] Zagal, J. H., & Cárdenas-Jirón, G. I. (2000). Reactivity of immobilized cobalt phthalocyanines for the electroreduction of molecular oxygen in terms of molecular hardness. *Journal of Electroanalytical Chemistry*, *489*(1), 96-100.

[123] El Hourch, A., Belcadi, S., Moisy, P., Crouigneau, P., Léger, J. M., & Lamy, C. (1992). Electrocatalytic reduction of oxygen at iron phthalocyanine modified polymer electrodes. *Journal of Electroanalytical Chemistry*, *339*(1), 1-12.

[124] Tse, Y. H., Janda, P., & Lever, A. B. P. (1994). Electrode with electrochemically deposited N, N', N'', N'''-tetramethyltetra-3, 4-pyridinoporphyrazinocobalt (I) for detection of sulfide ion. *Analytical Chemistry*,*66*(3), 384-390.

[125] Gulppi, M. A., Paez, M. A., Costamagna, J. A., Cárdenas-Jirón, G., Bedioui, F., & Zagal, J. H. (2005). Inverted correlations between rate constants and redox potential of the catalyst for the electrooxidation of 2-aminoethanethiol mediated by surface confined substituted cobalt-phthalocyanines. *Journal of Electroanalytical Chemistry*, *580*(1), 50-56.

[126] Retamal, B. A., Vaschetto, M. E., & Zagal, J. (1997). Catalytic electro-oxidation of 2-mercaptoethanol using cobalt phthalocyanine+ poly (2-chloroaniline) modified electrodes. *Journal of Electroanalytical Chemistry*,*431*(1), 1-5.

[127] Zhang, J., Tse, Y. H., Pietro, W. J., & Lever, A. B. P. (1996). Electrocatalytic activity of N, N′, N ″, N‴-tetramethyl-tetra-3, 4-pyridoporphyrazinocobalt (II) adsorbed on a graphite electrode towards the oxidation of hydrazine and hydroxylamine. *Journal of Electroanalytical Chemistry*, *406*(1), 203-211.

[128] Zagal, J. H. (1980) Electrocatalysis of Hydrazine Electrooxidation by Phthalocyamines Adsorbed on Graphite, Journal of Electroanalytical Chemistry, 109(1-3), 389-393.

[129] Uretazanartu, M. S. and J. H. Zagal (1982) Potentiodynamic Studies on Iridium Electrodes in Alkaline-Solution, Journal of the Electrochemical Society, 129(3), 141-141.

[130] Caro, C. A., Bedioui, F., & Zagal, J. H. (2002). Electrocatalytic oxidation of nitrite on a vitreous carbon electrode modified with cobalt phthalocyanine.*Electrochimica acta*, *47*(9), 1489-1494.

[131] Pournaghi-Azar, M. H., & Dastangoo, H. (2004). Electrocatalytic oxidation of nitrite at an aluminum electrode modified by a chemically deposited palladium pentacyanonitrosylferrate film. *Journal of Electroanalytical Chemistry*, *567*(2), 211-218.

[132] C.A. Caro, F. Bedioui, M.A. Páez, G.I. Cárdenas-Jirón, J.H. Zagal, (2004), J. Electrochem. Soc., 151 E32.

[133] Schöning, M. J., & Poghossian, A. (2002). Recent advances in biologically sensitive field-effect transistors (BioFETs). *Analyst*, *127*(9), 1137-1151.

[134] Sander, J., Schweinsberg, F., & Menz, H. P. (1968). Untersuchungen über die Entstehung cancerogener Nitrosamine im Magen. *Hoppe-Seyler´ s Zeitschrift für physiologische Chemie*, *349*(2), 1691-1697.

[135] Steinbach, F., & Zobel, M. (1978). Metal Phthalocyanines Used as Catalysts in Gas Phase Reactions. *Zeitschrift für Physikalische Chemie*, *111*(1), 113-123.

[136] Calvin, M., & Polanyi, M. (1938). Homogeneous catalytic hydrogenation.*Transactions of the Faraday Society*, *34*, 1181-1191.

[137] Razafindralambo, H., Paquot, M., Baniel, A., Popineau, Y., Hbid, C., Jacques, P., & Thonart, P. (1997). Foaming properties of a natural cyclic lipoheptapeptide belonging to a special class of amphiphilic molecules. *Food hydrocolloids*, *11*(1), 59-62.

[138] Heaton, F. W., & Uri, N. (1961). The aerobic oxidation of unsaturated fatty acids and their esters: cobalt stearate-catalyzed oxidation of linoleic acid.*Journal of lipid research*, *2*(2), 152-160.

[139] Brouwer, W. M., Piet, P., & German, A. L. (1985). The promoting role of polycations in the cobalt (ii) phthalocyanine tetrasodium sulfonate catalysed oxidation of thiols. *Journal of molecular catalysis*, *31*(2), 169-182..

[140] Santos, L. M., & Baldwin, R. P. (1986). Electrocatalytic response of cobalt phthalocyanine chemically modified electrodes toward oxalic acid and. alpha.-keto acids. *Analytical chemistry*, *58*(4), 848-852.

[141] Moser, F. H., & Thomas, A. L. (1983). The Phthalocyanines. Vol. 2 Manufacture and Applications.

[142] Evans, J. F. and T. Kuwana (1977) Radiofrequency Oxygen Plasma Treatment of Pyrolytic-Graphite Electrode Surfaces, Analytical Chemistry, 49(11), 1632-1635.

[143] Zagal, J., P. Bindra and E. Yeager (1980) A Mechanistic Study of O-2 Reduction on Water-Soluble Phthalocyanines Adsorbed on Graphite-Electrodes, Journal of the Electrochemical Society, 127(7), 1506-1517.

[144] Kobayashi, N. and Y. Nishiyama (1985) Catalytic Electroreduction of Molecular-Oxygen Using Iron or Cobalt 4,4',4'',4'''-Tetracarboxyphthalocyanine, Journal of Physical Chemistry, 89(7), 1167-1170.

[145] Osaka, T., K. Naoi, T. Hirabayashi and S. Nakamura (1986) Electrocatalytic Oxygen Reduction at (Tetrasulfonatophthalocyaninato)-Cobalt Incorporated Polypyrrole Film Electrode, Bulletin of the Chemical Society of Japan, 59(9), 2717-2722.

[146] Elzing, A., Van der Putten, A., Visscher, W., & Barendrecht, E. (1987). The cathodic reduction of oxygen at metal tetrasulfonato-phthalocyanines: influence of adsorption conditions on electrocatalysis. *Journal of electroanalytical chemistry and interfacial electrochemistry*, *233*(1), 99-112.

[147] Blomquist, J., Helgeson, U., Moberg, L. C., Johansson, L. Y., & Larsson, R. (1982). Simultaneous electrochemical and mössbauer measurements on polymeric iron phthalocyanine oxygen electrodes. *Electrochimica Acta*, *27*(10), 1453-1460.

[148] Toshiba Corp. Jpn. Kokai Tokkyo Koho Jp. Appl. (1985), 81/41, 673,24 March 1981, CA. 102, 754174.

[149] Savy, M. (1974) Study of Reduction of Oxygen on Monomer and Polymer Phthalocyanines .2. Iron Polyphthalocyanines Impregnated on Carbon Blocks of Y Acetylene, Electrochimica Acta, 19(7), 403-411.

[150] Meshitsuka, S. and K. Tamaru (1977) Photoelectrocatalysis by Metal Phthalocyanine Evaporated-Films in Oxidation of Oxalate Ion, Journal of the Chemical Society-Faraday Transactions, I 73, 236-242.

[151] Linkous, C., Klofta, T., & Armstrong, N. R. (1983). Photoactivated electrolysis on nonporous chlorogallium phthalocyanine thin film electrodes. *Journal of The Electrochemical Society*, *130*(5), 1050-1055.

[152] Halbert, M. K. and R. P. Baldwin (1985) Electrocatalytic and Analytical Response of Cobalt Phthalocyanine Containing Carbon Paste Electrodes toward Sulfhydryl Compounds, Analytical Chemistry, 57(3), 591-595.

[153] Chen, I., Mort, J., Jansen, F., Grammatica, S., & Morgan, M. (1985). Nature of electrophotographic images from amorphous silicon photoreceptors. *Journal of imaging science*, *29*(2), 73-75.

[154] Zagal, J. H. (1992) Metallophthalocyanines as Catalysts in Electrochemical Reactions, Coordination Chemistry Reviews, 119, 89-136.

[155] Obirai, J. and T. Nyokong (2004) Electrochemical studies of manganese tetraamminophthalocyanine monomer and polymer, Electrochimica Acta, 49(9-10), 1417-1428.

[156] Ozoemena, K. I., Nyokong, T., & Westbroek, P. (2003). Self-Assembled Monolayers of Cobalt and Iron Phthalocyanine Complexes on Gold Electrodes: Comparative Surface Electrochemistry and Electrocatalytic Interaction with Thiols and Thiocyanate. *Electroanalysis*, *15*(22), 1762-1770.

[157] ABE, T.; Taguchi, F.; Imaya, H.; Zhao, F.; Zhang J.; Kaneko M.: (1998), Highly active electrocatalyst by cobalt tetraphenylporphyrin incorporated in a Nafion membrane for proton reduction, *Polymer Advanced Technologies*, 9 559-562.

[158] Agboola, B. and T. Nyokong (2007) Comparative electrooxidation of sulphite by self-assembled monolayers (SAMs) of Co(II), Fe(II), Ni(II) and Mn(III) tetrakis benzylmercapto and dodecylmercapto metallophthalocyanines complexes on gold electrodes., Talanta, 72(2), 691-698.

[159] Sakamoto, K. and E. Ohno (1997) Synthesis and electron transfer property of phthalocyanine derivatives., Progress in Organic Coatings, 31(1-2), 139-145.

[160] Plenio, H. and C. Aberle (2001). Coupled molecular switches: A redox-responsive ligand and the redox-switched complexation of metal ions, Chemistry-a European Journal 7(20): 4438-4446.

[161] Kounaves, S. P. (1997). Voltammetric techniques. *Handbook of instrumental techniques for analytical chemistry*, 709-726.

[162] Osteryoung, J. G. and R. A. Osteryoung (1985) Square-Wave Voltammetry, Analytical Chemistry, 57(1), A101-&.

[163] Deangelis, T. P. and W. R. Heineman (1976) Electrochemical Experiment Using an Optically Transparent Thin-Layer Electrode, Journal of Chemical Education, 53(9), 594-597.

[164] Heineman, W. R., et al. (1975) Mercury Film Nickel Mini-Grid Optically Transparent Thin-Layer Electrochemical Cell, Analytical Chemistry, 47(8), 1364-1369.

[165] Deangelis, T. P. and W. R. Heineman (1976) Differential Pulse Anodic-Stripping Voltammetry in a Thin-Layer Electrochemical Cell, Analytical Chemistry, 48(14), 2262-2263.

[166] Gui, J. Y., et al. (1991) "Long Optical Pathlength Thin-Layer Spectroelectrochemistry - Study of Homogeneous Chemical-Reactions.", Journal of Electroanalytical Chemistry, 309(1-2), 73-89.

[167] Bornside, D. E., et al. (1987) On the Modeling of Spin Coating, Journal of Imaging Technology, 13(4), 122-130.

[168] Buck, R. P., (1978), Theory and Principles of Membrane Electrodes, Chapt. 1, Ion-Selective Electrodes in Analytical Chemistry, Vol. 1, H. Freiser, ed., Plenum Press, NY, U.S.A

[169] Ross, J. W. and M. S. Frant (1968). Mechanism of Interference at Solid State Membrane Ion Selective Electrodes, Applied Spectroscopy, 22(3): 228-&.

ÖZGEÇMİŞ

Adı Soyadı : Faruk DEMİR

Doğum Yeri ve Tarihi : İstanbul/1987

Yabancı Dili : İngilizce

E-Posta : fdemir@pendik.bel.tr

Öğrenim Durumu

Derece	Bölüm/Program	Üniversite/Lise	Mezuniyet Yılı
Lise	Fen	BEYOĞLU FINDIKLI LİSESİ	2004
Üniversite	Kimya Mühendisliği	MARMARA ÜNİVERSİTESİ	2010

İş Deneyimi

Yıl	Firma/Kurum	Görevi
2010-	PENDİK BELEDİYESİ	ÇEVRE DENETİM ŞEFİ

Bilimsel Eserler:

Uluslararası Hakemli Dergilerde Yayınlanan Makaleler

1. ÇAKIR, V., **DEMİR, F**., BIYIKLIOĞLU, Z., KOCA, A., KANTEKİN, H. (2013) Synthesis, characterization, electrochemical and spectroelectrochemical properties of metal-free and metallophthalocyanines bearing electropolymerizable dimethylamine groups, Dyes and Pigments, 98, (3), 414-421 .
2. **DEMIR, F**., ERDOGMUS, A., KOCA, A. (2013) Titanyl phthalocyanines: Electrochemical and Spectroelectrochemical Characterizations and Electrochemical Metal Ion Sensor Applications of Langmuir Films, Journal of Electroanalytical Chemistry, Accepted Manuscript.

Ulusal Konferans Bildirileri

1. **DEMİR, F**., KOCA, A. (2012). Electrochemical and In-Situ Spectroelectrochemical Characterization of Electroactive Titanyl Centered Phthalocyanine Complexes and Their Electrochemical Application Fields.XXVI National Chemistry Congress. Muğla, Turkey.